

Spring 5-31-1982

## Remote attitude measurement techniques

Frank John Elmer  
*New Jersey Institute of Technology*

Follow this and additional works at: <https://digitalcommons.njit.edu/dissertations>



Part of the [Electrical and Electronics Commons](#)

---

### Recommended Citation

Elmer, Frank John, "Remote attitude measurement techniques" (1982). *Dissertations*. 1268.  
<https://digitalcommons.njit.edu/dissertations/1268>

This Dissertation is brought to you for free and open access by the Electronic Theses and Dissertations at Digital Commons @ NJIT. It has been accepted for inclusion in Dissertations by an authorized administrator of Digital Commons @ NJIT. For more information, please contact [digitalcommons@njit.edu](mailto:digitalcommons@njit.edu).

## **Copyright Warning & Restrictions**

The copyright law of the United States (Title 17, United States Code) governs the making of photocopies or other reproductions of copyrighted material.

Under certain conditions specified in the law, libraries and archives are authorized to furnish a photocopy or other reproduction. One of these specified conditions is that the photocopy or reproduction is not to be “used for any purpose other than private study, scholarship, or research.” If a user makes a request for, or later uses, a photocopy or reproduction for purposes in excess of “fair use” that user may be liable for copyright infringement,

This institution reserves the right to refuse to accept a copying order if, in its judgment, fulfillment of the order would involve violation of copyright law.

**Please Note: The author retains the copyright while the New Jersey Institute of Technology reserves the right to distribute this thesis or dissertation**

Printing note: If you do not wish to print this page, then select “Pages from: first page # to: last page #” on the print dialog screen

The Van Houten library has removed some of the personal information and all signatures from the approval page and biographical sketches of theses and dissertations in order to protect the identity of NJIT graduates and faculty.

## INFORMATION TO USERS

This reproduction was made from a copy of a document sent to us for microfilming. While the most advanced technology has been used to photograph and reproduce this document, the quality of the reproduction is heavily dependent upon the quality of the material submitted.

The following explanation of techniques is provided to help clarify markings or notations which may appear on this reproduction.

1. The sign or "target" for pages apparently lacking from the document photographed is "Missing Page(s)". If it was possible to obtain the missing page(s) or section, they are spliced into the film along with adjacent pages. This may have necessitated cutting through an image and duplicating adjacent pages to assure complete continuity.
2. When an image on the film is obliterated with a round black mark, it is an indication of either blurred copy because of movement during exposure, duplicate copy, or copyrighted materials that should not have been filmed. For blurred pages, a good image of the page can be found in the adjacent frame. If copyrighted materials were deleted, a target note will appear listing the pages in the adjacent frame.
3. When a map, drawing or chart, etc., is part of the material being photographed, a definite method of "sectioning" the material has been followed. It is customary to begin filming at the upper left hand corner of a large sheet and to continue from left to right in equal sections with small overlaps. If necessary, sectioning is continued again—beginning below the first row and continuing on until complete.
4. For illustrations that cannot be satisfactorily reproduced by xerographic means, photographic prints can be purchased at additional cost and inserted into your xerographic copy. These prints are available upon request from the Dissertations Customer Services Department.
5. Some pages in any document may have indistinct print. In all cases the best available copy has been filmed.

**University  
Microfilms  
International**

300 N. Zeeb Road  
Ann Arbor, MI 48106

**Elmer, Frank John**

**REMOTE ATTITUDE MEASUREMENT TECHNIQUES**

*New Jersey Institute of Technology*

**D.ENG.SCI.**

**1982**

**University**

**Microfilms**

**International**

300 N. Zeeb Road, Ann Arbor, MI 48106

PLEASE NOTE:

In all cases this material has been filmed in the best possible way from the available copy.  
Problems encountered with this document have been identified here with a check mark ✓.

1. Glossy photographs or pages ✓
2. Colored illustrations, paper or print
3. Photographs with dark background ✓
4. Illustrations are poor copy
5. Pages with black marks, not original copy
6. Print shows through as there is text on both sides of page
7. Indistinct, broken or small print on several pages
8. Print exceeds margin requirements
9. Tightly bound copy with print lost in spine
10. Computer printout pages with indistinct print
11. Page(s)        lacking when material received, and not available from school or author.
12. Page(s)        seem to be missing in numbering only as text follows.
13. Two pages numbered       . Text follows.
14. Curling and wrinkled pages
15. Other \_\_\_\_\_

University  
Microfilms  
International

REMOTE  
ATTITUDE MEASUREMENT  
TECHNIQUES

by  
Frank John Elmer

Dissertation submitted to the Faculty of the Graduate School  
of the New Jersey Institute of Technology in partial fulfillment  
of the requirements for the degree of  
Doctor of Engineering Science  
1982

APPROVAL OF DISSERTATION

Remote Attitude Measurement Techniques

by Frank John Elmer

for Department of Electrical Engineering

New Jersey Institute of Technology

Approved: \_\_\_\_\_ Chairman

\_\_\_\_\_

\_\_\_\_\_

\_\_\_\_\_

Newark, N.J.  
April 1982



## VITA

Name: Frank John Elmer

Degree and date to be conferred: D. Eng. Sci. 1982

Secondary education: Manasquan High School, Manasquan, N.J.

Collegiate institutions attended	Dates	Degree	Date of Degree
Monmouth College	1968-70	A.A.	1970
Monmouth College	1970-72	B.S.E.E.	1972
Monmouth College	1972-75	M.S.E.E.	1975
New Jersey Institute of Technology	1975-82	D.Eng. Sci.	1982

Major: Electronic Engineering

Minors: Mathematics, Physics, Computer Science, Communications,  
Electro-optics

### Publications:

"Method of Determining Relative Orientation of Physical Systems"  
US Patent #4,134,681, 16 Jan 79  
"Optical Alignment Sensor", US Patent #4,035,654, 12 July 77  
"Transparent Optical Power Meter", US Patent #4,019,381,  
12 Jan 76.  
Numerous technical reports and IRIS papers.

### Positons held:

Electronic Engineer, Combat Surveillance and Target  
Acquisition Laboratory, Ft. Monmouth N.J. 1969-1978  
Electronic Engineer, Electronic Warfare Laboratory, Ft. Monmouth,  
N.J. 1978 to present

## ABSTRACT

Title of Dissertation: Remote Attitude Measurement Techniques

Frank John Elmer, Doctor of Engineering Science, 1982

Dissertation directed by: Dr. Stanley S. Reisman  
Associate Professor  
Department of Electrical Engineering  
New Jersey Institute of Technology

A method has been developed for solving practical problems which can be expressed in terms of physical geometry. These problems often involve combining directional information observed by remotely located sensors reported in their own respective local coordinate systems. To transform this information into a common coordinate system, the attitude of the sensors must be measured with respect to this common coordinate system.

Physical geometry is a generalization of mathematical geometry where objects define the endpoints of figures composed of ensembles of lines. A probabilistic approach has been taken which is based on the fundamental assumption that the objects can be partitioned (for analytical purposes) into volume elements which are very small compared to the distance between objects. This allows the set of directions to the partitioned object to be represented by an ensemble of lines. Each observable volume element is characterized by its normalized contrast which is proportional to the probability that the object lies in the direction specified by the line to that volume element. Thus, the direction to the object can be expressed in terms of a probabilistic vector.

A technique has been developed to measure the attitude of a remotely

located sensor based upon both sensors measuring the same set of two physical vectors. These measurements are reported in terms of probabilistic vectors and used to compute a probabilistic matrix which defines the attitude of the remote sensor. This probabilistic matrix can then be used to transform any vector measured by one sensor into its corresponding description in the other sensor's own local coordinate system. This allows directional information to be combined and thus physical geometry problems to be solved.

The engineering considerations of implementing a Remote Attitude Measurement, ReAtMent, system are presented including the development of an error budget necessary to insure that the ReAtMent system performs to the required accuracy.

An experimental section is presented which illustrates the concepts developed by using an electrooptical sensor to measure three physical vectors in several orientations. Two of these measured probabilistic vectors are used to compute a probabilistic attitude matrix. This matrix then operates on the remaining physical vector as reported in the reference orientation of the sensor to predict the probabilistic vector which would describe the same physical vector in the current orientation. The predicted and actually observed vectors are then compared to give a measure of the accuracy of the technique. Many of the concepts developed in this dissertation were thus validated experimentally.

As the study of ReAtMent is in its infancy, the present work should be used as a springboard for further research. Topics that may be of interest for future studies are suggested.

## PREFACE

Until recently, the study of attitude measurement has been largely confined to inertial attitude reference systems (i.e. gyroscopes) and some photographic schemes for determining the attitude of satellites in orbit. These systems are designed to measure their orientation with respect to the reference system used on the surface of the earth.

This study deals primarily with how two physically separated objects can determine their relative attitude, that is perform a Remote Attitude Measurement, ReAtMent; and extends previous work on attitude measurement by exploring the fundamental concepts on which ReAtMent techniques are based and developing the basic tool for ReAtMent, the Two Vector Method. Using the physical limitations on how directional information can be measured, a statistical approach is developed which allows the performance of a ReAtMent system to be analyzed in a probabilistic sense.

The study builds upon previous work in directional measurement, estimation of the attitude matrix, vector and quaternion algebra, statistics, and practical attitude measurement systems. Using these tools, it is possible to develop a firm theoretical framework for studying ReAtMent systems. The pure "pencil and paper" approach yields theoretically satisfying results which are useful for understanding how to analyze ReAtMent system performance. The integrals involved are quite complicated and a computerized implementation is necessary to analyze a practical ReAtMent system. A simple experiment is performed using a single electrooptical sensor and computerized

data reduction to illustrate and validate many of the concepts developed during the doctoral research.

While in residence at Ft. Monmouth, the author served as the project engineer on an exploratory development model of a state of the art ReAtMent system. This served as the testbed for many of the original ideas described below and provided insights into the fundamental problems with real life applications of ReAtMent, some of which would never have been brought to light by a purely theoretical approach.

## ACKNOWLEDGEMENT

In addition to my advisor, Dr. Stanley S. Reisman, the author wishes to acknowledge the help and encouragement given to him by several distinguished individuals over the years while this dissertation was in progress: Mr. William Bayha, for his help in formulating the expressions for the coefficients of the attitude matrix given the defining principal axis and angle of rotation; and Mr. Paul Michaels for his participation in many technical discussions related to various technical concepts developed by the author.

## TABLE OF CONTENTS

Chapter	Page
PREFACE.....	ii
ACKNOWLEDGEMENT.....	iv
INTRODUCTION.....	1
I. OVERVIEW OF FUNDAMENTAL CONCEPTS.....	2
A. Physical Geometry.....	2
B. Defining and Measuring the Direction to an Object.....	3
II. PROBABILISTIC VECTORS- A NEW ANALYTICAL TOOL.....	7
A. The Concept of Probabilistic Vectors.....	7
B. Continuous Probabilistic Vectors.....	8
C. Discrete Probabilistic Vectors.....	9
D. Describing Probabilistic Vectors in Terms of Base Pixels and Matrices.....	10
E. Combining Measurements Made in Different Coordinate Systems: The General ReAtMent Problem.....	12
F. Mathematical Basis of ReAtMent: The Two Vector Method.....	13
G. Physical Vectors: Generalizing the Two Vector Method for Separated Observers.....	17
III. THE PROBABILISTIC ANALYSIS OF A ReAtMent SYSTEM.....	19
A. Introduction.....	19
B. Mapping Probability into the $\theta, \emptyset$ Plane.....	20
C. Calculating the Direction of the Sum of Two Pixels....	26
D. Computability of Integrals.....	29
E. Calculating the Direction of the Difference Between Two Pixels.....	31
F. Calculating the Direction of the Crossproduct of Two Pixels.....	32
G. Calculating the Angle Between Two Pixels.....	34

H. Analysis of the Two Vector Method in Terms of Continuous Probabilistic Vectors.....	35
I. Analysis of the Two Vector Method in Terms of Discrete Probabilistic Vectors.....	37
J. Completing the Problem: Using the Computed Probabilistic Matrix.....	41
IV. STATE OF THE ART IN ATTITUDE MEASUREMENT.....	43
A. Mechanical Attitude Measurement.....	43
B. Inertial Attitude Measurement.....	46
C. Gravimetric Attitude Measurement.....	49
D. Electrostatic Attitude Measurement.....	50
E. Magnetic Attitude Measurement.....	51
F. Photogrammetric Attitude Measurement.....	52
G. Electromagnetic Attitude Measurement.....	53
H. Sonar Attitude Measurement.....	54
I. Electrooptical Attitude Measurement.....	54
J. Summary of the Major Forms of Attitude Measurement....	55
K. Considerations for ReAtMent Applications.....	57
V. THE GENERALIZED ReAtMent SYSTEM.....	59
A. Overview.....	59
B. Block Diagram and Component Descriptions of the Generalized ReAtMent System.....	60
1. Device to be Pointed.....	60
2. Position Measurement Means.....	61
3. Physical Vector Measurement Means.....	63
4. Computational Means.....	65
5. Object Direction and Range Measurement Means....	70
6. Communications Means.....	71
C. The "Simple" Generalized ReAtMent System.....	72
D. Errors in ReAtMent.....	73
E. Establishing a ReAtMent Error Budget.....	74



F. Summary of ReAtMent Considerations.....	78
VI. MEASURING PROBABILISTIC VECTORS WITH ELECTROOPTICAL SENSORS.....	79
A. Overview.....	79
B. What a Viewed Object Looks Like.....	81
C. Using the Direction to a Viewed Object as a Probabilistic Vector.....	83
D. The Concept of a Partitioned Focal Plane.....	83
E. Directional Properties of Electrooptical Systems.....	85
F. Converting Optical to Electrical Energy.....	92
G. Focal Plane Partitioning in Electrooptical Devices....	94
H. Expressing the Image of an Object as a Probabilistic Vector.....	100
I. Specific Example of a Television Camera with Computer Interface.....	104
VII. EXPERIMENTS IN ReAtMent.....	114
A. Object.....	114
B. Design of the Experiment.....	115
C. Directional Calibration of the Television Camera.....	117
D. Measurement of Probabilistic Vectors.....	127
E. The Experiment.....	129
F. Data Reduction.....	134
G. Results.....	138
VIII. CONCLUSIONS AND RECOMMENDATIONS FOR FURTHER RESEARCH.....	142
A. Conclusions.....	142
B. Recommendations for Further Research.....	144
APPENDIX A. LISTING OF DATA REDUCTION PROGRAM.....	146

APPENDIX B. VARIABLE LIST FOR DATA REDUCTION PROGRAM.....	157
APPENDIX C. MEASURED PROBABILISTIC VECTORS.....	158
APPENDIX D. SAMPLE RUN OF DATA REDUCTION PROGRAM.....	159
SELECTED BIBLIOGRAPHY.....	160
INDEX.....	165

## LIST OF TABLES

TABLE	Page
4.1 State of the Art Accuracy and Limiting Factors of Attitude Measurement Techniques	57
6.1 Derivation of Probabilistic Vector from Example Shown in Figure 6.5	101
7.1 Number of Members and Maximum Value of Measured Probabilistic Vectors	132
7.2 Results of Experimental Data Reduction	139

FIGURE	LIST OF FIGURES	Page
1.1	Partitioning Objects into Volume Elements Which Meet the Fundamental Assumption	2
2.1a	Physical Situation	15
2.1b	Observer in Reference Orientation	15
2.1c	Observer in Final Orientation	15
2.1d	Vectors Reported by Observer in His Own Local Coordinate System	15
3.1	Sum of Two Three Dimensional Unit Vectors	28
5.1	Generalized ReAtMent System Block Diagram	60
5.2	Basic Three Dimensional Triangle	75
6.1	Simple Optical Directional Measurement Model	83
6.2	Illustration of a Refractive Optical System	87
6.3	Illustration of an Array of Discrete Detectors in the Focal Plane	94
6.4	Illustration of Sensitive Focal Plane Scanned by Electron Beam	98
6.5	Object Viewed by a Partitioned Focal Plane Sensor with Plot of Probability Density	101
6.6	Numbering Scheme Used in Frame Store for Valid Pixels	107
6.7	Detail of Pixel Offset for Odd and Even Numbered Rows	107
7.1	The Calibration Triangle	118
7.2	Machinists Table Calibration Figure	121
7.3	Detail of Camera Mounting on Machinists Table	123
7.4	Camera Viewing Illuminated Slit During Calibration	124
7.5	Detail of the Fiber Optic Bundles in the Target Board	128
7.6	View of Setup to Measure Probabilistic Vectors	128
7.7	Typical Frame Store Image	131
7.8	View of Target Board from Behind Camera	131
7.9	Simplified Flowchart of Data Reduction Program	138

## INTRODUCTION

Remote Attitude Measurement, ReAtMent, is a tool for solving real world, three dimensional geometry problems. In such problems, observers independently measure, report, and act on data in their own local coordinate systems. This data is then transformed into a common coordinate system via a matrix computed by the ReAtMent system, and combined to solve the problem.

## CHAPTER I: OVERVIEW OF FUNDAMENTAL CONCEPTS

### A. PHYSICAL GEOMETRY

Spatial relationships between objects are analyzed by physical geometry. The commonly taught mathematical geometry is a subset of physical geometry where the objects are represented by infinitely small points. These points and the infinitely thin line segments which connect them are unique. This uniqueness provides the basis for asserting that two geometric quantities are actually exactly equal, thereby deducing that the other geometrical quantities must satisfy a given relationship. This absolute precision allows the development and proof of geometric theorems.

Mathematical and physical geometry converge when the following fundamental assumption holds: Objects defining the endpoints of a line segment are very small in comparison to the length of the line segment. When this fundamental assumption does not hold, it is possible to partition the objects into volume elements for which the assumption does hold, effectively creating an ensemble of line segments to replace the single line segment normally expected when using mathematical geometry. This ensemble is statistically describable by its expected value (or average) and its distribution.

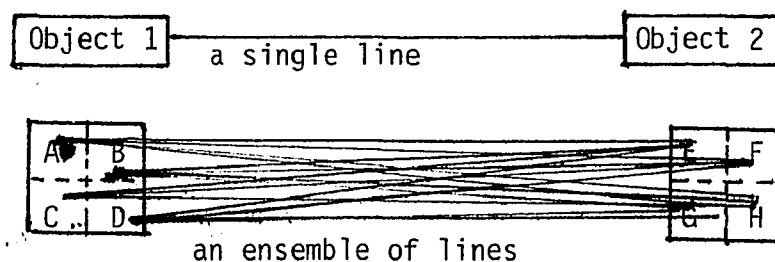


FIGURE 1.1. Partitioning Objects Into Volume Elements Which Meet the Fundamental Assumption

When a simple figure is formed by lines connecting objects in space, the result of partitioning the object into volume elements is that each of the lines, of the simple figure, becomes an ensemble of lines. Thus, the figure becomes an ensemble of geometric figures. However, all of the figures in the ensemble are not necessarily well behaved. This arises because the lines comprising these ill-behaved figures terminate on different volume elements of the objects. It is important to bear this in mind when doing a statistical analysis of real-world physical geometry problems such as are encountered in ReAtMent applications.

#### B. DEFINING AND MEASURING THE DIRECTION TO AN OBJECT

A line segment is described by its length and direction. The length is a scalar quantity and is therefore independent of the coordinate system used. However, the description of direction is strongly dependent on the coordinate system chosen. A direction is described by a unit vector pointing in that direction. The unit length is chosen to give the vector describing the direction the same two angular parameters as the direction itself.

The direction to an object can be defined as the ensemble of the unit vectors lying along the line segments joining volume elements of the observed object with volume elements of the viewing object.

The detectable volume elements of an observed object are those which have a clear line-of-sight to the viewing object and a non-zero contrast. The sensing object has no knowledge of the existence or whereabouts of undetectable volume elements of the viewed object. Similarly, the volume elements of the viewing object which have clear

line of sight to the observed object are the only ones which could possibly determine the direction of the viewed object. Therefore, for real objects, only a subset of the directions of the lines between all volume elements of the two objects are measurable. Consequently, the statistical parameters of the ensemble of measurable directions may differ from those of the full ensemble of the directions between all volume elements of the two objects.

Now consider how the directions in the ensemble are measured. If the separation between the two objects increases to the point where each object is very small compared to the distance between them, (i.e. the fundamental assumption is satisfied) then the detectable volume element of each object becomes the object itself and the ensemble reduces to a single line.

A directional sensor monitors a set of solid angles called pixels which cover the field-of-view, FOV, of the sensor. Each pixel reports the total energy received over its own instantaneous-field-of-view, IFOV, as a single value, the intensity of that pixel.

The presence of an object is detected by the difference between the intensities of the pixels viewing the background and those viewing the object. Since the intensity of a pixel is a single, scalar number, no information is obtained as to whether more than one object is within the IFOV of that pixel. Consequently, when partitioning the viewed object into detectable volume elements, there is no advantage in using a partition size smaller than the IFOV that pixel subtends at the range to the object.

Now consider the limitations imposed by the combination of sensor



and object on directional measurement. The portion of the sensor which directs energy onto the detectors associated with individual pixels (e.g. the lenses of an optical system) are characterized by a modulation transfer function, MTF. The temporal MTF of the sensor is a measure of how the pixel responds to a change in the energy received with time. The spatial MTF is a measure of the ability of the sensor to discern contrast within a given angular subtense of the image.

The detectable elements of the object have a non-zero contrast. That is they radiate a different amount of energy toward the sensor in the passband of the detector than does the background. The definition of the contrast of a pixel is  $[\text{brightest pixel} - \text{pixel under discussion}] / [\text{brightest pixel} - \text{dimmiest pixel}]$ . The spatial MTF of the sensor multiplies the spatial power spectrum of the scene to give the spatial power spectrum of the image as reported by the sensor. As an example, consider a scene consisting of a checkerboard pattern with a contrast of 1.0 (the best possible) between adjacent squares. If the MTF of the sensor were 0.8 at the corresponding spatial frequency, then the squares in the image would appear to have a contrast of 0.8 instead of 1.0.

Once the contrast between squares falls to the noise level of the sensor, the squares become indistinguishable. This occurs when the size of the square just subtends the diffraction limit of the sensor (assuming an ideal sensor). However, in practice, the effects of aberrations in the parts of the sensor which direct energy onto the detectors, effectively limit the size of the image of a bright point source (the ideal viewed object) and thus the spatial resolution

achievable by the sensor.

Usually, the pixel size selected for the directional sensor is made slightly larger than the theoretical diffraction limit to insure that pixel size, rather than the MTF of the energy collecting portion of the sensor, limits the spatial resolution of the sensor.

## CHAPTER II: PROBABILISTIC VECTORS - A NEW ANALYTICAL TOOL

### A. THE CONCEPT OF PROBABILISTIC VECTORS

In order to treat the ensemble of directions from one physical object to another as a single analytic entity, the concept of a probabilistic vector was developed.

The probability associated with each individual measurable direction in the ensemble is proportional to the contrast of the volume element in the viewed object to which it points. Consider the case where a point source in a uniform background is imaged onto a single detector of the directional sensor. The pixel corresponding to this detector is the only one whose intensity is different from the rest. Therefore, the object (the point source) must be within the IFOV of that pixel with a probability of 1.0. If the image were now spread out to cover several pixels, the probability of the object being within that set of pixels is still 1.0. Therefore, the integral over the set of the probability associated with each pixel must be a constant equal to 1.0. However, the individual pixels may have different intensities, with the brightest having the highest probability of containing the object. Thus, it is appropriate to select the set of pixels whose contrast exceeds a reasonable threshold and normalize the contrast of these pixels so that they sum to 1.0. This normalized contrast corresponds to the probability of the direction to the object being within the IFOV of the respective pixels.

If the pixels are allowed to have infinitesimal IFOV such that they form a continuum, the probability density becomes a continuous

distribution over the solid angle covered by the set of pixels. If, on the other hand, the design of the sensor is such that the IFOV of each pixel is of a finite size, then the probability density must be represented as a series of discrete values because each detector's output is a single number, thus no information is obtained from the detector to resolve any finer detail in the probability distribution. It is then reasonable to assume that the probability distribution within a finite pixel is uniform.

On the basis of the above discussion, a probabilistic vector,  $P$ , can be defined as a set of  $n$  vectors,  $P_m$ , each having an associated probability,  $p_m$ , as shown by equation 2.1.

$$P = \left\{ (P_{mx}\hat{i} + P_{my}\hat{j} + P_{mz}\hat{k} + p_m) \mid \sum_{m=1}^n p_m = 1.0 \right\} \quad (\text{eq. 2.1})$$

where  $P_{mx}\hat{i} + P_{my}\hat{j} + P_{mz}\hat{k}$  is the  $m^{\text{th}}$  vector in the set and  $p_m$  is the probability associated with that  $m^{\text{th}}$  vector

## B. CONTINUOUS PROBABILISTIC VECTORS

A vector describing a direction has two independent angular parameters. The most convenient set of angular parameters to work with in describing the output of a directional sensor are azimuth,  $\theta$ , and elevation  $\emptyset$ . This arises because most directional sensors are mounted in an azimuth over elevation gimbal.  $\theta$  physically varies between zero and  $2\pi$  while  $\emptyset$  physically varies between  $\pi/2$  and  $-\pi/2$ . However, this can pose a problem because  $\theta$  and  $\emptyset$  are pointwise orthogonal<sup>1</sup> but not mutually orthogonal<sup>2</sup>.

To facilitate analysis,  $\theta$  and  $\emptyset$  are mapped into a Cartesian

1. Pointwise orthogonal means that at every point  $d\theta$  is perpendicular to  $d\emptyset$ .

2. Mutually orthogonal means that the  $d\theta$  at any point is orthogonal to  $d\emptyset$  taken at any other point.

coordinate system in which the spherical angular parameters of  $\theta, \phi$  are directly substituted for the usual  $x, y$ .

A further difficulty is encountered due to the singularity at  $\phi = \pi/2$ . It should be remembered however that the actual values of  $\theta$  and  $\phi$  correspond to the principal values of the arc trigonometric functions of  $\theta$  and  $\phi$ . Thus, a physically contiguous set of pixels (i.e. the set of solid angles which cover a larger continuous solid angle) can be mapped into separated disconnected regions in a Cartesian plot of  $\theta, \phi$ . To circumvent this difficulty, let the  $\theta, \phi$  plane extend from  $-4\pi$  to  $+4\pi$  for both  $\theta$  and  $\phi$ . In this expanded plane, any physically contiguous set of pixels will map into a simply connected region, greatly simplifying the required calculations without impairing their mathematical integrity.

An infinitesimal single pixel centered at  $\theta, \phi$  has an IFOV bounded in its own local coordinates by  $(\theta-d\theta, \phi-d\phi), (\theta-d\theta, \phi+d\phi), (\theta+d\theta, \phi+d\phi), (\theta+d\theta, \phi-d\phi)$ . Thus the area in the  $\theta, \phi$  plane represented by the infinitesimal pixel is  $4d\theta d\phi$ . In concert with the discussion above concerning the information content of the pixel, the probability distribution over the region in the  $\theta, \phi$  plane representing the pixel is uniform and equal to  $1/(4d\theta d\phi)$ . The form of the continuous probabilistic vector is given by equation 2.2 where the terms are as defined for equation 2.1, except that  $p_{\theta\phi}$  is the probability associated with the point at  $\theta, \phi$ .

$$P = \{ \cos(\theta)\cos(\phi)\hat{i} + \sin(\theta)\cos(\phi)\hat{j} + \sin(\phi)\hat{k} + p_{\theta\phi} \} \quad (\text{eq. 2.2})$$

### C. DISCRETE PROBABILISTIC VECTORS

The probabilistic vector describing a single pixel has a uniform

distribution (in its own local coordinate system) whose integral over the pixel is equal to its normalized contrast. To compute this normalized contrast, let all pixels whose contrast exceeds a given threshold (depending on the noise level of the sensor and the confidence level required) be assigned to the set of pixels known to contain the direction to the object. The total probability associated with this set can therefore be assigned a probability of 1.0. To determine their normalized contrast, all pixels in this set have their actual contrast divided by the sum of the contrasts of the pixels assigned to this set.

Thus the direction to an object can be described by a set of pixels with associated probabilities. Since each pixel has a uniform distribution, the expected direction of the ensemble of directions represented by that pixel is simply the centroid of the solid angle covered by that pixel. This expected direction can be expressed as a vector and used to represent the pixel with the understanding that the solid angle (i.e. IFOV) of the pixel is "small". Thus, the set of pixels can be represented as an ensemble of vectors with associated probabilities. As there are a finite number of vectors in this ensemble, the resulting probability distribution is a set of discrete values. Therefore, the probabilistic vector is described as discrete.

#### D. DESCRIBING PROBABILISTIC VECTORS IN TERMS OF BASE PIXELS AND MATRICES

Consider the entire FOV of the sensor to be a single pixel, or a sensor with a single pixel. Let the sensor be mounted in a two axis gimbal on the sensing object. To express the FOV of the pixel in the sensing object's coordinate system, the set of directions represented

by the pixel in its own local coordinate system must be operated on by the matrix representing the combined effect of the rotations performed by the gimbal in moving the sensor from its aligned position to point at the viewed object.

The typical elevation over azimuth gimbal rotates first about the Y axis by the elevation angle,  $\emptyset$ , (assuming the pixel to be centered on the X axis of the sensor which is initially aligned with the X axis of the sensing object), and then about the Z axis by the azimuth angle,  $\theta$ . The transformation matrix (i.e. attitude matrix),  $[T]$ , which operates on the pixel (i.e. any pixel of the sensor) is formed by the multiplication of two simple matrices as shown below.

$$\begin{aligned}
 [T] &= \begin{bmatrix} \cos(\emptyset) & 0 & -\sin(\emptyset) \\ 0 & 1 & 0 \\ \sin(\emptyset) & 0 & \cos(\emptyset) \end{bmatrix} \begin{bmatrix} \cos(\theta) & \sin(\theta) & 0 \\ \sin(\theta) & \cos(\theta) & 0 \\ 0 & 0 & 1 \end{bmatrix} \\
 &= \begin{bmatrix} \cos(\emptyset)\cos(\theta) & \cos(\emptyset)\sin(\theta) & -\sin(\emptyset) \\ \sin(\emptyset)\cos(\theta) & \sin(\emptyset)\sin(\theta) & 0 \\ \sin(\emptyset)\cos(\theta) & \sin(\emptyset)\sin(\theta) & \cos(\emptyset) \end{bmatrix} \quad (\text{eq. 2.3})
 \end{aligned}$$

As an example of a common application, consider a surveyor's theodolite. The sensor is the telescope. The intersection of the crosshairs gives a pixel with a "small" IFOV centered on the X axis of the telescope. The vector representing this pixel directly along the

X axis of the telescope is  $\begin{bmatrix} 1 \\ 0 \\ 0 \end{bmatrix}$  and the transformation matrix,  $[T]$ ,

is as given by equation 2.3. The direction,  $D$ , of an object centered in the crosshairs is given in probabilistic vector form by equation 2.4.

$$D = \{\cos(\theta)\cos(\emptyset)\hat{i} + \sin(\theta)\cos(\emptyset)\hat{j} + \sin(\emptyset)\hat{k} + 1\} \quad (\text{eq. 2.4})$$

where  $D$  is expressed in the coordinate system of the body of the theodolite. If the telescope is now replaced by a sensor containing

many pixels, the same process can be used to express the direction of that pixel in the coordinate system of the body of the mounting gimbal.

#### E. COMBINING MEASUREMENTS MADE IN DIFFERENT COORDINATE SYSTEMS: THE GENERAL ReAtMent PROBLEM

Consider the most general case of a triangle in three dimensions formed by two observers and a third object. One observer determines the relative locations of both the other observer and the object. The first observer wishes to tell the second observer in what direction to point the device toward the object. To be of any use, this information must be expressed in the local coordinate system of the second observer. A ReAtMent system must be used to measure the attitude of the second observer and to transform the data measured by the first observer into the coordinate system of the second observer, so that he can use it to point the device.

In the above case, the triangle in three dimensions was solved in the coordinate system of the first observer. Now consider a variation of the problem such that the two observers can determine each other's relative location and independently measure the direction to the object in their own coordinate systems. This is the generalized ReAtMent problem where the measured data must be transformed into a common coordinate system to solve the triangle (via the angle, side, angle technique).

All three dimensional geometric figures can be solved by decomposing them into triangles in three dimensions (by constructing lines as necessary) described in a common coordinate system.



## F. MATHEMATICAL BASIS OF ReAtMent: THE TWO VECTOR METHOD

The fact that a triangle in three dimensions is actually independent of the coordinate system used to describe it, forms the basis of the Two Vector Method. A triangle, formed by the observer and two objects, is measured once by the observer in his reference orientation and once in his final orientation. If the relative location of the observer and the two objects has not changed, the triangle has not changed. Thus, the difference in the descriptions the directions to the respective objects must be due solely to the change in orientation of the observer.

Whatever series of rotations is made by the observer as he progresses from his reference orientation to his final orientation, there exists a unique single rotation about a unique axis which would have accomplished the reorientation of the observer in a single step. This axis is called the principal axis of rotation, PAR. The angle is called the angle of rotation, AR.

When the vector describing the direction to an object is rotated about the PAR by the AR in the opposite sense to the rotation of the observer, the vector still physically points in the same direction, but its description has changed. If this vector is decomposed into components parallel and perpendicular to the PAR, it will be seen that the two parallel components (before and after rotation) are identical. The difference in description must thus be due to the components perpendicular to the PAR. Therefore, the difference between the two descriptions of the same physical vector (i.e. the difference vector) must be perpendicular to the PAR.

Calculating the difference vectors (one for each of the two objects) and taking their crossproduct results in a vector parallel to the PAR. Normalizing this crossproduct gives the direction of the PAR.

If the two measurements of the same physical vector are decomposed into components parallel and perpendicular to the PAR, the AR can be calculated from the angle between the components perpendicular to the PAR.

If the two objects are far enough away from the observer so that the fundamental assumption (i.e. objects small compared to distance between them) is satisfied, then the physical geometry triangle between them becomes a simple mathematical geometry triangle and the directions to the objects can be represented by deterministic vectors as shown in figure 2.1

Figure 2.1a shows that  $\hat{M}$  and  $\hat{L}$  are unit vectors describing the direction to object 1, and are thus the same physical vector. Similarly,  $\hat{P}$  and  $\hat{Q}$  describe the direction to object 2. In the reference orientation of the observer (figure 2.1b)  $\hat{M}$  and  $\hat{Q}$  are measured. In the final orientation of the observer, (figure 2.1c)  $\hat{L}$  and  $\hat{P}$  are measured. In figure 2.1d these measured vectors are shown in the local coordinate system of the observer.

If  $[A]$  is defined as the attitude matrix of the observer (i.e.  $[A]$  operates on any vector measured by the observer to express that vector in the reference coordinate system), then

$$\hat{M} = [A]\hat{L} \quad (\text{eq. 2.5})$$

$$\hat{Q} = [A]\hat{P} \quad (\text{eq. 2.6})$$

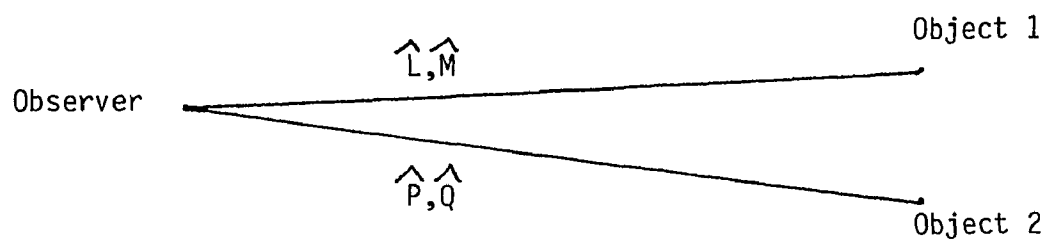


Figure 2.1a. Physical Situation

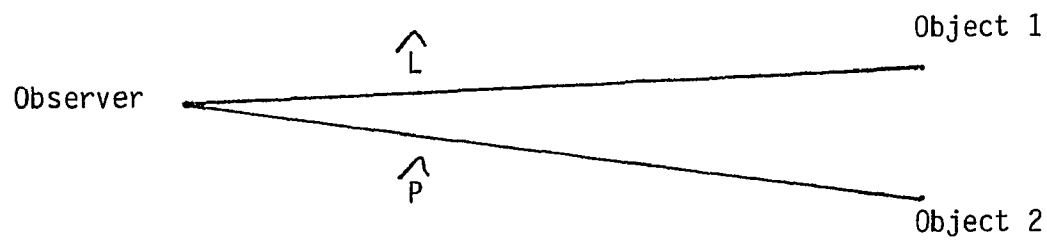


Figure 2.1b. Observer in Reference Orientation

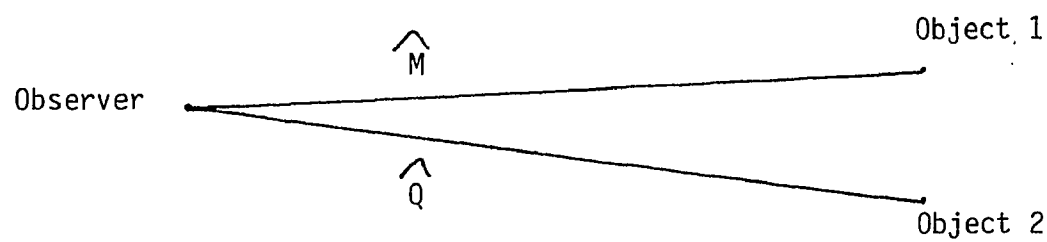
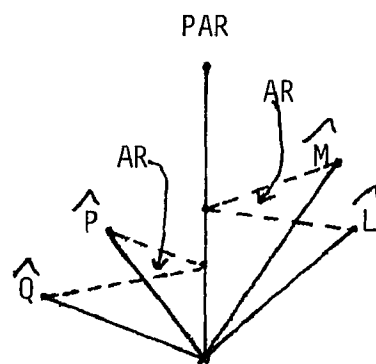


Figure 2.1c. Observer in Final Orientation



Origin of Observer's Coordinate System

Figure 2.1d. Vectors Reported by Observer in His Own Local Coordinate System

Since  $(\hat{L}-\hat{M})$  and  $(\hat{P}-\hat{Q})$  are perpendicular to the PAR then by the discussion above,

$$\text{PAR} = (\hat{L}-\hat{M}) \times (\hat{P}-\hat{Q}) \quad (\text{eq. 2.7})$$

It should be noted that if  $(L-M)$  is parallel to  $(P-Q)$  the PAR can be found by

$$\text{PAR} = (\hat{L} \times \hat{P}) \times (\hat{M} \times \hat{Q}) \quad (\text{eq. 2.8})$$

Let  $s$  be the magnitude of the projection of  $M$  or  $L$  on the PAR, thus

$$s = \hat{M} \cdot \hat{\text{PAR}} = \hat{L} \cdot \hat{\text{PAR}} \quad (\text{eq. 2.9})$$

form the perpendicular components of  $M$  and  $L$  respectively as

$$G = (\hat{L} - s\hat{\text{PAR}}) \quad (\text{eq. 2.10})$$

$$H = (\hat{M} - s\hat{\text{PAR}}) \quad (\text{eq. 2.11})$$

then the AR can be calculated from

$$\text{AR} = \arctangent[(G \times H)/(G \cdot H)] \quad (\text{eq. 2.12})$$

It should be noted that the sense of the angle of rotation and the sense of the principal axis of rotation will match if this notation is followed. Thus, if the two vector method is used in a test case, the calculated PAR may be of the opposite sense than expected, but if so, then the AR will also have the opposite sign. Thus when  $[A]$  is calculated, as shown below, the expected  $[A]$  will be obtained.

If the components of the PAR are expressed as

$$\text{PAR} = \alpha \hat{i} + \beta \hat{j} + \gamma \hat{k} \quad (\text{eq. 2.13})$$

then the coefficients of  $[A]$  can be calculated as shown in equation 2.14.

$$[A] = \begin{vmatrix} a_{11} & a_{12} & a_{13} \\ a_{21} & a_{22} & a_{23} \\ a_{31} & a_{32} & a_{33} \end{vmatrix} \quad (\text{eq. 2.14})$$

where<sup>3</sup>

$$a_{11} = \cos^2(AR/2) - (1 - 2\alpha^2)\sin^2(AR/2)$$

$$a_{12} = -\gamma \sin(AR) + 2\alpha\beta \sin^2(AR/2)$$

$$a_{13} = \beta \sin(AR) + 2\alpha\gamma \sin^2(AR/2)$$

$$a_{21} = \gamma \sin(AR) + 2\beta\alpha \sin^2(AR/2)$$

$$a_{22} = \cos^2(AR/2) - (1 - 2\beta^2)\sin^2(AR/2)$$

$$a_{23} = -\alpha \sin(AR) + 2\beta\gamma \sin^2(AR/2)$$

$$a_{31} = -\beta \sin(AR) + 2\gamma\alpha \sin^2(AR/2)$$

$$a_{32} = \alpha \sin(AR) + 2\gamma\beta \sin^2(AR/2)$$

$$a_{33} = \cos^2(AR/2) - (1 - 2\gamma^2)\sin^2(AR/2)$$

#### G. PHYSICAL VECTORS: GENERALIZING THE TWO VECTOR METHOD FOR SEPARATED OBSERVERS

The Two Vector Method given above holds exactly for the case of one observer viewing two objects, first from a reference orientation and then again from his final orientation. In order to apply the Two Vector Method in determining the relative orientation of two separated observers, the two observers must be mathematically moved to share a common origin of their coordinate systems. This can be accomplished by expressing the respective directions to the two objects as members of uniform vector fields (i.e. physical vectors).

Every member of a uniform vector field is mathematically indistinguishable from that member of the field which passes through the origin of the coordinate system. The member of the uniform vector field describing the direction to an object from one observer is mathematically the same as a different member of the same field which passes through the origin of another observer's coordinate system. Thus, this uniform vector field can be thought of as a physical vector.

Thus, the Two Vector Method can be generalized to cover the case

3. This form of the expressions for the matrix coefficients is after a derivation by Mr. William Bayha.

of separated observers by requiring that each observer measure the same two physical vectors. If both observers are colocated, it can be seen that this reduces to the case of a single observer measuring the same two physical vectors from two different orientations.

When separated observers view the same object, a triangle in three dimensions is formed. In general, the two sides of the triangle intersecting at the object are not parallel, but if the object is sufficiently far away from the observers, then these two sides become effectively parallel (i.e. within the measurement accuracy of the observer). Consequently if the two observers were to both be aligned with each other, the object would appear to be in the same direction to each observer, allowing the direction to the object to be defined in terms of a uniform vector field, and thus as a valid physical vector.

Thus, for two separated observers who each measure the respective directions to two distinct, distant objects, the Two Vector Method can be used to determine their relative orientation. This allows a ReAtMent system based on an implementation of the Two Vector Method to be constructed using appropriate physical vector measurement means on each of the two platforms whose relative attitude is to be determined, a means of communicating the measured physical vectors to a computational means which performs the Two Vector Method algorithm, and a means for communicating the measured attitude back to the respective platform so that it can act on the information<sup>4</sup>.

4. F.Elmer. "Method of Determining Relative Orientation of Physical Systems", US Patent # 4,134,618. 16 Jan 79

## CHAPTER III: THE PROBABILISTIC ANALYSIS OF A ReAtMent System

### A. INTRODUCTION

The next task is to perform a theoretical analysis of the Two Vector Method using probabilistic vectors in order to understand the statistical aspects of the problem and to provide a tool for the analysis of an actual ReAtMent system.

Physical geometry problems are best handled by a probabilistic analysis as they are described by figures composed of ensembles of lines. When the size of the objects involved approach a point relative to the length of the lines, the ensemble of lines shrinks to a single line and the results of a probabilistic analysis must converge to that obtained via a conventional mathematical geometric analysis.

Another factor in analyzing the performance of a ReAtMent system is repeatability. Given the same physical situation, i.e. the observers and the objects have not moved, repeated measurements will produce differing results due to the effect of random errors in the directional measurement means. Thus an ensemble of geometric figures will be obtained for the same physical situation.

Assuming stationarity, the results of using the ensemble of repeated measurements will have the same statistics as the results obtained from using the ensemble of directions obtained by the probabilistic analysis. As a gedanken, imagine an object which subtends two pixels in the sensor's FOV. The sensor as a subsystem will indicate one pixel or the other as being the direction to the object, and track accordingly. If the two pixels are of different intensity during one measurement, stationarity implies that the relative frequency of selecting the brighter pixel as the direction to the

object is proportional to the normalized contrast of that pixel. Thus if one pixel were twice as bright as the other, that pixel would be selected as the direction to the object by the sensor subsystem 2/3 of the time.

Leaving the gedanken, the desired end result of using the ReAtMent system is to point something at the object. In an analytical sense, this requires a calculation of the probability distribution of the direction to that object. Given this, the effectiveness of pointing that something at the object can be evaluated (e.g., the probability of a hit on a detected aircraft by an air defense weapon). The necessary tools to perform the probabilistic analysis of a ReAtMent system are developed below.

#### B. MAPPING PROBABILITY INTO THE $\theta, \phi$ PLANE

The concept of mapping probabilistic vectors as a probability distribution on a Cartesian plot of the angular parameters  $\theta$  and  $\phi$  has been introduced.<sup>5</sup> The major advantage in using this approach is that the standard tools of statistical analysis can be directly applied to data in this form.

Briefly, the major theorems employed are the following:

1. When constructing a set from subsets, the region where two subsets intersect is assigned the probability density formed by the sum of the respective subset probabilities at each point.
  2. When an operation is performed on independently chosen members of two or more sets, the probability of the result is the product of the respective probabilities.
5. See section B of chapter II



3. The integral of the probability of any given parameter over the  $\theta, \emptyset$  plane is exactly equal to 1.0.

The use of the  $\theta, \emptyset$  plane produces a problem in determining the analytic form of the probability density as a function of the  $\theta, \emptyset$  as the parameters are pointwise orthogonal rather than uniformly orthogonal and have singularities at  $\emptyset = +\pi/2$  and  $-\pi/2$ .

Consider the case of mapping the probabilistic vector represented by a single pixel of a sensor into the  $\theta, \emptyset$  plane. In local sensor coordinates, the pixel represents a uniform probability density over a region bounded by  $(\theta - \Delta\theta, \emptyset - \Delta\emptyset)$ ,  $(\theta - \Delta\theta, \emptyset + \Delta\emptyset)$ ,  $(\theta + \Delta\theta, \emptyset + \Delta\emptyset)$ , and  $(\theta + \Delta\theta, \emptyset - \Delta\emptyset)$ .

For the reasons given above in the discussion on expressing pixels in terms of base pixels and matrices, each vector representing an infinitesimal solid angle within the IFOV of the pixel is operated on by the transformation matrix  $[T]$  to determine the corresponding coordinates in the  $\theta, \emptyset$  plane. This point in the plane is then assigned the probability density of  $1/(4d\theta d\emptyset)$  where  $d\theta$  and  $d\emptyset$  are given in the sensor local coordinate system. The probability distribution in the  $\theta, \emptyset$  plane is constructed by repeating this procedure until all of the IFOV of the pixel has been covered by the infinitesimal solid angles.

This can be seen by examining the mapping of a sensor pixel centered on the X axis of the sensor (i.e.  $\theta = \emptyset = 0$ ) and of half angle  $\Delta\theta$ ,  $\Delta\emptyset$ . In chapter 2 vectors, the probability density of the pixel in sensor coordinates,  $f_{\theta\emptyset}(\theta, \emptyset)$ , is given by definition 3.1.

$$f_s(\theta_s, \emptyset_s) = \begin{cases} 1/(4\Delta\theta\Delta\emptyset) & \text{for } -\Delta\theta < \theta_s < \Delta\theta \text{ and } -\Delta\emptyset < \emptyset_s < \Delta\emptyset \\ 0 & \text{otherwise} \end{cases} \quad (\text{def. 3.1})$$

The set of directions represented by this pixel  $P_s$ , is a set of probabilistic vectors defined as

$$P_s = \{\cos(\theta_s)\cos(\emptyset_s)\hat{i} + \sin(\theta_s)\cos(\emptyset_s)\hat{j} + \sin(\emptyset_s)\hat{k} + f_s(\theta_s, \emptyset_s)\} \quad (\text{def. 3.2})$$

Refer back to the discussion of how pixels may be represented in terms of a base pixel and matrix which maps the base pixel onto the  $\theta\emptyset$  plane as  $P_r$ . Call this base pixel  $P_s$  (expressed in sensor coordinates) and the matrix  $[M_s]$ . The transformed pixel in body coordinates,  $P_b$ , will be given by

$$P_b = [M_s]P_s \quad (\text{eq. 3.1})$$

As a result of this transformation, the density of  $P_b$  will be non-uniform. To show this clearly, some dummy variables will be introduced to simplify the algebra required. Thus let

$$[M_s] = \begin{bmatrix} a & b & c \\ d & e & f \\ g & h & i \end{bmatrix} \quad (\text{def. 3.3})$$

$$R = \sin(\theta_s) \quad (\text{def. 3.4})$$

$$S = \cos(\theta_s) \quad (\text{def. 3.5})$$

$$P = \sin(\emptyset_s) \quad (\text{def. 3.6})$$

$$Q = \cos(\emptyset_s) \quad (\text{def. 3.7})$$

Then from equation 3.1 obtain

$$\cos(\theta_r)\cos(\emptyset_r) = aSQ + bRQ + cP = \textcircled{2} \quad (\text{eq. 3.2})$$

$$\sin(\theta_r)\cos(\emptyset_r) = dSQ + eRQ + fP = \textcircled{3} \quad (\text{eq. 3.3})$$

$$\sin(\emptyset_r) = gSQ + hRQ + iP = \textcircled{4} \quad (\text{eq. 3.4})$$

The circled numbers are dummy variables whose value is equal to one side of the correspondingly numbered equation. This notation is used to help keep track of where the dummy variables come from as the

analysis progresses and to provide an easy means of locating their defining equations. Equations 3.2 and 3.3 can be combined to eliminate  $\theta_r$  and yield

$$\tan(\theta_r) = \frac{dSQ + eRQ + fP}{aSQ + bRQ + cP} = (5) \quad (\text{eq. 3.5})$$

This gives two equations (3.4 and 3.5) which are immediately solvable for  $\theta_r$  and  $\theta_s$  in terms of  $\theta_s$  and  $\theta_s$ . Using the property of the transformation matrix that its inverse is given by its transpose<sup>6</sup>, it is possible to solve directly for  $\theta_s$  and  $\theta_s$  in terms of  $\theta_r$  and  $\theta_r$ , thus

$$\tan(\theta_s) = \frac{b\cos(\theta_r)\cos(\theta_r) + e\sin(\theta_r)\cos(\theta_r) + h\sin(\theta_r)}{a\cos(\theta_r)\cos(\theta_r) + d\sin(\theta_r)\cos(\theta_r) + g\sin(\theta_r)} = (6) \quad (\text{eq. 3.6})$$

$$\sin(\theta_s) = \frac{c\cos(\theta_r)\cos(\theta_r) + d\sin(\theta_r)\cos(\theta_r) + i\sin(\theta_r)}{a\cos(\theta_r)\cos(\theta_r) + d\sin(\theta_r)\cos(\theta_r) + g\sin(\theta_r)} = (7) \quad (\text{eq. 3.7})$$

The Jacobian of the transformation is defined as

$$J(\theta_s, \theta_s) = \begin{vmatrix} \frac{\partial \theta_r}{\partial \theta_s} & \frac{\partial \theta_r}{\partial \theta_s} \\ \frac{\partial \theta_r}{\partial \theta_s} & \frac{\partial \theta_r}{\partial \theta_s} \end{vmatrix} \quad (\text{def. 3.8})$$

Thus the density of  $\theta_r, \theta_r$  is given by

$$f_{\theta_r, \theta_r}(\theta_r, \theta_r) = \frac{f_{\theta_s, \theta_s}(\theta_s, \theta_s)}{J(\theta_s, \theta_s)} = (8) \quad (\text{eq. 3.8})$$

and the Jacobian is shown to be

$$(9) = \frac{[(R^2Q^2(ae-bd) + RPQ(af-cd) + SPQ(ce-bf) + S^2Q^2(ae-bd))(-gSP-hRP+iQ) - (SP^2(af-cd) + RP^2(bf-ce) + SQ^2(af-cd) + RQ^2(bf-ce))(-gRQ+hSQ)]}{[(2)^2(1-(5)^2)(1-(4)^2)]} \quad (\text{eq. 3.9})$$

Thus a calculable (although quite complicated) analytical expression (equation 3.8) has been found for the density of the pixel in the 6. This is true for any unitary, orthogonal matrix.

$\theta_r, \emptyset_r$  plane.

Consider the special case where the transformation matrix  $[M_s]$  is the identity matrix. This means that the sensor is in its reference position and shares the same coordinate system (ignoring translation of the origin) as the body to which it is attached. After a little algebra, the Jacobian (equation 3.9) turns out to be equal to  $1/\cos(\emptyset)$ . Thus, the density of  $f_{\theta\emptyset}$  is proportional to  $\cos(\emptyset)$ .

This is not inconsistent. The parameters  $\theta, \emptyset$  have a singularity at  $\emptyset = +\pi/2$  and  $-\pi/2$ , where the Jacobian becomes zero. Thus when a finite solid angle (e.g. a pixel) is centered on the plane where  $\emptyset$  equals zero it subtends a minimum measure of the angular parameters  $\theta$  and  $\emptyset$ . However, if moved to a region where  $\emptyset$  is near  $\pi/2$  the apparent measure of the pixel in terms of  $\theta$  increases while the measure of  $\emptyset$  remains constant.

To help in visualizing this point, consider a gedanken where a small square of paper is placed on a standard desk top globe. The small square of paper represents a fixed amount of solid angle originating at the center of the globe. Place the square on the equator, and assume that the square covers 10 degrees of latitude by 10 degrees of longitude. Now move the paper up in latitude and measure the difference in longitude between the corners of the square. Note that the top corners appear to subtend a greater number of degrees of longitude than the bottom corners of the square. Also note that the difference in latitude between the top and bottom of the square is still 10 degrees. Now place the square so that it is centered at one

of the poles. The 4 corners of the square will now differ in longitude by 90 degrees.

Now imagine that the square is cut up into areas subtending exactly 1 degree by 1 degree. If the square is on the equator, 100 very nearly square pieces will result. Each will have very nearly the same area. In contrast, if the square had been centered on the pole, 1800 pieces would have been cut<sup>7</sup>. They would not all have the same area.

Consider that the entire square represents the probability of something being in the set of directions subtended by the solid angle covered by the square. Since the square of paper is of a uniform thickness, imagine that this thickness represents the probability density. Thus, each little piece we have cut from the square represents the probability of that something being in the solid angle subtended by that little piece. Thus, a probability density which is physically uniform (like the paper) may be expressed as a non-uniform density when it is described by the parameters  $\theta$  (longitude) and  $\emptyset$  (latitude), depending on where the center of the distribution is located on the  $\theta, \emptyset$  plane.

Leaving the gedanken, it can be seen that what was thought to be a uniform distribution in the pixel itself is actually uniform; however, because it is described by the pointwise orthogonal parameters  $\theta, \emptyset$ , this distribution should be written as

$$f_{\theta_s \emptyset_s}(\theta_s, \emptyset_s) = \frac{\cos(\emptyset_s)}{4 \Delta \theta \sin(\Delta \emptyset)} \quad (\text{def. 3.9})$$

7. 360 degrees of longitude by 5 degrees of latitude.

The  $\cos(\emptyset_s)$  in the above definition arises because of the dependence of the distribution on  $\cos(\emptyset)$ . The  $\sin(\Delta \emptyset)$  replaces the  $\Delta \emptyset$  expected because the integral of  $f_{\emptyset_s \emptyset_s}$  over  $\Delta \theta, \Delta \emptyset$  must equal 1.0 to be consistent with the definition of the pixel as having a uniform spatial probability distribution. For a pixel centered on the X axis (i.e.  $\theta = \emptyset = 0$ ), the  $\cos(\emptyset)$  is very nearly 1.0 while the  $\sin(\Delta \emptyset)$  is very nearly  $\Delta \emptyset$ . This brings the above expression for  $f(\theta, \emptyset)$  (def. 3.9) into agreement with the former expression (def. 3.1) and explains the assumptions and resulting approximations which hold for the former expression.

To summarize this discussion on mapping directional probabilities onto the  $\theta, \emptyset$  plane, a rather complicated expression (eq. 3.8) has been derived for analytically performing the required mapping. This lays the foundation for the analysis which follows as all directional probability distributions can now be represented on a common  $\theta, \emptyset$  plane in analytic form.

### C. CALCULATING THE DIRECTION OF THE SUM OF TWO PIXELS

Given that the probability density of each pixel has been mapped into the  $\theta, \emptyset$  plane as given above, it is possible to compute the direction of the sum of two pixels as a probabilistic vector and represent this probabilistic vector as a pixel (or collection of pixels).

First examine the two dimensional case. Let the first pixel be such that  $\theta_1 - \Delta \theta < \theta < \theta_1 + \Delta \theta$ , and let the second pixel be such that  $\theta_2 - \Delta \theta < \theta < \theta_2 + \Delta \theta$ . Let  $\theta_a$  be any member of the first pixel and  $\theta_b$  be any member of the second pixel. Then it can be shown

that<sup>8</sup> the azimuth of the sum,  $\theta_s$ , is given by

$$\theta_s = (\theta_a + \theta_b)/2 \quad (\text{eq. 3.10})$$

Thus the bounds of  $\theta_s$  are given by

$$\frac{\theta_1 + \Delta\theta_1 + \theta_2 + \Delta\theta_2}{2} > \theta_s > \frac{\theta_1 - \Delta\theta_1 + \theta_2 + \Delta\theta_2}{2} \quad (\text{eq. 3.11})$$

If  $\theta_a$  and  $\theta_b$  are written as

$$\theta_a = \theta_1 + d\theta_1 \quad (\text{def. 3.10})$$

$$\theta_b = \theta_2 + d\theta_2 \quad (\text{def. 3.11})$$

then equation 3.10 can be solved for  $d\theta_2$  and used to form the density of the sum as

$$f_{\theta_s}(\theta_s) = \int_{\theta_1}^{\theta_1 + \Delta\theta_1} f_{d\theta_1}(\theta_1) f_{d\theta_2}(2\theta_s - \theta_1 - \theta_2 - d\theta_1) d(d\theta_1) \quad (\text{eq. 3.12})$$

The expected value of  $\theta_s$  can be written as

$$E(\theta_s) = \int_{(\theta_1 + \theta_2 - \Delta\theta_1 - \Delta\theta_2)/2}^{(\theta_1 + \theta_2 + \Delta\theta_1 + \Delta\theta_2)/2} \theta_s f_{\theta_s}(\theta_s) d\theta_s \quad (\text{eq. 3.13})$$

As a check, consider the special case of  $d\theta_1$  and  $d\theta_2$  having symmetrical densities; then  $E(\theta_s) = (\theta_1 + \theta_2)/2$  as expected. The two dimensional case is thus seen to correspond to the well known one of the sum of two independent random variables.

This analysis can be expanded directly to three dimensions. Writing the equations directly in terms of  $\theta_s$ ,  $\emptyset_s$ , and a constant of proportionality, k:

8. Assuming infinitesimally small pixels

$$k\cos(\theta_s)\cos(\phi_s) = \cos(\theta_1+d\theta_1)\cos(\phi_1+d\phi_1) + \cos(\theta_2+d\theta_2)\cos(\phi_2+d\phi_2) \quad (\text{eq. 3.14})$$

$$k\sin(\theta_s)\cos(\phi_s) = \sin(\theta_1+d\theta_1)\cos(\phi_1+d\phi_1) + \sin(\theta_2+d\theta_2)\cos(\phi_2+d\phi_2) \quad (\text{eq. 3.15})$$

$$k\sin(\phi_s) = \sin(\phi_1+d\phi_1) + \sin(\phi_2+d\phi_2) \quad (\text{eq. 3.16})$$

While it is possible to solve these equations directly for the member of one pixel which will combine with the given member of the other to form a given member of the sum, it is more instructive to solve the problem geometrically. From the two dimensional case, it is clear that the sum vector lies in the same plane as the two vectors which were added. Thus

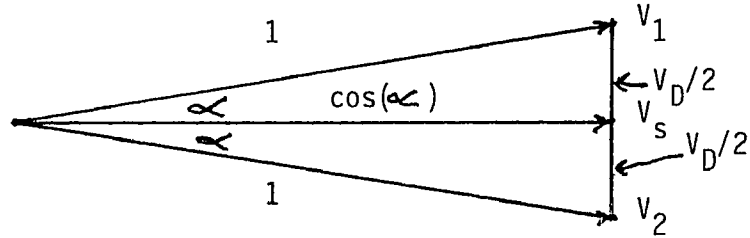


Figure 3.1 Sum of Two Three Dimensional Unit Vectors

In this figure, it is apparent that the angle,  $2\alpha$ , between the two members of probabilistic vector sets,  $V_1$  and  $V_2$  can be found directly from the dot product of the two unit vectors. Thus

$$\begin{aligned} \cos(2\alpha) &= \cos(\theta_1+d\theta_1)\cos(\phi_1+d\phi_1)\cos(\theta_2+d\theta_2)\cos(\phi_2+d\phi_2) \\ &\quad + \sin(\theta_1+d\theta_1)\cos(\phi_1+d\phi_1)\sin(\theta_2+d\theta_2)\cos(\phi_2+d\phi_2) \\ &\quad + \sin(\phi_1+d\phi_1)\sin(\phi_2+d\phi_2) \end{aligned} \quad (\text{eq.3.17})$$

Now doing some straightforward vector algebra

$$V_2 = V_1 - 2(V_D/2) = V_1 - 2(V_1 - \cos(\alpha)V_s) = -V_1 + 2\cos(\alpha)V_s \quad (\text{eq. 3.18})$$

$$\textcircled{19} = \tan(\theta_2+d\theta_2) = \frac{2\cos(\alpha)\sin(\theta_s)\cos(\phi_s) - \sin(\theta_1+d\theta_1)\cos(\phi_1+d\phi_1)}{2\cos(\alpha)\cos(\theta_s)\cos(\phi_s) - \cos(\theta_1+d\theta_1)\cos(\phi_1+d\phi_1)} \quad (\text{eq. 3.19})$$

$$\textcircled{20} = \sin(\phi_2+d\phi_2) = 2\cos(\alpha)\sin(\phi_s) - \sin(\phi_1+d\phi_1) \quad (\text{eq. 3.20})$$



Equation 3.17 provides a reasonable means of calculating the angle. Using this in equation 3.18, the member of the second pixel which combines with the given member of the first pixel to form the desired sum can be found with equations 3.19 and 3.20. Introducing  $\theta_a, \phi_a$  as the general member of the first pixel with parameters  $\theta_1 + d\theta_1, \phi_1 + d\phi_1$ , and denoting the probabilities of the members of the first and second pixels respectively as  $f_1$  and  $f_2$ , the probability density of the sum,  $f_s$  can be written as

$$f_s(\theta_s, \phi_s) = \int_{\phi_1 - d\phi_1}^{\phi_1 + d\phi_1} \int_{\theta_1 - d\theta_1}^{\theta_1 + d\theta_1} f_1(\theta_a, \phi_a) f_2(\tan^{-1}(\textcircled{19}), \sin^{-1}(\textcircled{20})) d\theta_a d\phi_a \quad (\text{eq. 3.21})$$

The expected value of the representative vector of the sum is found to be

$$E(\theta_s, \phi_s) = \int_{\text{lower bound } \theta_s}^{\text{upper bound } \theta_s} \int_{\text{lower bound } \phi_s}^{\text{upper bound } \phi_s} \theta_s \phi_s f_s(\theta_s, \phi_s) d\theta_s d\phi_s \quad (\text{eq. 3.22})$$

Once the density of the sum (equation 3.21) has been found, the limits of the integrals in equation 3.22 can be determined. In general, these upper and lower limits are functions of  $\theta, \phi$  rather than constants. Thus, while this integral is conceptually satisfying, it is quite difficult to evaluate in closed form.

#### D. COMPUTABILITY OF INTEGRALS

In so far as these integrals are derived from real numbers and represent probability distributions derived from physically realizable situations, the computability of the integrals is guaranteed. However, the closed form analytic solutions of the integrals may be far too complicated to work with in studies of real applications.

A practical way around this difficulty, using computerized analysis, can be derived as follows: Visualize the operation of the procedure described for forming the sum of two pixels. Two probability distributions have been mapped in the  $\theta, \phi$  plane which represent two pixels to be operated upon (in the case above, by addition). To form the probability density of the result, begin by partitioning each pixel into small regions each represented as a discrete probabilistic vector with an associated finite probability; perform the operation on the two recently formed discrete probabilistic vectors; map the resulting probabilistic vector onto the  $\theta, \phi$  plane and assign a point probability mass at that spot equal to the product<sup>9</sup> of the probabilities associated with the two discrete probabilistic vectors; repeat this process using all possible pairs of discrete probabilistic vectors; now partition the portion of the  $\theta, \phi$  plane covered by the point masses into regions of a size comparable with that of the partitions of the original two pixels, and assign to each region the sum of the point probability masses lying within that region. This effectively constructs a discrete probability distribution of approximately the same angular resolution as the distributions of the original two pixels.

It is important to realize that the process described here preserves the information content of the directional sensor's output since the pixels reported by the sensor have spatially uniform probability distributions specified by a single number (the normalized contrast). Thus this technique is preferable to the strictly

9. Assuming that the probability distributions are independent.

analytical approach for the study of actual ReAtMent system performance.

However, the derivation and subsequent use of the analytic expressions for the sum, difference, cross product, dot product, and angle between two pixels is essential to develop a firm theoretical grasp of the actual operations being performed and their consequences in specific applications.

#### E. CALCULATING THE DIRECTION OF THE DIFFERENCE BETWEEN TWO PIXELS

The concept of the sum of two pixels or sets of directions resulting in some form of "average" direction is reasonably easy to grasp. Not so for the difference. The best way to visualize this is to look back at figure 3.1 and see that  $V_D$  is the difference vector between  $V_1$  and  $V_2$ . This  $V_D$  is in a direction perpendicular to the direction of the sum of  $V_1$  and  $V_2$  and lies in the same plane as those two vectors.<sup>10</sup> Thus the difference vector can be thought of as the tangent to the unit vector representing the sum of the two vectors. This establishes the basis for considering the difference between two probabilistic vectors to be thought of a direction (and hence a probabilistic vector) rather than a vector difference in the ordinary sense.

Thus the "difference of two pixels" means the direction of the difference. A vector difference is computed by taking the negative (i.e. opposite sense) of the vector to be subtracted and adding it to the other vector.

To take the negative of a pixel mapped in the  $\theta, \emptyset$  plane, let

10. More specifically, each member of  $V_D$  lies a plane defined by the specific members of  $V_1$  and  $V_2$  which generated that member of  $V_D$ .

$$f_n(\theta, \emptyset) = f_p(-\theta, -\emptyset) \quad (\text{def. 3.12})$$

where  $f_p$  is the density of the original pixel and  $f_n$  is the density of the negative of that pixel.

Thus to find the difference between two pixels  $P_1$  and  $P_2$ , form the negative of  $P_2$  as  $N_2$  (i.e.  $N_2 = -P_2$ ) as above where

$$f_{N_2}(\theta, \emptyset) = f_{P_2}(-\theta, \emptyset) \quad (\text{def. 3.13})$$

then express the difference between  $P_1$  and  $P_2$  as the sum of  $P_1$  and  $N_2$  and compute as given above for the sum of two pixels.

#### F. CALCULATING THE DIRECTION OF THE CROSSPRODUCT OF TWO PIXELS

The concept of the crossproduct of two pixels is not intuitively obvious. Referring to figure 3.1, the crossproduct of the two vectors  $V_1$  and  $V_2$  is perpendicular to the plane of the two vectors (i.e., into the page for  $V_1 \times V_2$ ). Thus, the direction of the crossproduct of two pixels can be thought of as perpendicular to their plane.

The crossproduct,  $P_c$ , of a member of the first pixel,  $P_1$  with a member of the second pixel,  $P_2$ , is defined as

$$\begin{aligned} P_c = P_1 \times P_2 &= \begin{vmatrix} \hat{i} & \hat{j} & \hat{k} \\ P_{1x} & P_{1y} & P_{1z} \\ P_{2x} & P_{2y} & P_{2z} \end{vmatrix} \\ &= (P_{1y}P_{2z} - P_{1z}P_{2y})\hat{i} + (P_{1z}P_{2x} - P_{1x}P_{2z})\hat{j} + (P_{1x}P_{2y} - P_{1y}P_{2x})\hat{k} \\ &= m\cos(\theta_c)\cos(\emptyset_c)\hat{i} + m\sin(\theta_c)\cos(\emptyset_c)\hat{j} + m\sin(\emptyset_c)\hat{k} \quad (\text{eq. 3.23}) \end{aligned}$$

where  $m$  is a constant of proportionality and the direction of the crossproduct has parameters  $\theta_c$  and  $\emptyset_c$ .

Given specific members of the probabilistic vectors  $P_c$  and  $P_1$ , there is a set of the members of  $P_2$  which will combine with

the specified member of  $P_1$  to form the specified member of  $P_c$ . Thus the probability added to the probability already assigned to that particular member of  $P_c$  should be the product<sup>11</sup> of the probabilities assigned to the specific member of  $P_1$  and the set of those members of  $P_2$  which combine with the specific member of  $P_1$  to form that particular member of  $P_c$ . This process forms the probability distribution of  $P_c$ .

To derive this probability, first start by setting the dot product of  $P_c$  and  $P_1$  to zero.<sup>12</sup> Thus,

$$0 = \cos(\theta_1)\cos(\phi_1)\cos(\theta_c)\cos(\phi_c) + \sin(\theta_1)\cos(\phi_1)\sin(\theta_c)\cos(\phi_c) + \sin(\phi_1)\sin(\phi_c) \quad (\text{eq. 3.24})$$

Solving for  $\phi_1$  as a function of  $\theta_1$  obtain

$$\cos^2(\phi_1) = 1/((\cos^2(\theta_1)\cos^2(\phi_c) + \sin^2(\theta_1)\sin^2(\theta_c) + 2\cos(\theta_1)\sin(\theta_1)\cos(\theta_c)\sin(\theta_c)(\cot^2(\phi_c) + 1.)) = \textcircled{25} \quad (\text{eq. 3.25})$$

Note that this equation has two branches. When plotted on the  $\theta, \phi$  plane, the probability of  $\theta_c, \phi_c$  will be the product of the line probability (from equation 3.25) over each pixel. Thus

$$f_{\phi_c} = \int_{P_1} f_{P_1}(\theta_1, \pm \cos^{-1}(\textcircled{25})) d\theta_1 \int_{P_2} f_{P_2}(\theta_2, \pm \cos^{-1}(\textcircled{25})) d\theta_2 \quad (\text{eq. 3.26})$$

and the expected value,  $E_{P_c}$ , of the crossproduct is given by

$$E_{P_c}(\theta_c, \phi_c) = \int_{\text{lower bound of } \phi_c}^{\text{upper bound of } \phi_c} \int_{\text{lower bound of } \theta_c}^{\text{upper bound of } \theta_c} \theta_c \phi_c f_{P_c}(\theta_c, \phi_c) d\theta_c d\phi_c \quad (\text{eq. 3.27})$$

where the limits on the integral are the bounds of  $\theta_c, \phi_c$ . As was the case with the sum of two pixels, it is much more efficient to restrict the limits of the integral to the minimum bounds which will

11. Again, assuming independence of the distributions of  $P_1$  and  $P_2$ .

12. Since  $P_c$  is by definition perpendicular to  $P_1$  and  $P_2$

enclose the region of the  $\theta, \emptyset$  plane where  $f_{p_c}(\theta_c, \emptyset_c)$  is different from zero, than to find the limits as a function of  $\theta, \emptyset$ . Again, this integral is intelectually quite satisfying, but unfortunately quite difficult to evaluate in closed form.

#### G. CALCUATING THE ANGLE BETWEEN TWO PIXELS

This is relatively straightfoward as the angle between two vectors is a scalar rather than a vector quantity. Thus if we define the two pixels  $P_1$  and  $P_2$  as above, the dot product of these two pixels is a scalar random variable  $\gamma = \cos(\alpha)$ , where  $\alpha$  is the angle between the two pixels. Consider a given value of  $\alpha$  and a particular member of one pixel  $(\theta_1, \emptyset_1)$ . The locus of all members of the other pixel  $(\theta_2, \emptyset_2)$  which have an angular difference of  $\alpha$  lie on the intersection of a cone of half angle centered at  $\theta_1, \emptyset_1$  with the other pixel. Thus

$$\gamma = \cos(\theta_1)\cos(\emptyset_1)\cos(\theta_2)\cos(\emptyset_2) + \sin(\theta_1)\cos(\emptyset_1)\sin(\theta_2)\cos(\emptyset_2) + \sin(\emptyset_1)\sin(\emptyset_2) \quad (\text{eq. 3.28})$$

Then

$$\gamma - \sin(\emptyset_1)\sin(\emptyset_2) = \cos(\theta_1)\cos(\theta_2) + \sin(\theta_1)\sin(\theta_2) = \cos(\theta_1 - \theta_2) \\ \cos(\emptyset_1)\cos(\emptyset_2) \quad (\text{eq. 3.29})$$

and therefore

$$\textcircled{30} = \theta_2 = \cos^{-1}\left(\frac{\cos(\alpha) - \sin(\emptyset_1)\sin(\emptyset_2)}{\cos(\emptyset_1)\cos(\emptyset_2)}\right) \quad (\text{eq. 3.30})$$

thus

$$f_{\alpha}(\alpha) = \int_{P_1} f_1(\theta_1, \emptyset_1) \int_{P_2} f_2(\textcircled{30}, \emptyset_2) d\emptyset_2 d\theta_1 d\emptyset_1 \quad (\text{eq 3.31})$$

The expected value is therefore

$$E(\alpha) = \int_{\text{lower bound of } \alpha}^{\text{upper bound of } \alpha} f_{\alpha}(\alpha) d\alpha \quad (\text{eq 3.32})$$

As was the case with the other integrals derived above, this is also very satisfying, but difficult to evaluate in closed form.

#### H. ANALYSIS OF THE TWO VECTOR METHOD IN TERMS OF CONTINUOUS PROBABILISTIC VECTORS

The purpose of the above derivations of the sum, difference, crossproduct, and angle between two pixels (i.e., sets of directions) is to develop the tools necessary to analyze the Two Vector Method in probabilistic terms. The Two Vector Method is the mathematical basis for ReAtMent and has been derived<sup>13</sup> for the simple case of discrete vectors. The derivation for the probabilistic case very closely parallels this.

Using the same notation, consider that  $\hat{L}, \hat{M}, \hat{P}$ , and  $\hat{Q}$  are given in the form of probabilistic vectors. The PAR is calculated by equation 2.7 using the technique described for taking the difference and crossproduct of probabilistic vectors.

Next, the measured probabilistic vectors,  $\hat{L}, \hat{M}, \hat{P}$ , and  $\hat{Q}$ , are decomposed into components parallel and perpendicular to the PAR. Since only the perpendicular components are of interest, the most straightforward method of calculating them is to use a double cross-product as indicated in equation 3.33 .

$$V = (\text{PAR} \times V) \times \text{PAR} \quad (\text{eq. 3.33})$$

where V can represent any of the vectors L,M,P, or Q. The major reason for using this procedure rather than the one suggested by 13. See derivation in section F of chapter I.

equations 2.9, 2.10, and 2.11 is that the scalar  $s$  in equation 2.9 becomes a random variable with a conditional probability distribution. This can provide major unnecessary complications in attempting to compute the proper probability distribution for the respective perpendicular components. In contrast, the proper probability densities are computed directly via equation 3.33.

Using equation 3.31 the probability density of the AR can be computed. However, it must be noted that this is a conditional probability distribution which depends on the member of the PAR selected. Thus at this point, it is more reasonable to define the probabilistic matrix directly as having the parameters of PAR and AR and a probability density of  $f_{\text{PAR},\text{AR}}$ . The elements of the matrix are as defined by equation 2.14 and the probability density is defined by

$$f_{\text{PAR},\text{AR}} = f_{\text{PAR}}(\text{PAR})(f_{\alpha}(\alpha) + f_{\beta}(\beta))/2 \quad (\text{eq. 3.34})$$

where  $f_{\text{PAR}}$  is the density of the PAR member selected,  $f_{\alpha}(\alpha)$  and  $f_{\beta}(\beta)$  are the probability densities of  $\alpha$ , and  $\beta$  respectively as calculated using equation 3.31 where  $\alpha$  is the angle between the components perpendicular to the PAR of one physical vector (e.g. the angle between the perpendicular components of  $\hat{L}$  and  $\hat{M}$ ) and  $\beta$  is the corresponding angle between the components perpendicular to the PAR of the other physical vector.

The process described above for calculating the probabilistic attitude matrix, which results from the use of probabilistic vectors in the Two Vector Method, is a straightforward extension of the analysis of the Two Vector Method using the tools developed in this chapter. While the analysis as given is correct and theoretically quite



satisfying, the notations one is forced to use to express the analysis in terms of continuous functions tend to obscure the overall chain of thought. Furthermore, the integrals which must be evaluated during the course of the analysis are at best quite difficult (although guaranteed possible by their physical realizability) to express in closed form. This complicates the analysis of even the most simple case to the point where it is impractical to perform.

Fortunately, in the real life applications of the analysis given above, the physical vectors are measured with sensors whose outputs are reported in terms of discrete probabilistic vectors (i.e. collections of pixels with discrete assigned probabilities). This leads to a computerized approach to the analysis which is based on the above but is considerably less complicated.

#### I. ANALYSIS OF THE TWO VECTOR METHOD IN TERMS OF DISCRETE PROBABILISTIC VECTORS.

In chapter II the concept of expressing the output of a directional sensor in terms of discrete probabilistic vectors was introduced. This allows replacement of the continuous distributions described above by finite sets of vectors represented by point probability masses on the  $\theta, \emptyset$  plane.

Paralleling the analysis above, the difference vectors between measurements of the same physical vector are formed by computing the normalized (i.e. unit length) vector difference between each possible pair of members of the two measurements. Using the notation introduced in the derivation of the Two Vector Method, if L consisted of  $\{L_1, L_2, \text{ and } L_3\}$  and M consisted of  $\{M_1, M_2, \text{ and } M_3\}$  then the vector

pairs  $L_i - M_j$  would be formed and normalized where the indices  $i$  and  $j$  run from 1 to 3. The probability assigned to the difference vector  $L_i - M_j$  would be the product of the probability associated with  $L_i$  and that associated with  $M_j$  based on the independent selection of one from  $L$  and one from  $M$ . The same process is performed for the other difference vector  $P - Q$ .

The point probability masses which result from the formation of these difference vectors can be grouped in partitions of the  $\theta, \emptyset$  plane with a solid angular subtense similar to that represented by each original member of the measured vector set (e.g.  $L_1$ ). These partitions of the  $\theta, \emptyset$  plane can now be represented by discrete members of the probabilistic vector difference and their assigned probabilities be the sum of the point probability masses in the respective regions. This allows a possible reduction in the number of members of the difference vector from the product of the number of members in the two vectors being differenced.

The discrete difference vectors having been computed, equation 2.7 can be used to form the PAR. Again, the crossproduct operation is performed on each possible pair of the members of the two difference vectors used and the point probability mass assigned to the resulting crossproduct is the product of the probabilities assigned to the respective members chosen. The area covered by the crossproduct in the  $\theta, \emptyset$  plane is again partitioned into regions whose solid angular subtense is similar to that of the original members of the measured physical vector.

Now the conditional probability distribution of the AR must be

computed. Choosing each member of the PAR in turn, use equation 2.12 to calculate the AR for each possible pair of the members of L and M and for each possible pair of the members of P and Q (substituting P for L and Q for M in equation 2.12), assigning to each result the product of the probabilities of the respective members of the PAR and measured vectors used to compute it. Partition the range of the values of the AR into lengths of similar angular subtense as that of the measured members of the physical vectors.

Note the overall result. Each member of the PAR has a number of possible values of AR associated with it, and thus each combination of a member of the PAR and a value of the AR has a probability associated with the combination. If this combination of PAR and AR is expressed as a matrix (per equation 2.14) and associated with a probability, then by definition a member of a probabilistic matrix results. The set of all such members is the probabilistic attitude matrix which represents the output of the ReAtMent system.

While this derivation follows the course laid by the continuous analysis of the section above, there exists some additional information which can be used to increase the accuracy of the probabilistic attitude matrix. This arises from the examination of the case where the measured vectors consist of a single member (corresponding to the derivation of the Two Vector Method in chapter II). By virtue of the fact that the difference in the two observations of the direction to the object (i.e. a physical vector) is due to the equivalent of a physical rotation of the observer by AR about the PAR, the calculation of the value of the AR must be the same (within the accuracy of the

pixel size) for equation 2.12, whichever physical vector is chosen.

Thus when calculating the value of AR, using selected members of L and M, roughly the same value should be obtained using the selected members of P and Q in equation 2.12. If this is not the case, then the computed PAR and AR can not transform the selected members of both L into M and P into Q. Therefore, the probability assigned to this combination of PAR and AR should be zero and not that according to the discussion above.

Furthermore, the PAR used with selected members of the measured vectors must be roughly perpendicular to the respective difference vectors. Again, if this is not the case, then the combination of PAR,AR is not capable of transforming the selected members of both L into M and P into Q, and should be assigned a probability of zero.

This additional information can lead to significant computational savings as many combinations of selected members of the measured vectors will not be valid. That is, that no possible physical reorientation of the observer could result in those particular members of L and M being transformed into those particular members of P and Q. This means that the calculation of the members of the PAR by the exhaustive technique given in the beginning of this section is not optimal as it may contain many members with an actual probability of zero, but a finite assigned probability. Even more significant than the computation of potentially extraneous members of the PAR, is the refinement of the computation afforded by the check on the AR. This means, however, that the integral of the probabilities over the remaining members of the probabilistic matrix may not be 1.0. Since

the actual PAR,AR combination is guaranteed to be among the remaining members, the appropriate procedure would be to normalize the probabilities associated with the remaining members to arrive at the correct distribution.

Thus, the most efficient approach is to select all possible sets of one member from each measured vector, compute the PAR, check the two values computed for the AR for consistency, and assign the product of the probabilities of each member used to the combination of PAR,AR. After this, normalize the probabilities assigned to the surviving combinations of PAR,AR.

#### J. COMPLETING THE PROBLEM: USING THE COMPUTED PROBABILISTIC MATRIX

Once the probabilistic attitude matrix is available, it must be used to transform an observed probabilistic vector into the other coordinate system. The procedure is straightforward. Each member of the probabilistic matrix is used in turn on each member of the observed probabilistic vector, and the result assigned the product of the probabilities associated with the respective matrix and vector used. This results in a probabilistic vector whose density represents the probability of the direction of the observed object being correctly expressed by the corresponding member of that vector.

In the case of discrete probabilistic vectors and matrices, the probability of the respective results can be mapped into the  $\theta, \phi$  plane by point masses. The area covered can be partitioned into regions whose solid angular subtense is comparable to that of the observed vector. This results in a compact (minimum number of members) probabilistic vector which predicts the normalized contrast of the

object as seen in the other coordinate system.

## CHAPTER IV: STATE OF THE ART IN ATTITUDE MEASUREMENT

Before proceeding to the analysis of an actual ReAtMent system, it is necessary to understand the current state of the art in attitude measurement technology and how it relates to the basic concepts introduced in chapter I.

### A. MECHANICAL ATTITUDE MEASUREMENT

This is the earliest form of attitude measurement. It allows a direct measurement of the relative orientation of one object (usually gimbal mounted) with respect to its reference orientation. Consider an object mounted on a shaft so that it is free to rotate about that shaft, or more conveniently, consider that the shaft is part of the object and that the shaft is free to rotate in a mounting bracket. The exact orientation of the object can be specified by the angle by which the shaft has rotated from some reference position.

In this case, the PAR is the axis of the shaft and the AR is the angle of the shaft rotation. The attitude matrix  $[A]$  which transforms any directional measurement made by the object in its current orientation to the equivalent expression in its reference orientation with respect to its mounting frame can be found by equation 2.14.

This gives only one degree of freedom to the orientation of the object. To give the object one more degree of freedom, attach a shaft to the first mounting bracket so that is perpendicular to the shaft attached to the object, and then mount this "second object" (the object with its mounting frame) in a second mounting bracket similar to the first (but obviously larger). The same equation, 2.14, can be used to yield another attitude matrix which transforms any directional

measurement made in the current orientation of the "second object" into the equivalent expression in its reference orientation with respect to its mounting frame.

Now attach a shaft to this "third object" (the mounting bracket holding the mounting bracket which holds the object) and mount this in a similar mounting frame. The same equation, 2.14, can be used to generate an attitude matrix  $[A_3]$  which transforms any directional measurement made by the third object in its current orientation into the equivalent expression in its reference orientation with respect to its mounting frame.

The original object is now free to assume any orientation with respect to the mounting frame holding the third object. When the original object makes a directional measurement, the information is first transformed into the coordinate system of the second object by  $[A_1]$ , then into the coordinate system of the third object by  $[A_2]$ , and finally into the coordinate system of the mounting bracket holding the third object by  $[A_3]$ . This last mentioned coordinate system is usually the one shared by the platform carrying the original object, and consequently the coordinate system the information is desired in.

The three successive transformations can be mathematically combined into a single attitude matrix  $[A]$  by

$$[A] = [A_3][A_2][A_1] \quad (\text{eq. 4.1})$$

If the shafts are mutually perpendicular and their center lines intersect at a common point (such mounting gimbals are usually designed this way) which is the origin of the coordinate system of the original



object, then these shafts define the axis of a convenient coordinate system when the original object is in its reference position (i.e. aligned to share this coordinate system). In this convenient, often used special case, each of the attitude matrices,  $[A_1]$ ,  $[A_2]$ , and  $[A_3]$  become simple matrices which are functions of one parameter each commonly referred to as the Euler angles. A great deal of information is contained in the literature concerning Euler angles, principally in texts on mechanics. There are currently several variations of the Euler angles in common use. They differ by the order of rotation about the axes (one does X first, the other Y, etc.) and the sense of the positive rotation (i.e. one says counterclockwise, the other clockwise). These are all special cases of equation 4.1. In general, however, equation 4.1 can be used even if the respective axes are not perpendicular as is occasionally necessary in certain applications.

This technique of mounting the original object in a series of gimbals, measuring the shaft rotation angles mechanically, and then using equation 4.1 to generate the attitude matrix, is called mechanical attitude measurement. This technique forms a critical part of most ReAtMent systems as the directional sensors typically used have small fields of view and must be gimbal mounted in order to be pointed roughly in the direction of the physical vector to be measured. Consequently, mechanical attitude measurement is often an integral part of a directional measurement system.

The most common form of shaft angle measurement device is a simple pointer attached to the shaft with the angle read out manually

via a dial. This is usually accurate to about 1 mil ( $1/6400$  of a full circle). The more accurate mechanisms make use of various gearing arrangements to make a pointer rotate through a larger angle than the shaft, thus allowing smaller rotations to be measured (e.g., a theodolite is usually good to about 0.001 mill and uses vernier scales). Electrical readout devices range from simple rotary switches (good to roughly 5 degrees) to sophisticated optical encoders (10 to 12 bit parallel output direct reading) or incremental encoders (good to about 0.01 mill and require counting from a reference). These devices are undergoing continual improvement and the reader is urged to contact reputable vendors directly to obtain current information.

The direct extension of mechanical attitude measurement to ReAtMent is not possible since mechanical attitude measurement relies on the original object rotating successively about known axes. Objects in free space (i.e. not gimbal mounted) generally do not have this characteristic movement, thus mechanical attitude measurement can be used as a critical subsystem for a directional measurement device, but is not capable of forming a ReAtMent system by itself.

#### B. INERTIAL ATTITUDE MEASUREMENT

This is an attempt to extend mechanical technology to ReAtMent by gimbal mounting a "gizmo", which is supposed to remain aligned with some inertial coordinate system, as the platform whose attitude is to be measured moves. The relative orientation of this gimbal mounted "gizmo" can then be measured by mechanical means.

If this "gizmo" does, indeed, remain aligned with some inertial system then the attitude of each of two separated platforms can

be measured relative to this standard inertial coordinate system and the relative orientation of the two platforms determined (i.e. a ReAtMent performed).

The problem is that no such "gizmo" exists which will remain perfectly aligned with an inertial coordinate system. A very good approximation to remaining aligned with a vector in an inertial coordinate system is possible using the spin axis of a gyroscope. As a minimum of two physical vectors are necessary to provide enough information to perform an attitude measurement, at least two gimbal mounted gyroscopes are necessary in an inertial attitude measurement system. These two gyroscopes are usually mounted with their axes perpendicular to maximize the sensitivity of the measurement, however, numerous schemes have been tried over the years and reported in the literature.

The problem with gyroscopes is drift. Over a period of time, the axis of the gyroscope will start to precess (i.e. nutate or wobble) due to the effects of acceleration not parallel to the spin axis and slight imbalances in the mass of the gyro. This is inherent in the mechanical design of the gyroscope and can not be designed out. However, design efforts have succeeded in minimizing these effects using laser machining and air bearings. Typical gyroscopes in common use today have drift rates of between 0.1 to 1 milliradian per hour.

Another device used is the laser gyro. The basic operating principle is that the velocity of energy propagation (i.e. electromagnetic waves) is effectively independent of the velocity of the medium it is propagating in (at least for non-relativistic velocities). Thus, when two coherent laser beams are propagated along different

paths and both illuminate the same detector, the phase difference due to the different path lengths will result in an interference pattern on the detector. If the device is stationary, the intensity of the light seen by the detector will be constant. When the device moves, the rotation about the axis perpendicular to the path will move the detector closer to one of the incoming beam phase fronts and further from the other. The phase change, due to one beam traveling a longer inertial distance than the other, results in the equivalent of interference fringes being seen at the detector. By counting these fringes the amount, and hence the rate of rotation, can be measured. Using three laser gyros the "equivalent" of the Euler angles can be measured. Again, the problem is drift of the electrical and mechanical parameters of the laser gyro.

In some systems, small changes or torques are measured and integrated to give the current orientation of the object. One example of this is the fluidic rate sensor used on some aircraft. This instrument senses the inertial deflection of a jet of air to sense the rotation about the axes perpendicular to the axis of the air jet.<sup>14</sup> The jet of air cools thermal sensors and the deflection of the air jet is sensed by the change in temperature between sensors on opposite sides of the stream. The present application is primarily for the autopilot rather than for attitude measurement. If used for an inertial attitude measurement, two jets would be required as each measures the equivalent of only two of the Euler angles.

14. Garner, D. "The Electro-fluidic Autopilot", Sport Aviation, August 1980, Volume 29, No. 8, pg. 16-24

In essence, inertial attitude measurement is sufficiently accurate for many applications, but it suffers from drift and the need to be periodically updated. Again, the devices are being constantly improved and the reader is urged to contact reputable vendors directly to obtain current information.

The "gizmo" that is actually needed is a physical vector measurement device. Ideally, the axis of a spinning gyroscope represents a physical vector in inertial space. Thus it can readily be seen from the discussion in the chapter II that the inertial attitude measurement systems require at least two gyros. The mathematics evolved over the years to obtain the attitude of the system from the measurements of the gyroscope angles (or equivalently the integrals of their rates of change) are thus not inconsistent with the Two Vector Method. The advantage to be gained from applying the Two Vector Method directly is elimination of many of the approximations resorted to in the more conventional algorithms applied to inertial systems.

However, inertial attitude measurement systems are not true ReAtMent systems as such because they only determine the relative orientation of a single object to a "reference inertial" coordinate system, and not the relative orientation of two separated objects directly.

### C. GRAVITIMETRIC ATTITUDE MEASUREMENT

The basis for this type of attitude measurement is a measurement of a single physical vector, the local gradient of the potential energy field. Given quiescent conditions (i.e. no net acceleration), and limiting the discussion to a small region near the surface of the

earth, the gravitimetric field is essentially uniform. Thus the surfaces of equipotential are effectively flat (i.e. level). This means that the gradient points downward and the direction "down" defines a physical vector. However, since only one physical vector is measured, gravitimetric attitude measurement is only a partial attitude measurement technique.

The most common example of this type of attitude measurement is performed via a spirit level. For example, when a surveyor's transit is set up, it is first leveled by adjusting the legs of the tripod until a bubble is in the center of the bubble level. This establishes the azimuthal plane of the transit as being horizontal, and thus the elevation plane as being vertical. However, when two such transits are set up, their coordinate systems will not be identical. A difference in azimuth will exist. The various procedures for computing this azimuth difference (and hence correction factor) amount to the measurement of another physical vector. Gravitimetric attitude measurement has thus performed only a partial attitude measurement.

The major problem with gravitimetric attitude measurement is that it can only be used accurately where the gravitimetric field is uniform and under static conditions. Therefore, gravitimetric attitude measurement is unsuitable for applications aboard a ship, plane or spacecraft. Since it only deals with the orientation of the object with respect to a reference rather than another system, it is not a true ReAtMent technique.

#### D. ELECTROSTATIC ATTITUDE MEASUREMENT

This is a partial attitude measurement technique used in much

the same fashion as gravimetric attitude measurement. The physical vector measured is the electric field near the surface of the earth. This electric field has a very nearly vertical gradient. The standard sensor consists of a source of radioactive ions and collection electrodes. The stream of ions drift along the electric field lines and are collected on electrodes. The charge induced on the respective electrodes indicates the direction of the ion stream and therefore the direction of the electric field.

The principal use of this device is as a very low cost, light weight, vertical reference of the autopilot used on remotely piloted vehicles. Obviously, any nearby object (power lines, metal structures, etc.) can disrupt the electric field, thus the device has very limited use.

#### E. MAGNETIC ATTITUDE MEASUREMENT

This is another partial attitude measurement technique in common use. The physical vector measured is the gradient of the earth's magnetic field. Usually, only the horizontal component of the field is measured. This is the direction of "magnetic north" usually measured by a compass. Over a limited area and away from metallic objects, this direction qualifies as a physical vector.

Magnetic and gravimetric partial attitude measurement techniques are usually combined to provide a total attitude measurement capability. In applications where the primary purpose of the attitude measurement system is to align the device with the "reference" coordinate system on the surface of the earth under static conditions, this combination works very well. The surveyor's transit is an

excellent example. The bubble level measures the physical vector "down" and the compass measures the physical vector "the horizontal component of the magnetic field gradient". When two such transits, each measuring the same two physical vectors, are set up so that the respective vectors appear to have the expected respective descriptions, then the two transits can be said to be aligned with the "reference" coordinate system and thus aligned with each other.

It should be noted that the use of the horizontal component of the gradient of the magnetic field is sufficient, if the transit is first leveled. If, however, the two transits are set up in some arbitrary fashion, then all three components of the gradient of the magnetic field must be measured. This can be done via a vector magnetometer. Thus, magnetic and gravimetric attitude measurement techniques can be combined under appropriate conditions to yield a true ReAtMent system, where the relative orientation of two objects (e.g., the transits in the example above) can be determined.

#### F. PHOTOGRAMMETRIC ATTITUDE MEASUREMENT

This technique accomplishes ReAtMent in a very cumbersome way by applying the rules of perspective geometry to objects of known size and distance in the field-of-view of the sensor. Remote attitude measurement is possible in the sense that the relative orientation of the viewed object and the sensor can be determined. More often, however, the orientation of the viewing device is computed relative to salient features of the scene, such as the horizon or the edge of the moon. This technique arose mainly from photo reconnaissance applications where it is necessary to establish the orientation of the



viewing system so that observed objects can be located. Variations on this idea which have sensors look at the edge of the moon and the horizon of the earth have been used for space applications. The use of lines-of-sight to various objects in the scene for the computations involved is the fundamental reason why this technique works. The results of the dissertation research are likely to find direct application here. By selecting two lines of sight to features in the scene sufficiently distant from the sensor (this qualifies them as physical vectors) and measuring their apparent directions by the position of these features on the image of the scene, it is possible to use the Two Vector Method to compute the attitude of the viewing device directly (assuming that the locations of the scene features and the sensor are known in some reference coordinate system). This can result in a considerable savings in both time and computational effort over present techniques.

#### G. ELECTROMAGNETIC ATTITUDE MEASUREMENT

Remote attitude measurement is accomplished by direction sensing techniques developed for radio frequencies (e.g., time of arrival, interferometric phase measurements between receiving antennas, and directional antenna rotation). This technique is not in common use due to the relatively poor directional accuracy possible (primarily due to diffraction and multipath effects at the long wavelengths used). As the frequency is increased into the millimeter wave region, ReAtMent systems become feasible. However, due to the relative infancy of this technology, and the existence of practical ReAtMent systems using electrooptical techniques, it appears unlikely that this technique

will be used except for very special applications.

#### H. SONAR ATTITUDE MEASUREMENT

Given the present state-of-the-art in acoustic technology, it appears feasible to construct a ReAtMent system using sound waves instead of electromagnetic waves. Surface acoustic waves with submillimeter wavelengths have been demonstrated. The ability to form images using sound waves (e.g., some of the latest infrasound medical body scanners) gives rise to the possibility of using the same techniques as those in electromagnetic, photogrammetric, or electrooptical attitude measurement.

#### I. ELECTROOPTICAL ATTITUDE MEASUREMENT

The basis of electrooptical attitude measurement is the measurement of the direction of the line-of-sight to a distant object which serves as a physical vector. The use of two such measurements allows the Two Vector Method to be used directly.

The major difference between electrooptical attitude measurement and photogrammetric attitude measurement is that in the latter, the lines of sight used are selected from an image while electrooptical attitude measurement systems need not necessarily form an image. For example, imagine a sensor viewing two pulsing lights in the distance. A photogrammetric approach would select the pixels representing those lights on the basis of their temporal variation as being the desired salient features of the scene and report their directions accordingly. An electrooptical approach would detect and measure the directions of the two lights by pointing a device (e.g., a quadrant detector) directly at the flashing light without necessarily ever forming an

image of the scene.

In addition to the obvious physical vector of the line-of-sight between two objects, it is possible to use the direction of polarization of a beam of light emitted by the viewed object as one of the physical vectors. It is possible to construct a ReAtMent system using a single cooperative viewed object (possibly the other station ) which emits a polarized beam of light toward the viewer. This approach was used for the PAM <sup>15</sup>.

Overall, electrooptical attitude measurement appears to be the best for ReAtMent applications because the physical vectors used are not affected by motion of the platform, and very high directional accuracy is obtainable due to the short wavelengths used.

#### J. SUMMARY OF THE MAJOR FORMS OF ATTITUDE MEASUREMENT

The fundamental form of attitude measurement is mechanical because the relative orientation of the sensor to the platform (whose attitude is being measured) is most often measured by this technique.

The techniques which rely on the measurement of a single physical vector are classified as partial attitude measurement techniques because they are incapable of making a true attitude measurement by themselves as at least two physical vectors must be measured. Two such techniques, (e.g. gravimetric and magnetic) must be combined to yield a true attitude measurement. Often, as in the example cited

15. The Position and Attitude Monitor (PAM): an electrooptical state-of-the-art ReAtMent system .

above of the surveyor's theodolites, the function of the ReAtMent system is merely to indicate when the platform is aligned in some preferred orientation, rather than to actually measure the relative orientation between the coordinate systems of two objects.

Inertial attitude measurement tries hard but doesn't quite measure up to the definition of ReAtMent, mainly because it employs an intermediate "inertial reference" frame which may or may not be common to the two stations whose relative attitude is being measured. As a quick example of this, consider a platform on the earth and one on the moon at the time of their initialization. Let both platforms be launched into earth orbit and approach each other. Because of the relative motion of the earth and the moon, the inertial reference frame of the earth platform and the moon platform would be different. Therefore, inertial reference systems carried by the platforms would not be able to determine the relative orientation of one platform to the other.

Electromagnetic, electrooptical, sonar, and photogrammetric attitude measurement essentially are similar as each uses the direction of a "line-of-sight" as the physical vectors measured. The differences stem mainly from the wavelength of the energy used and the operational environments for which they are best suited. At present, there are no known programs involving sonar for attitude measurement, however, it would appear that this technology would be a reasonable choice for deep sea underwater applications.

Based on the resolution available and the demonstrated real time capability, electrooptical attitude measurement is the best choice for systems designed to operate in the earth's atmosphere or space.

TABLE 4.1 State of the Art Accuracy and Limiting Factors of Attitude Measurement Techniques

Technology	Type	Limiting Factor	State of the Art Accuracy
Mechanical	Direct	Resolution and Speed	0.001 microradians
Inertial	Indirect	Drift	8 milliradians with 1 milliradian/hour drift
Gravitimetric	Partial	Acceleration	0.001 microradians
Electrostatic	Partial	Local field Perturbations	10 microradians
Magnetic	Partial	Local field Perturbations	10 microradians
Photogrammetric	Remote	Optical Resolution	1 microradian
Electromagnetic	Remote	Directional Resolution	0.5 milliradians
Sonar	Remote	Directional Resolution	10 microradians (estimated from imaging system resolution)
Electrooptical	Remote	Optical Resolution	0 .1 milliradian (PAM,1978) < 1 microradian achievable

#### K. CONSIDERATIONS FOR ReAtMent APPLICATIONS

The need for ReAtMent arises when data from two separated systems must be combined to solve a three dimensional geometry problem. The amount of separation can be great, as in the case of an aircraft and a ground station, or small, as in the case of two systems mounted on the same platform.

The choice of what physical vectors to measure is dependent on the accuracy required and the operational environment of the

ReAtMent system. In the case where the two systems are merely to be aligned with each other and are relatively close to the surface of the earth under static conditions, the choices of the physical vectors "down" and "north" are reasonable. These can be easily measured by the combination of gravimetric and magnetic techniques.

If one system must (for operational reasons) be completely self-contained, then inertial technology (although it is not a ReAtMent system in the strict sense) is the obvious choice. If possible, a ReAtMent system should be used to initially align and periodically update the inertial systems. However, drift problems pose an inherent limitation to the accuracy obtainable.

Under conditions where it is possible to measure the line of sight to two different distant objects or the stations are inter-visible, electrooptical technology with the Two Vector Method is indicated.

The practical applications of ReAtMent call for something to be pointed as a result of the attitude measurement. In such pointing applications, mechanical attitude measurement is the obvious choice. The output of the ReAtMent system must be considered along with the device being pointed as a single system. The nature of the composite system is to close the tracking loop via the observational device - ReAtMent system - pointed device rather than by having the pointed device acquire and track the object itself. Thus, as in chapter II, the analysis of the ReAtMent system must be carried to the point where the probability of the object being in the FOV of the pointed device is calculated.

## CHAPTER V: THE GENERALIZED ReAtMent SYSTEM

### A. OVERVIEW

In order to analyze the generalized ReAtMent system, it is necessary to specify each of the major components in sufficient detail to fully characterize the function performed by that component. This form of functional description allows whatever specific hardware implementation selected for each given component to have its parameters substituted directly into the generalized analysis developed below.

We begin this analysis by considering the generalized ReAtMent problem as described in chapter I. An observation device on one platform detects an object and wishes to have another device on the other platform pointed so as to view the object.

The first step is to measure the relative position of one of the platforms in the other's local coordinate system. The next step is to measure the direction and range (or equivalently the relative position) of the object. The next step is to measure the relative attitude between the two platforms expressed in the form of a matrix. The last step is to use the computed attitude matrix to transform the direction of the object (computed from the three dimensional triangle) into the coordinate system of the device to be pointed.

There are several factors which combine to determine the mix of technologies selected to implement a solution to the ReAtMent problem in any given situation: 1. The specific geometrical problem to be solved (i.e. a single three dimensional triangle or a more complicated figure composed of several three dimensional triangles); 2. The precision

necessary to solve the figure (i.e. provide closure of the endpoints of the various sides of the triangles to within the volume of the object defining those endpoints) and thus perform the mission in a practical sense; 3. The environment in which the systems must perform (i.e. in space, airborne, underwater, on the ground, or any combination of these); 4. The size, configuration, and weight restrictions imposed by the platforms and or overall mission; and 5. The physical vectors which can be measured subject to the above constraints.

#### B. BLOCK DIAGRAM AND COMPONENT DESCRIPTIONS OF THE GENERALIZED ReAtMent SYSTEM

The block diagram of the generalized ReAtMent system is shown below in figure 5.1.

PLATFORM 1

Position Measurement Means *
Physical Vector #1 Measurement Means
Physical Vector #2 Measurement Means *
Computational Means
Device to be pointed
Communications Means

PLATFORM 2

Position Measurement Means *
Physical Vector #1 Measurement Means
Physical Vector #2 Measurement Means *
Computational Means
Object Direction Measurement Means
Communications Means

\* indicates item may not be present on both systems or may reside at a separate location and be tied in via the communication means

Figure 5.1 Generalized ReAtMent System Block Diagram

In order to keep this analysis as general as possible and yet provide a reasonable guide to essential subsystem characteristics, each of the subsystems shown in figure 5.1 above will be discussed in functional detail.



## 1. DEVICE TO BE POINTED

The device to be pointed is selected by the application. Based on the expected range to the object and the expected size of the object, the device will usually be designed with a beamwidth covering roughly twice the size of the object at the minimum expected range. This will insure that if the line defining the center of the beam is on the object, that the object will be correctly covered by the beam. Thus, the ReAtMent system must be able to define the direction to the object to within better than one half of the beamwidth (or FOV) of the object to be pointed.

In general, the device to be pointed will not be able to acquire and track the object at which it is to be pointed. If this were the case then the ReAtMent system would become superfluous. The object is detected and tracked by one platform and commands are relayed to the other platform carrying the device to be pointed.

In the generic sense, the apparatus used to point the device itself must be considered as a part of the device. This apparatus is given a command to point in a specified direction in its own local coordinate system. Therefore, the output of the ReAtMent system must be in the form of this command.

## 2. POSITION MEASUREMENT MEANS

The purpose of this component is to determine the relative position of one platform to the other in the local coordinate system of one of the platforms. This can take many forms. If the two platforms are intervisible and a device onboard one is able to determine the range and direction to the other platform, then this

device serves as the position measurement means. If the two platforms are not intervisible, then it is necessary to use some intermediate coordinate system to locate the position of each platform. This introduces a complication, as now the attitude of at least one of the platforms must be known relative to the intermediate coordinate system. As an example of this, consider two aircraft on opposite sides of a mountain range and let the first aircraft be flying level on a known heading. At a given instant of time, the locations of both aircraft are measured in terms of latitude, longitude, and height above sea level. It is possible to solve for the length and direction of the line between the two aircraft in terms of the ground coordinate system. Since one aircraft is flying level, the slope of the line in ground coordinates and aircraft coordinates is the same. Since the aircraft is flying on a known azimuth, this can be appropriately added to the azimuth of the line between the aircraft expressed in ground coordinates, to give the azimuth of the line in aircraft coordinates. The length of the line between the aircraft is independent of the coordinate system used. Thus the relative position of the second aircraft has been determined in the coordinate system of the first aircraft.

To continue the example just a bit further, consider that the level aircraft has used onboard radar to locate the relative position of an unknown aircraft. The simple triangle in three dimensions between the two aircraft and the unknown aircraft can be solved for the length and direction of the line from the second aircraft to the unknown aircraft. Thinking back to the discussion on partitioning

objects into volume elements so that the fundamental assumption applies in order to express the problem in terms of physical geometry, the three dimensional triangle formed by the three aircraft represents an ensemble of triangles. This requires that the endpoints of each line be located within the volume of the respective aircraft, and establishes a fundamental requirement for the accuracy of the means used to locate each of the three aircraft. If the radar were only able to locate the unknown aircraft to within a volume of space equal to  $1 \text{ km}^3$ , then as far as the physical geometry problem is concerned that unknown aircraft has a volume of  $1 \text{ km}^3$ , and the best possible ReAtMent system would only be able to point the device (e.g., a narrow beamwidth communications link) to somewhere within that  $1 \text{ km}^3$  volume.

Leaving the example, it can be seen that the position measurement means shown in figure 5.1 can be either on the respective platforms or at some separate location. The accuracy of these position measurement means determines the overall accuracy of the triangle in three dimensions which is solved, and hence the ability to perform the overall mission. For this reason, the position measurement means are usually specified without regard to the ReAtMent system used to determine the relative attitude between the two platforms.

### 3. PHYSICAL VECTOR MEASUREMENT MEANS

The key to specifying the physical vector measurement means is in first very carefully selecting the physical vectors to be measured and insuring that the parameters selected to be measured actually represent physical vectors. This must be done with an appreciation for

the operating environment in which the ReAtMent system must function. The physical vectors selected must be measurable from both platforms throughout their allowed range of attitudes and motions. Thus, while the physical vectors representing the gradient of the gravimetric and magnetic fields may be reasonable choices for a fixed ground based application, they would not necessarily be good choices for shipboard use. Similarly, the use of the directions to two convenient stars may be excellent choices for a spaceborne application, they may not be good choices for a ground based system which must operate during the day.

The other consideration is how accurately the selected physical vectors must be measured. For problems involving relatively short ranges (e.g., an anti-aircraft weapon and its associated radar), the physical geometry problem may indicate that pointing accuracies on the order of (object size divided by range) radians may be sufficient, say 5 milliradians for purposes of discussion, then the physical vectors need only be measured to roughly 10 times better accuracy (0.5 milliradians) so as not to limit the accuracy of the overall system by ReAtMent system performance. This rule-of-thumb is based on the author's experience and should be investigated by a parametric study of the particular application in which the performance of all elements of the overall system are taken into account.

Quite often the physical vector measurement means will involve mechanical attitude measurement to report the attitude of the measuring sensor tracking the direction of the physical vector. This facet of the problem must also be addressed by considering the output

of the directional sensor to be the final direction reported by the measurement system to the computational means.

#### 4. COMPUTATIONAL MEANS:

For all practical purposes, the author's experience has indicated that the computational accuracy requirements are easily met by the hardware readily available today. In general, quantities will not be measured to much more than 12 or 16 bit precision. Thus the use of a machine with a 32 bit real word length (1 bit sign, 24 bit mantissa, 1 bit exponent sign and 6 bit exponent) is quite adequate for ReAtMent computations.

The speed requirement for performing the necessary computations, however, may be quite another matter. To illustrate the amount of computations required, follow the analysis of the Two Vector Method given in chapter II. The formation of the two difference vectors, takes 6 additions. The formation of the crossproduct of these difference vectors takes 6 multiplications and 3 additions. Normalizing this result to obtain the PAR requires 3 multiplications, 2 additions, 1 square root, and 3 divisions. Computing  $s$  takes 3 multiplications and 2 additions. Computing  $G$  takes 3 multiplications and 3 additions. Computing  $H$  also takes 3 multiplications and 3 additions. Computing  $G \cdot H$  takes 3 multiplications and 2 additions. Computing  $|G \times H|$  takes 9 multiplications, 5 additions and 1 square root. Computing the AR with these results takes 1 division and 1 arctangent. Somewhat better accuracy can be obtained by normalizing the two difference vectors,  $G$ , and  $H$  immediately after they are calculated, adding a total of 12 multiplications, 8 additions, 4 square roots, and 12

divisions to the procedure. Thus the total number of operations just to compute the Two Vector Method is 42 multiplications, 34 additions, 6 square roots, 16 divisions, and 1 arctangent.

To calculate the attitude matrix, equation 2.14, given the PAR and AR, requires 1 division, 31 multiplications, 12 additions, 2 sines, and 1 cosine, assuming that the  $\sin(AR)$ ,  $\sin^2(AR/2)$ , and  $\cos^2(AR/2)$  terms are computed only once. This attitude matrix must now be used to operate on the vector describing the reported direction to the object which takes another 9 multiplications and 6 additions. Multiplying this unit vector by the range to the object from the sensor and subtracting the vector to the other platform results in another 3 multiplications and 3 additions. (This solves the 3 dimensional triangle in the coordinate system of the platform which detected the object.) Normalizing the result to give a vector command to the device to be pointed requires yet another 3 multiplications, 2 additions, 1 square root, and 3 divisions.

Thus to perform one full ReAtMent computation requires a grand total of 88 multiplications, 58 additions, 7 square roots, 19 divisions, 1 arctangent, 1 cosine and 2 sines. For any given computer system, the average time to perform each of these functions is usually specified. Thus it is possible to compute the total average time required to perform a ReAtMent calculation after all data has been fed into the computational means. The required update rate for pointing the device at the object determines the processing speed required by the computational means. Some consideration should also be given to the form of the data reported by the physical vector measurement means, the object

direction measurement means, and the position measurement means as well as the form of the command for the device to be pointed. Often these inputs and outputs are available in the form of two angles. Therefore, some conversion must take place to express these in unit vector form. The most logical place to do this is in the computer itself as leaving the data in the form of only two rather than three quantities would reduce the data rate required of the communications means.

Taking all of this into account, approximately 10 to 15 percent should be added to the minimum calculated time to allow for overhead in the programming. This discussion gives a rough idea of the computational effort involved in implementing a ReAtMent system for the case where the measured physical vectors are simple and discrete (i.e they consist of only one pixel). For the probabilistic case, as discussed above in section I of chapter III on analyzing the Two Vector Method in terms of probabilistic vectors, all combinations of the pixels of the 4 measurements of the two physical vectors would have to be used to compute the PAR and AR for each case (including the check for consistency between the two possible values of the AR), each valid result of this computation would then be used with all possible combinations of the pixels in the probabilistic vector representing the direction to the object would then be used to construct the probabilistic vector representing the computed direction to the object. This process obviously would involve a very considerable amount of calculation, but may be necessary in some cases for particular applications.

A highly efficient and compact program can be written for a dedicated computational means in a combination of hardware and firmware. This combination uses firmware to take advantage of the machine architecture to minimize the number of operations and hence the time required. For example, this might involve routing an incoming number directly from the input/output bus into one of the data inputs of the arithmetic logic unit (the part of the processor which actually performs the arithmetic functions) rather than first storing the data from the input/output bus in memory and then reading it from memory into the arithmetic logic unit. Dedicated input/output driver hardware might be used to perform the necessary code conversions between the data format used by the communication means and the format used by the computer. This form of programming produces the absolute maximum possible speed in performing the required computations, but requires both a dedicated computer and an extraordinary amount of programming effort.

The next best choice is to write the program entirely in assembly language using available firmware commands wherever possible. This also involves a great deal of programming effort, but can produce a very rapid computation. One step further along the same option is to use prewritten general purpose routines to perform the input/output functions and standard mathematical procedures (e.g., the square root). The main advantages to this use of assembly language is that proper structuring of the program can minimize the overhead associated with the use of subroutines and subscripted variables. This can save approximately 5 to 10 percent of the time and storage required if the



program were written in a high level language.

The use of a high level language, such as FORTRAN or ALGOL results in a considerable reduction in programming time and effort over the use of assembly language. The major reason for this is that the program can be written in modularized segments which can be individually tested and linked together by an executive routine. Also, special functions, such as sine, square root, and format conversion are built into the language.

Perhaps the easiest language to write the required programs in is BASIC. This language is an interpretive, interactive language with built in special functions which makes translating the program flowchart into code straightforward and relatively easy. Debugging is greatly facilitated by the interactive nature of the language. The price paid is in execution time. The program source code is "thought about anew, line by line by line by line ..." (after an overall symbol table has been developed) each time the program is executed. This results in a program written in BASIC running as much as several hundred times slower than if the program were written in ALGOL or FORTRAN, and as much as a few thousand times slower than if assembly language is used.

Thus it is apparent that the choice of the programming language used involves a tradeoff between the time required for performing the programming and executing the program. The question of using a dedicated processor, microcomputer, general purpose minicomputer, or large scale computer in a timeshare or batch mode is also a tradeoff between processing speed, cost, size, and weight constraints, and

availability. For example, consider a remotely controlled machine tool in a factory which is required to measure its attitude relative to the workpiece. This application can be met by having one set of physical vector measurement means on the workpiece and another set on the tool, both linked to a central computer. Since time is not critical, but high accuracy is, the appropriate choice would probably be to use a general purpose minicomputer programmed in a high level language. In contrast, consider a problem where a satellite must point a narrow beamwidth communication device at an approaching spacecraft already in contact with another satellite. The need for high speed updates to the pointed device, because of rapid changes in the satellite's attitude, combined with the size, weight, and power restrictions, makes a dedicated processor with firmware and special hardware the appropriate choice for the computational means of the ReAtMent system.

## 5. OBJECT DIRECTION AND RANGE MEASUREMENT MEANS

This subsystem (in combination with the position measurement means) determines the net accuracy of the solution to the three dimensional triangle between the two platforms and the detected object. Obviously, the first consideration is to select the appropriate technology to detect and track the object. The next step is to integrate this with a means of determining the range to the object. Finally, as mentioned above in the discussion of the position measurement means, the object direction and range measurement means must be able to determine the relative location of the object to within the volume of the object if the three dimensional triangle solved by the ReAtMent system is to correspond to the actual physical situation.

In contrast to the position measurement means, the object direction and range measurement means must be located on one of the platforms. This subjects this subsystem to the constraints of size and weight imposed by the platform.

## 6. COMMUNICATIONS MEANS

The separation between the two platforms requires that some means be used to communicate between them. The communications net may also include another station where the computational and/or position measurement means are located. The data that must be transferred by the communications means consists mainly of angular measurements (at most 6 sets corresponding to the 4 physical vector measurements, the direction to the object, and the pointing command) and range measurements (at least the separation between the platforms and the range to the object). The amount of data transferred is also dependent on the number of pixels in each probabilistic vector. Given the required update rate of the ReAtMent system, it is possible to estimate the minimum necessary capacity of the communications means in terms of bits per second.

This will only be a first approximation as there are other factors which will influence the selection of the communications means. One major factor is the selection of the technology to be used. Aside from the conventional radio data links, it may be desirable to use optical data links, or even hard wire systems. Potential interference with the other subsystems of the ReAtMent system is also a consideration. For example, a large dish antenna may obstruct the view of the object direction and range measurement means. Another

consideration is immunity from transmission noise. This might be accomplished by the use of error detection/correction coding and/or spread spectrum techniques which provide processing gain. Yet another consideration is the requirement for synchronous or asynchronous operation.

In general, the communications means will be the last major subsystem to have its parameters determined other than the selection of the technology (i.e. radio, optical, etc.) used to implement it. This is because the communications means does not play a determining factor in the overall accuracy or performance capabilities of the ReAtMent system, except for the speed of operation, and this is usually limited by the computational means.

#### C. THE "SIMPLE" GENERALIZED ReAtMent SYSTEM

For the moment, step back and consider the simplest possible generalized ReAtMent system. For such a system, the following assumptions are made: 1. The sizes of the two platforms and the object are very small compared to the distances separating them, thus the problem reduces to one single, deterministic three dimensional triangle; 2. The lines of sight to two very distant bright point sources are the physical vectors measured, thus the physical vectors are measurable as deterministic rather than probabilistic vectors; and 3. The beamwidth of the device to be pointed is sufficient to cover many times the size of the object, thus some "slop" is provided for pointing errors introduced by the ReAtMent system.

#### D. ERRORS IN ReAtMent

Starting with the simple, generalized ReAtMent system defined

above, it is possible to examine the effect of errors introduced by the ReAtMent system. This type of error manifests itself in terms of the ReAtMent system reporting a valid, but incorrect attitude matrix. This is not an inconsistency of terms. A ReAtMent system based on the Two Vector Method will always generate a valid attitude matrix in the sense that it is both orthogonal and unitary. However, because of errors in the physical vector measurement means, the incorrect PAR and AR may be computed. This is in contrast to some of the other attitude measurement schemes in which errors manifest themselves as errors in the individual matrix coefficients. Although the resulting matrices look reasonable, such coefficient errors result in invalid matrices in the sense that the matrix is no longer unitary or orthogonal. The effect of using an invalid matrix is that the length of the vector, or the angles between two vectors operated upon by the same matrix may not be preserved, preventing a correct solution to a physical geometry problem. A singular value decomposition (see Golub) can be used to find a least squares estimation in terms of a linear, orthogonal matrix, but even here, there is no useful way to specify the error associated with the matrix.

A more efficient way to define the level of error in an attitude matrix is by the maximum angular difference between a vector operated on by the measured (i.e. calculated) attitude matrix,  $[M]$ , and the correct matrix  $[C]$ . Call this maximum angular error  $E_{\max}$ .

Imagine a vector,  $V$ , operated on first by the inverse of the correct matrix, and then by the measured matrix. If the two matrices  $[C]$  and  $[M]$  are the same then the vector will be transformed back

upon itself and will suffer no transformation error due to the measured matrix. If, however,  $[M]$  is different from  $[C]$  then the operation can be combined into a single error matrix  $[E]$  as shown in definition 5.1.

$$[E] = [M][C]^{-1} \quad (\text{def. 5.1})$$

This matrix allows the angular error,  $E_V$ , (resulting from the use of the measured rather than the correct matrix) to be evaluated for any vector,  $\hat{V}$ , by using equation 5.1.

$$\cos^{-1}(E_V) = ([E]\hat{V}) \cdot \hat{V} \quad (\text{eq. 5.1})$$

It can now be seen that if  $\hat{V}$  is parallel to the PAR of  $[E]$  then there will be no transformation error. If  $\hat{V}$  is perpendicular to the PAR of  $[E]$  then the error will be a maximum with a value equal to the AR of  $[E]$ ,  $AR_{[E]}$ . Thus if  $[E]$  is specified for a ReAtMent system, then the maximum tolerable transformation error is specified for the ReAtMent system.

#### E. ESTABLISHING A ReAtMent SYSTEM ERROR BUDGET

The real question for the designer of a ReAtMent system is how accurate each of the major subsystems must be to yield a specified overall system accuracy. To arrive at a starting estimate, first evaluate the problem using the worst case anticipated and assume a perfect ReAtMent system exists. The basic triangle in three dimensions is shown in figure 5.2.

In this figure, the angle,  $\alpha$ , range to the object,  $R$ , and interplatform separation,  $D$ , are measured in the coordinate system of platform 1, giving enough information to solve the triangle. Thus the angle,  $\beta$ , is calculated by equation 5.2.

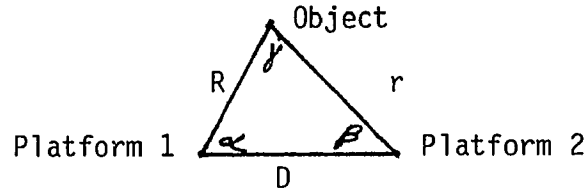


Figure 5.1 Basic Three Dimensional Triangle

$$\beta = \tan^{-1} \left( \frac{R \sin \alpha}{D - R \cos \alpha} \right) \quad (\text{eq. 5.2})$$

$$d\beta = \frac{D \sin \alpha \partial R + R \sin \alpha \partial D + R(D \cos \alpha - R) \partial \alpha}{(R^2 + D^2 - 2DR \cos \alpha)} \quad (\text{eq. 5.3})$$

The equation 5.3 gives the total derivative of  $\beta$  in terms of the partial derivatives of  $R$ ,  $D$ , and  $\alpha$ . Thus it is possible to predict the magnitude of the error in  $\beta$  based on errors in these parameters. This is the critical parameter of interest since it is the one which corresponds to the pointing accuracy of the device on platform 2 which is to be pointed at the object. The range to the object from platform 2 can be calculated from equation 5.4.

$$r = \frac{R \sin \alpha}{\sin \beta} \quad (\text{eq. 5.4})$$

The criterion for saying that the triangle has been solved directly is that the line of length  $r$  and angle  $\beta$  starting at platform 2 must terminate within the volume of the object. If the object can be assigned an effective radius,  $R_{\text{obj}}$ , as seen from the platforms then the allowable error in the angle  $\beta$  is given by equation 5.5 as

$$\Delta \beta = \tan^{-1} \left( \frac{R_{\text{obj}}}{r} \right) \quad (\text{eq. 5.5})$$

Looking at equation 5.3, it would seem that the worst case occurs when  $D$  and  $R$  are approximately equal and  $\alpha$  is close to zero. This corresponds to the object being almost on top of platform 2. This is

an unrealistic case because if this were so, the device to determine the range and direction to the object would have been located on platform 2, making the ReAtMent system unnecessary. In the same light, if  $\alpha$  were near  $\pi$ , this would correspond to the object being nearer to platform 1 and the device to be pointed would have been located on platform 1, again making the ReAtMent system unnecessary.

In a realistic case,  $\alpha$  would be between  $\pi/4$  and  $\pi/2$  and  $R$  would be on the same order of magnitude as  $D$ , meaning that the error in  $\beta$  would be roughly equal to the error in  $\alpha$ .

Since the object direction and range measurement means is supposed to produce a line from platform 1 and terminating within the volume of the object, it is reasonable to start the development of the error budget with this subsystem. Let  $R_{\max}$  be the maximum range to the object and then the half-beamwidth of the object direction measurement means is given by  $\tan^{-1}(R_{\text{obj}}/R_{\max})$ . The accuracy of the range measurement should then be  $\pm R_{\text{obj}}$ , or expressed as a fraction  $R_{\text{obj}}/R_{\max}$ .

The effective radius of the respective platforms, ( $P_1$  and  $P_2$ ), and the maximum separation between the platforms,  $D_{\max}$  determine the required accuracy of the position measurement means to be  $(P_1 + P_2)/2D_{\max}$  (or the smaller of  $P_1$  or  $P_2$ ) in range and  $\tan^{-1}(P_2/D_{\max})$  in angle.

Assuming that a perfect ReAtMent system is used, specifying the above accuracies should guarantee that the three dimensional triangle is solved to the accuracy permitted by the physical geometry. In a real ReAtMent system, there will be an error matrix  $[E]$ , as described



above, which could produce a maximum error of  $AR_{[E]}$  in the pointing angle  $\beta$ . Equation 5.3 should therefore be amended to include a term  $AR_{[E]}$  to account for the ReAtMent system error. Clearly, this error should be less than  $\tan^{-1}(R_{obj}/R_{max})$  and in general should be about 1 or two orders of magnitude below this value to make the error contribution of the ReAtMent system negligible in comparison with the other major system components.

To examine the effect of specifying the error matrix angle of rotation, consider that if a physical vector  $V$  were measured by platform 1, it would appear to platform 2 as  $[C]V$ , but would be reported as if it were  $[E][C]V$  with a maximum possible error of  $AR_{[E]}$ . Since both platforms have roughly (if not exactly) the same physical vector measurement means accuracy, the combined measurement accuracy must be better than  $AR_{[E]}$ . Assuming a gaussian distribution and using a  $3\sigma$  level of confidence, it is reasonable to specify the accuracy of the physical vector measurement means as being  $(1/6)AR_{[E]}$ .

This analysis has now covered the critical subsystems whose accuracy must be specified to determine how accurately the triangle in three dimensions can be solved. For various reasons, it may not be possible to obtain the various accuracies specified using the worst case, first cut methodology suggested above. Furthermore, the various errors do not combine in a nicely separable fashion to allow an easy analytical tradeoff between the accuracies of the various components. Therefore, it is suggested that the techniques developed in previous chapters be used in a computerized parametric analysis of the

worst expected case to determine realistic tradeoffs between the accuracy specifications for the various subsystems.

#### F. SUMMARY OF ReAtMent CONSIDERATIONS

In order to specify the technologies used and the accuracies required of the various components of the ReAtMent system, it may be necessary to evaluate the physical geometry of the overall system in its worst case. This determines the required accuracies of the position measurement means, the object direction and range measurement means, the device to be pointed, and the ReAtMent system. The operational environment in which the system is required to work determines the available physical vectors and thus the technologies necessary to measure them to the accuracy required.

The velocities and relative rotational rates of the platforms determine the required update rate to keep the device pointed at the object. This drives the specification of the computational means throughput rate and the capacity of the communications means.

The above formulas are first cut approximations to the accuracies of the various systems which would be required to solve the overall problem to the limits imposed by the actual physical geometry. Tradeoffs must usually be made for cost, weight, and other reasons, thus it is necessary to perform a parametric analysis of the worst case to determine the allowable tradeoffs.

## CHAPTER VI: MEASURING PROBABILISTIC VECTORS WITH ELECTROOPTICAL SENSORS

### A. OVERVIEW

The first five chapters have progressed from the basic concepts of ReAtMent through the analysis of a generalized ReAtMent system. Before performing some simple experiments to illustrate some of the concepts developed, it is worthwhile to digress slightly and study a class of electrooptical sensors which are capable of reporting physical vectors directly in terms of probabilistic vectors. These sensors (in particular a television camera) will be used in the experimental work reported in the next chapter.

### B. WHAT A VIEWED OBJECT LOOKS LIKE

Section B of chapter I showed that detectable volume elements of a viewed object are essentially those on its surface (i.e. have a clear line-of-sight) which have a non-zero contrast (i.e. the energy emitted by the volume element over the optical passband of the observer is different from that of the background).

For objects in the atmosphere, two other factors must be taken into account. The most obvious is absorption of some of the energy by the molecules in the path between the object and the observer, Resulting in a net loss of energy received from the object and hence a reduction in the apparent contrast of the object. The other effect is the scattering of the energy by particles in the path, which has the effect of increasing the volume of space emitting a detectable energy difference from the background. Thus, this effect can cause an apparent alteration in the size or shape of the viewed object.

However, since the energy density, due to the scattering, is always less than from the source itself, the region surrounding the object will have a lesser contrast than the object itself.

This gives credence to the use of a probabilistic vector to describe the direction to the object. Those regions with a detectable energy difference can not be ruled out as candidates for the location of the object based on the information available to the sensor.

The calculation of the apparent size and shape of an object due to scattering and transmission losses through the atmosphere is, in general, quite complex and far beyond the scope of this discussion. The interested reader should consult The Infrared Handbook for a concise treatment of the fundamental physics and the current (i.e. 1978) state-of-the-art in these topics. On the basis of the author's personal observations and reading of applicable literature, it is reasonable to assume that the effects of scattering are appreciable only when the object (or a portion of the path) passes through an aerosol and the source is significantly brighter than the background. Common examples of this are streetlights in a fog, or the halo around the moon when seen through high clouds. When the object is a dark source (i.e. emits less energy than the background) the effect of scattering will be to reduce the apparent size of the source. Common examples of this are a red fire hydrant seen in a fog, or an aircraft viewed in daylight through thin clouds. Perhaps the most striking common example of shape and size alteration is a searchlight (or high intensity flashlight) in a fog. The scattering produces a large bright region just in front of the unit and makes the beam appear as a bright

column, while diminishing the apparent size of the dark body of the unit.

Thus, when designing a ReAtMent system where the direction to a viewed object is to be used as a probabilistic vector, it is highly desirable to select an object which appears as a bright point source. This will give a high contrast (making acquisition easier by the observer) and effects of scattering will at most increase the apparent size of the object in a symmetrical fashion.

#### C. USING THE DIRECTION TO A VIEWED OBJECT AS A PROBABILISTIC VECTOR

When is it appropriate to use the direction to a viewed object as a physical vector? This question must be answered carefully in the design of a ReAtMent system based on electrooptical directional measurement. The most important consideration is that the object be sufficiently distant from the two observers (see figure 5.1) so as to appear to be in the same direction to either observer (within the accuracy of their respective directional measurement means). In a real world triangle in three dimensions, illustrated in figure 5.1, this is impossible since the apex angle of the triangle will always be finite. However, if this angle can be effectively brought to zero at the angular quantization level used to solve the triangle, then the two long legs of the triangle will become effectively parallel. Thus the direction of these two legs will both be members of a uniform vector set and fulfill the definition of a physical vector.

The quantization error in angular measurement is effectively set at one half the angular subtense of the largest pixel in the observer's sensor. Denoting the total angular subtense of the largest pixel as

$L_{obs}$ , the apparent radius of the object as  $R_{obj}$ , the distance between the object and the observers as  $D$ , then the range,  $r$ , beyond which the apex angle can effectively be considered as zero is given in equation 6.1.

$$r = 2D/L_{obs} \quad (\text{eq. 6.1})$$

The range beyond which the object will appear as a point source is given by equation 6.2.

$$r = 2R_{obj}/L_{obs} \quad (\text{eq. 6.2})$$

Thus for a deterministic solution to the ReAtMent problem, the viewed objects, whose directions define measured physical vectors, must be beyond the ranges given by both equations 6.1 and 6.2.

To examine the case for describing a physical vector as a probabilistic vector, allow the separation,  $D$ , to go to zero so that there is only one observer. Now equation 6.1 is satisfied for any range and if the viewed object is closer than the range specified in equation 6.2, it may subtend more than one pixel. The direction to this object is now given as a probabilistic vector, yet, it satisfies the criteria to qualify as a physical vector.

The common practice in specifying the direction to an object which subtends more than one pixel is to specify the pixel containing the centroid of the outline of the object. This is based on the premise that all pixels fall into one of two classes, either they include some of the image of the object, or they don't. The resulting uniform probability density in each pixel, judged to contain some portion of the object, makes the pixel containing the centroid of the outline the most likely pixel, MLP, to still include the viewed

object if the range to the object were to increase to the point where the object appears in only one pixel. By using a probabilistic vector to describe the direction to the object, a better approximation to the MLP is possible, since those pixels containing less of the image of the object would have a lower contrast and thus a smaller assigned probability. The MLP would be chosen as the one containing the "center of probability mass". Thus, the use of probabilistic vector theory represents an improvement in the state-of-the-art in determining the direction to an object.

#### D. THE CONCEPT OF A PARTITIONED FOCAL PLANE

The lens of a sensor serves to map directions in space (which are characterized by two angular parameters) into points on the focal plane (characterized by two linear parameters). To illustrate this, consider the simple thin lens and focal plane portrayed in figure 6.1.

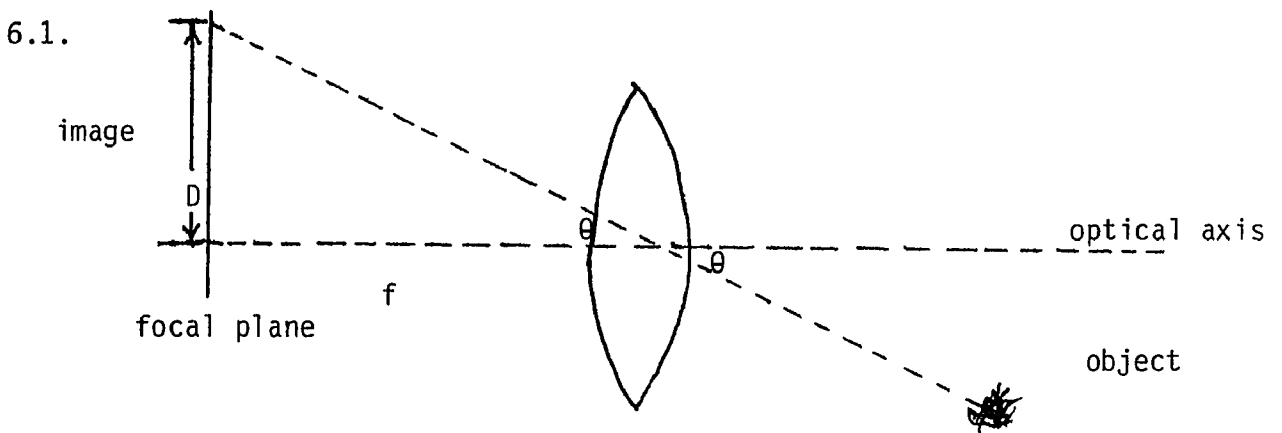


Figure 6.1 Simple Optical Directional Measurement Model

Before using this simple optical directional measurement model, it is necessary to justify some of the implicit assumptions used. This model is based on the use of geometric optical ray tracing which treats optical energy as if it were composed of streams of photons

that behave independently of each other. This approach works well for systems whose dimensions are usefully quantized in increments which are on the order of many wavelengths. For most optical devices this approach is valid as the smallest dimensions of component regions are on the order of tens of microns while the wavelength (for visible light) are on the order of half a micron. Also, the dimensions of the lenses themselves and the active areas of the focal plane are on the order of tens of millimeters (or hundreds of thousands of wavelengths).

Since we are interested in measuring the direction to an object which represents a physical vector, the rays originating from incremental elements of the object's surface which arrive at the sensor are all effectively parallel. The design of the optical system represented by the ideal thin lens shown in figure 6.1 is such that all parallel incoming rays will be deflected so as to meet at a common point on the focal plane which is at a distance,  $f$ , from the center of the thin lens. Since all rays converge at a point, it is easy to obtain the location of this point on the focal plane by tracing the ray which passes through the center of the lens. This ray is not deflected by its passage through the lens, thus, if it makes an angle of  $\theta$  entering the lens, it will still have the same angle (relative to the optical axis) upon exiting the lens. Thus, the distance,  $D$ , on the focal plane between the point image of the viewed object and the intersection of the optical axis with the focal plane, is calculated as shown in equation 6.3.

$$D = f \tan(\theta) \qquad \qquad \qquad (\text{eq. 6.3})$$



Thus, there is a 1 to 1 mapping of  $\theta$  into  $D$ . If the focal plane is partitioned into regions  $\Delta D$  wide, this effectively partitions the field-of-view of the sensor into a set of contiguous, nonoverlapping pixels with non-uniform individual fields-of-view. The relationship between  $\theta$  and  $D$  is given in equation 6.4.

$$d\theta = d(\arctan(D/f)) = (1/(1 + (D/f)^2))d(D/f) = (f + D^2/f)^{-1}dD \text{ (eq. 6.4)}$$

Thus, if the increments of  $D$  are uniform, then the pixels near the center of the focal plane will subtend larger angles than the pixels near the edge of the field-of-view. The center pixel ( $D = 0$ ) will have a field-of-view subtending an angle of  $\Delta D/f$  radians. This varying pixel subtense must be accounted for when using electro-optical devices.

In spite of this, the partitioning of the focal plane results in a set of pixels which cover the total field-of-view without overlapping. This can be shown from the non-overlapping of the partitioned regions on the focal plane and the 1 to 1 mapping of between  $\theta$  and  $D$ . Thus, a true point image can fall in one and only one pixel. The partitioning of the focal plane also allows the energy received by the respective regions to be reported independently. Thus the partitioned focal plane allows the image of an object subtending more than one pixel to be reported as a probabilistic vector.

#### E. DIRECTIONAL PROPERTIES OF ELECTROOPTICAL SYSTEMS

An actual optical sensor will not have a simple thin lens, but rather an optical system consisting of a number of optical components such as lenses, prisms, and mirrors. Each of these optical systems are characterized by the presence of front and rear nodal points.

This allows the optical system to be modeled as a "black box" when determining its directional transfer properties. To understand why this is possible, it is necessary to remember that the optical system is specifically designed to form an image on the focal plane. This means that the incoming parallel rays from one element of the scene will all be deflected so as to all converge at one spot in the focal plane and thus form the image of that object.

When measuring the physical vector representing the direction to an object, consider the object to be partitioned into volume elements approaching a mathematical point. Do the same for the volume elements of the front of the optical system. Each of the lines (i.e. rays) joining volume elements of the respective bodies is a member of a uniform vector field which defines the physical vector.

At this point, a rigorous analysis requires the use of an optical analysis technique known as a ray trace, where each of the incoming rays is traced through the optical system (using Snell's law and the principles of reflection) to the point at which the ray intersects the focal plane. In chapter 2 of Ehling's book on Range Instrumentation a very concise treatment of geometrical optics is given for refractive optical systems. Similar results hold for reflective optical systems. For the convenience of the reader, some of the essential, well known, definitions are given below:

1. Nodal points are characterized by the fact that a ray emerging from the rear of a nodal point of an optical system is parallel to the ray impinging on the front nodal point of an optical system. Nodal points are always located on the optical axis. Every refractive

optical system has at least two nodal points and every reflective optical system has at least one nodal point.

2. The aperture stop limits the size of the bundle of rays which traverse the optical system. This is usually expressed as an  $F/\#$  which is the ratio of the focal length of the optical system to the diameter of the entrance pupil. The brightness of the image is inversely proportional to the square of the  $F/\#$ .

3. The field stop limits the field-of-view of the optical system. In general, a ray trace must be performed to determine which aperture (or lens diameter) serves as the field stop. For the thin lens shown in figure 6.1, the field-of-view is limited by the extent of the focal plane. For the thick lens shown in figure 6.2, the field stop is formed by the diameter of the aperture behind the rear lens, while the aperture stop is formed by the diameter of the front lens.

4. The focal length of the optical system is defined as the distance from the principal point of the lens to the plane of best average image definition.

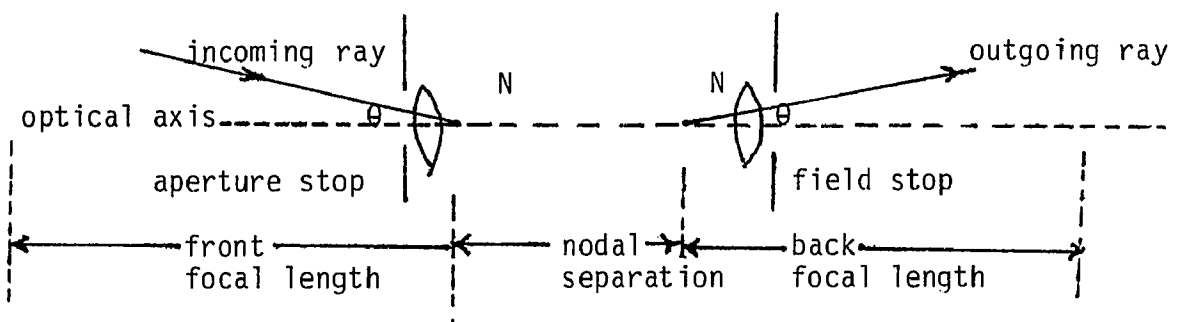


Figure 6.2 Illustration of a Refractive (Thick Lens) Optical System.

5. The principal points of an optical system are defined by the property that a small point object placed at one principal point will form

an image of the same size at the other principal point. If the initial and final medium have the same index of refraction (e.g., air in front of and behind the lens) then the principal and nodal points coincide.

Using the above, well known, definitions, it is possible to analyze the directional transfer characteristics of the refractive (thick lens) axially symmetric optical system shown in figure 6.2. The incoming ray shown is a selected member of the set of incoming rays whose extension (dotted line) would pass through the front nodal point making an angle of  $\theta$  with the optical axis. By performing a ray trace, using the actual indices of refraction and curvatures of the lenses, it can be shown that this ray will exit the optical system in a direction which makes the same angle  $\theta$  with the optical axis when extended back into the optical system (dotted line) through the rear nodal point. This is a direct consequence of the deliberate design of the optical system used to form the image on the focal plane. Since the distance to the viewed object defining the physical vector is many orders of magnitude larger than the nodal separation, it is usually possible to ignore the separation and treat the optical system as an equivalent thin lens located at the rear nodal point, as shown in figure 6.1. In this respect, it is possible to model the optical system of an electrooptical sensor as a "black box" with two nodal points and a restriction on the maximum angle that an incoming ray (i.e. direction) can make with the optical axis and still be within the field-of-view of the sensor.

Since not all optical systems are radially symmetric (about the

optical axis) it may be necessary to specify the projected angle that an incoming ray makes with the optical axis on two mutually orthogonal planes (analogous to an azimuth and an elevation plane). This is especially true in the case of a scanning optical system such as a FLIR (forward looking infrared) or a television camera where the fields-of-view in the horizontal and vertical planes are different. It should also be mentioned that in the case of "folded" optical systems where the optical axis changes spatial orientation (e.g., via a mirror) as it passes from the front lens through the optical system to the focal plane, the direction of the optical axis in free space is considered to be defined by the optical axis external to the electro-optical device.

Finally, it should be remembered that the simple model of a thin lens placed at the location of the rear nodal point of the actual optical system, is adequate for a first cut analysis of the directional measurement properties of an electrooptical device. However, in the cases where the directional resolution of the electrooptical device is not limited by the partition size of the optical plane, but rather by the performance of the optics, it is necessary to perform a ray trace or actual measurement of the optical system to account for the effects of diffraction, the various aberrations (spherical aberration, coma, astigmatism, curvature of field, and chromatic aberrations) as well as lens defects such as decentration, distortion, and flare. The net result of these problems is to make the bundle of incoming rays to converge at a spot rather than at a single point on the focal plane. A brief description of these well known aberrations and defects is

given in Ehling (and other optical texts) which will be condensed here for the convenience of the reader.

Diffraction is the result of the wave properties of light incident on a finite aperture which limits the angular resolution possible with an ideal optical system. The diffraction limit is given in equation 6.5.

$$\alpha = 1.22\lambda/D \quad (\text{eq. 6.5})$$

where  $\alpha$  is the angular resolution in radians,  $\lambda$  is the wavelength of the light, and D is the diameter of the aperture.

Spherical aberration is produced when rays incident on different zones of the lens focus at different places along the optical axis (i.e. have different focal lengths). This results as a point object being imaged as a blurred circle.

Coma results from the lateral magnification not being constant in all annular zones of the lens. This results in the central rays imaging at one point while the outer rays image alongside rather than at that point.

Astigmatism is an aberration which causes an off-axis point source to be imaged as two mutually perpendicular short lines located at different distances from the lens.

Curvature of field refers to the differences between the surface of least confusion (i.e. best focus) and a plane.

Chromatic aberration results because the lens material has different indices of refraction for different wavelengths of light. This results in the lens having different focal lengths for different wavelengths of light. Since the energy from the scene contains many

many different wavelengths (i.e. is polychromatic), the image of a point source in the scene is a series of monochromatic rings.

Among the lens defects, decentration occurs when the center of curvature of the lens does not coincide with the optical axis, making the lens act as if it were an ideal lens plus a thin prism. Hence, the optical axis deflects as it passes through the center of the lens.

Distortion refers to the image forming at a location other than that predicted by geometric optics and can be due to variations in the index of refraction of the lens, or surface curvatures. Usually, distortion results in a radial displacement of the image due to the symmetry in the manufacturing process for the lens.

Again, if the partition size of the focal plane limits the angular resolution, then the optical system can be modeled via the simple equivalent thin lens. However, if the performance of the optical system is the limiting factor, then the appropriate ray trace analysis or a suitable calibration procedure must be performed to establish the actual field-of-view of each pixel and the "leakage" of the image of a point source from one pixel to the adjacent pixels. It should be noted that various image processing techniques exist to "enhance" the image obtained in the presence of such leakage. However, these methods are largely empirical in nature and rely on some knowledge of the "ideal" image. The interested reader should consult texts on image processing for details.

It is interesting to note that the probabilistic vector approach is not severely degraded by such leakage. The energy leaked into the

adjacent pixels is usually much weaker than the energy incident on the intended pixel. This results in the equivalent of some of the probability mass associated with a pixel spilling over into adjacent pixels. When analyzed in terms of information content, and speaking of the simple case where the image of the object should lie entirely within one pixel based on its geometrical angular subtense, the sensor has received sufficient information to know that the object 1. is present, 2. lies in the solid angle subtended by a group of pixels, 3. the solid angle represented by the group of pixels covers, but does not necessarily correspond to the actual angular subtense (i.e. shape) of the viewed object, 4. Those pixels known to contain both the background and a part of the object will have a lesser contrast than those pixels which contain only the object. In this case, the adjacent pixels contain false information (i.e. they do not actually view a part of the object). Thus too fine an angular resolution has been attempted. The probabilistic vector approach will "correct" for this by declaring the object to lie within a group of pixels (or equivalently a larger single pixel) which does cover the direction to the object. In this sense, the probabilistic vector methodology can be said to generate a minimal solid angle within which the direction to the object is known to be, consistent with the information available to the sensor.

#### F. CONVERTING OPTICAL TO ELECTRICAL ENERGY

In order to process the energy reaching the focal plane, it must be converted into an electrical signal via a suitable detector. Before discussing the various methods of partitioning the focal plane,



it is worthwhile to digress for a moment to give the reader an overview of some of the various mechanisms by which optical energy is converted into electrical energy in electrooptical sensors.

When a semiconductor material such as silicon, PbS, HgCdTe, etc. is illuminated with photons having the required energy to produce free carriers in the bulk of the material, the conductivity of the semiconductor changes. This is known as the photoconductive effect. When these free carriers are produced in the depletion region of a p-n junction, the voltage across the junction changes. This is known as the photovoltaic effect.

When a photoemissive surface (e.g., Cs-Sb) is illuminated with photons of sufficient energy, electrons are freed from the surface and can be swept to a anode by an electric field to produce a current. This is known as the photoelectric effect. If the electrons acquire enough energy from the accelerating field, they can cause the emission of many more electrons from the surface of the anode. These electrons can then be swept to a higher voltage anode, etc. until a suitable current is produced. This process is known as photomultiplication.

When photons impinge on a crystalline responsive element (e.g. triglycine sulphate, triglycide flurobreyllate, or triglycine selenate, abbreviated TGS, TGFB, and TGS<sub>e</sub> respectively) the induced temperature rise alters the dipole moment of the crystal and produces an observable external electric field. This is known as the pyroelectric effect.

The interested reader is referred to chapters 8 and 9 of Kruse

et al, Elements of Infrared Technology for a detailed description of the photovoltaic effect and to The Infrared Handbook for a state-of-the-art (1978) detailed discussion of these effects and their applications in converting optical energy into electrical signals. The major reason for reviewing these effects is that they are all used in electrooptical devices with partitioned focal planes, and the characteristics of these techniques influence how the focal planes are partitioned.

#### G. FOCAL PLANE PARTITIONING IN ELECTROOPTICAL DEVICES

All of these effects have been implemented in single pixel detectors and in arrays of detectors placed in the focal plane. First, examine the focal plane structure of an array of discrete detectors as illustrated in figure 6.3. Using this approach, each individual detector requires a separate amplifier which means that at least one lead per detector must exit the focal plane. Also, there must be both physical, electrical, and optical isolation of the detector from its neighbors. This prevents an array of discrete detectors from forming a set of pixels which cover the entire field-of-view of the sensor if the optics were capable of forming a true point image of a point source in the scene.

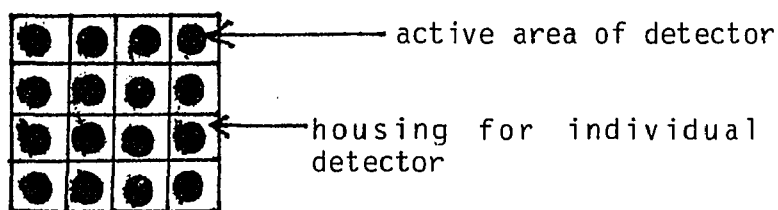


Figure 6.3 Illustration of an Array of Discrete Detectors in the Focal Plane

To illustrate this, consider the case where the point image falls on the housing of the detector rather than the active area of the detector. The point source in the scene (and hence the direction in space which it represents) would then be in a blind region where it would not be detected, although it is within the overall limits of the sensor's field-of-view. This situation can be remedied by using a less perfect lens which would present a spot rather than a point image on the focal plane. Assuming that the spot size is just slightly smaller than the detector active area, and that the insensitive region (due to the housings for the individual detectors) between adjacent detectors is much smaller than the size of the active area, then the spot would image on at least one and at most four of the detectors.

Under these conditions, consider this approach in defining the field-of-view of a single detector. Assume that the boundary of the image spot is defined by the minimum detectable energy contour. That is to say that the image spot cannot be detected unless some part of its boundary falls within the active area of the detector. Then the field of view of a detector would in effect be defined by the angle subtended by the region between the active areas of the detectors on either side of the given detector.

Thus for an array of discrete detectors, it is necessary to match the diameter of the spot image to be at least the largest distance between active detector areas (taking the shape of the active area and the layout of the array into account) and at most the minimum separation between the active areas of the non-adjacent detectors. This insures that the entire field of view is covered by the set of

reported pixels.

It is interesting to consider the case where the spot overlaps two or more detectors. Here, an above threshold contrast would be indicated on the two detectors (i.e. pixels). The shape and optical energy distribution of the image spot can be assumed to take the form of an ellipse and ellipsoidal gaussian distribution respectively. The energy incident on each detector would be the integral of the optical energy density over the portion of the spot on the active area of each detector. While this is impossible to state explicitly in the general case, it is reasonable to assume that the energy would divide roughly as the proportion of the spot in the field of view of the respective pixels. This lends credance to the concept of probabilistic vectors as developed in previous chapters.

Another implementation of a partitioned focal plane is where the sensitive material is spread continuously and uniformly over the focal plane but is scanned by an electron beam (e.g. a television camera). The incident illumination produces a non-uniformity on the scanned side of the sensitive material which can be modeled as an array of elemental capacitors, each corresponding to an elemental layer of the sensitive area. This is illustrated in figure 6.4 which also shows the appropriate models to describe vidicons using a photo-conductive, pyroelectric, or silicon diode sensitive material. The interested reader is referred to chapter 13 of The Infrared Handbook for a more detailed explanation of this technology. For the purposes of defining the field-of-view of the individual pixels, the technology employed to generate the charge distribution scanned by the electron

beam, is not significant. This is because the size of the region of the focal plane represented by the elemental capacitor in the model is much smaller (typically on the order of 1 micron) than the electron beam diameter (approximately 35 microns). Thus, the electron beam covers many elemental capacitors, drawing current more rapidly from those capacitors in the center of the beam than those in the skirts of the beam. This means that if the electron beam were pulsed for a fixed amount of time onto a fixed place in the sensitive area (i.e. not scanning) the region of discharged elemental capacitors would grow with the time that the beam is left on. Thus, the scanning action of the beam determines the width of the region swept out on the focal plane.

The incident constant illumination from the scene can be assumed to provide a steady charging current to the elemental capacitors. Thus, the current in the beam, due to the sensitive surface area, is a measure of the optical energy (product of the illumination and time) incident on the focal plane. Since the amount of stored charge is limited by the shunt resistance along the scanned surface, it is possible to arrive at a condition of saturation where the amount of beam current does not increase as the level of surface illumination increases. Practical vidicons take care of this problem by selecting an appropriate "integration time" for each pixel which is the time between interrogations of the same pixel by the scanning electron beam. This integration time coupled with the dwell time on a fixed place of the sensitive area effectively determines the radius of the region of elemental capacitors which may be discharged. Thus, a

limit is placed on the extent of the pixel in the focal plane by the electron beam diameter, the integration time, and the dwell time.

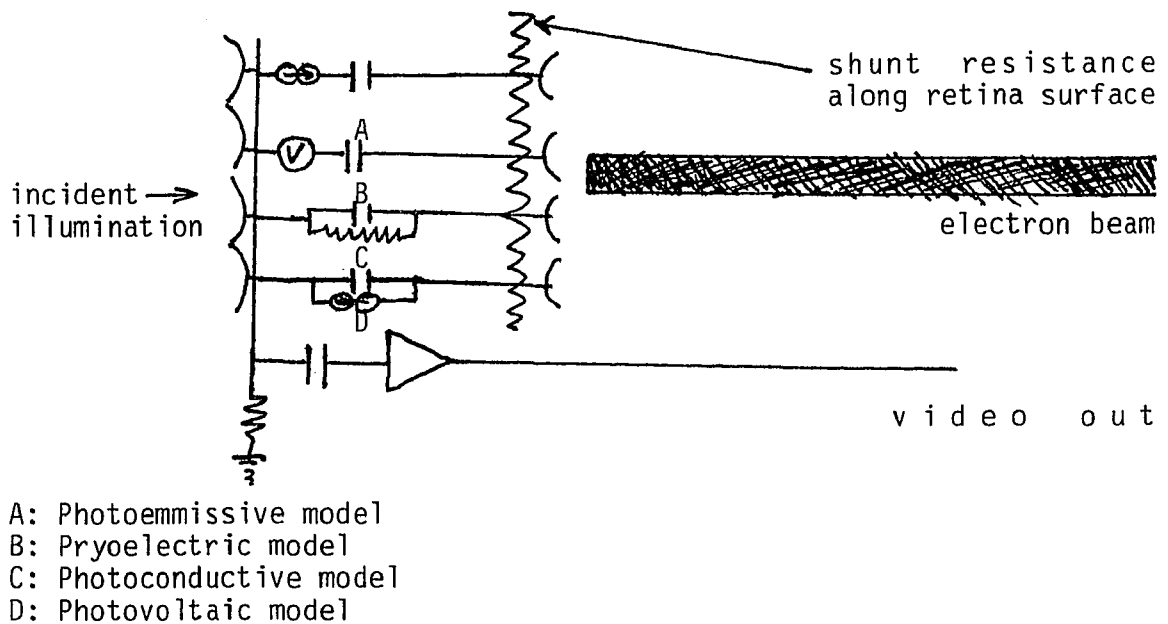


Figure 6.4 Illustration of Sensitive Focal Plane Scanned by Electron Beam.

Figure 6.4 is obviously not drawn to scale because it is intended to represent the general case rather than any specific technology. The surfaces of the sensitive material are shown as wavy lines rather than planar surfaces to indicate that the regions on either side of the model are associated with the respective elemental capacitors. Also, it is obvious that for any specific application, there would only be one type of model present as the sensitive material would be either photoemissive, pyroelectric, photoconductive, or photovoltaic, but not a combination of these (assuming the current technology, it may be desirable to fabricate such a structure for special applications).

Another consideration on this focal plane is the lateral thermal conductivity and the shunt resistance along the surface of the

sensitive material. This tends to spread out an image by indirectly inducing a signal in the elemental regions adjacent to the illuminated ones. However, this effect is intentionally minimized in the design of the sensitive surface.

Since the electron beam is scanned over the interior surface of the sensitive material, the analog video output corresponds to that of a single detector scanned over the same total field-of-view. Consider that the most common mode of scanning is a raster scan with a 2 to 1 interlace. This means that the odd numbered lines are scanned first and then the even numbered lines. If the useable diameter of the electron beam is used to define the width of the area scanned in one line (defining the useable diameter of the beam as the diameter of the set of elemental capacitors discharged under saturation conditions), then the length of the pixel is defined by the length of time which the video output is integrated before sampling and the scan rate. If the scan rate were relatively slow in terms of the integration interval, then the area swept out on the focal plane by the beam can be modeled as an ellipse with almost flat sides parallel to the major axis. It is therefore obvious that a set of such pixels cannot cover the focal plane unless they overlap. This is not critical for purposes of presenting an image, but is undesirable for the purpose of using the sampled values of the video as a measure of the intensities of the pixels since this makes it quite difficult to adequately define the instantaneous field-of-view of a given pixel because of the overlap.

A more practical approach is to repetitively sample the video

output using a very narrow aperture time analog-to-digital converter, which effectively freezes the beam in one position. If the sampling interval is long enough, it produces the equivalent of an array of discrete detectors. This makes the comments regarding the determination of the field-of-view of an array of the discrete detectors apply to the class of electron beam scanned electrooptical sensors.

A similar approach can be made in analyzing the behavior of electrooptical systems which scan the instantaneous field-of-view of a single detector to cover the total field-of-view. If the detector output is sampled over a sufficiently narrow time interval, the detectors instantaneous field-of-view is effectively fixed in space. If the sampling is repetitive, then the equivalent focal plane structure is again an array of discrete detectors.

#### H. EXPRESSING THE IMAGE OF AN OBJECT AS A PROBABILISTIC VECTOR

The preceeding sections have covered what a viewed object looks like, why its direction represents a physical vector, the concept of a partitioned focal plane, the directional properties of optical systems, how optical energy is converted into electrical energy, and how the focal plane is effectively partitioned in electrooptical devices. These sections have provided the necessary background to discuss the core of this chapter: how the image of an object on a partitioned focal plane can be expressed as the probabilistic description of a physical vector.

Consider the situation shown in figure 6.5 where an object is viewed by a partitioned focal plane electrooptical sensor. The object is sufficiently distant from the two observers (for clarity, only one



observer (i.e. sensor) is shown) so that the direction to that object represents a physical vector. However, this object subtends a solid angle greater than the IFOV of one pixel. If the object is partitioned into volume elements which image in only one pixel, then (assuming a uniform background), the contrast of that pixel will depend on the percentage of the IFOV of the pixel which is filled by the volume element of the object (assuming a uniform contrast object).

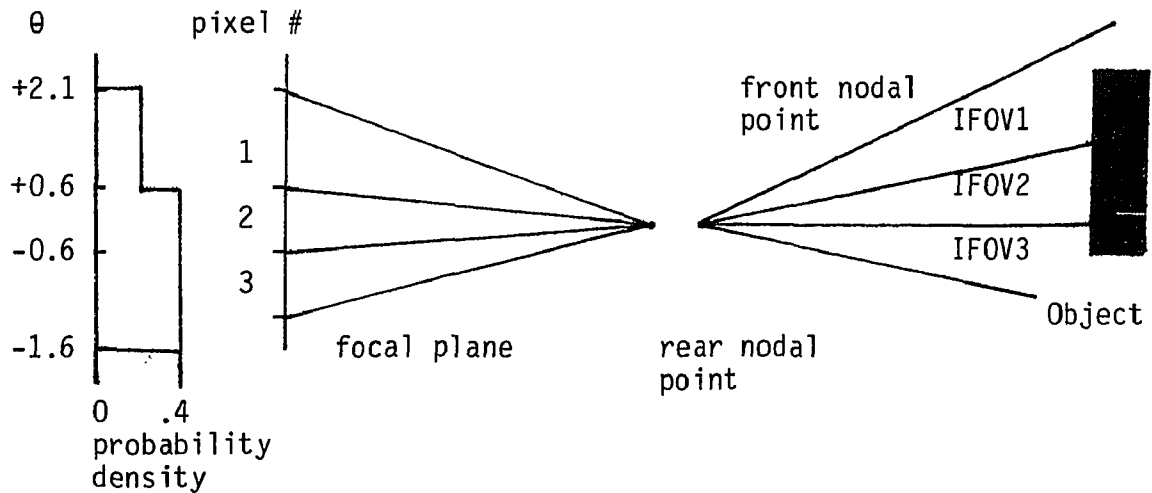


Figure 6.5 Object Viewed by a Partitioned Focal Plane Sensor with Plot of Probability Density

Pixel #	IFOV (mr)	Center $\theta$ (mr)	Raw Contrast	Normalized Contrast	Probability Density	Base Pixel Prob. Density
1	1.5	1.35	0.5	0.3	0.3	0.2/mr
2	1.2	0	1.0	0.5	0.5	0.4/mr
3	1.0	-1.10	0.4	0.2	0.2	0.4/mr

Table 6.1 Derivation of Probabilistic Vector From Example Shown in Figure 6.5

Figure 6.5 is stylized to illustrate the important features of the focal plane, rear node of the optical system, the fields of view of the various pixels, and the relative extent of the viewed object into the IFOV's of the respective pixels. The pixels are deliberately

of different sizes to illustrate the most general case. The raw contrast of the pixels are obtained by computing the percentage of the pixel field-of-view in which the object appears. The column labeled center of pixel,  $\theta$ , is the angular direction of the center of the pixel, considering the front nodal point of the optical system as the origin of the "apparent sensor coordinate system". This terminology is carefully chosen as the front nodal point appears to be the origin of the sensor coordinate system to the world beyond the sensor. However, as stated above, the rear nodal point of the optical system is the origin of the coordinate system used to define the subtense of each pixel on the focal plane.

It is appropriate to use the front nodal point as the apparent origin. Physical rotation of the sensor about an axis which passes through this point will change the directions in free space represented by the individual pixels in the manner expected as the result of operating on these directions by the matrix generated using that axis and angle. To see why this is true, consider that the position of the image on the focal plane is determined by the angle which incoming ray makes with the optical axis when that ray passes through the front nodal point. The rotation of the sensor about the front nodal point changes the angle that the ray makes with the optical axis directly by the angle of rotation (for the case where the axis is perpendicular to the ray and the optical axis). If a rotation were performed about the rear nodal point, the spatial location of the front nodal point of the optical system would change, thus changing the direction of the ray from the object to the sensor in free space.

Looking at table 6.1 and figure 6.5, once the raw contrast has been measured for each pixel, the algebraic sum of the contrasts (i.e. 2) is divided into the contrast of each pixel to obtain the normalized contrast. This is done without regard for the differing sizes (i.e. angular subtense ) of the pixels. The justification for this is given in sections A and C of chapter II. Thus, the discrete probabilistic vector representing the direction to the object is given by the set  $\{(-1.35 \text{ mr}, 0.3), (0 \text{ mr}, 0.5), (1.1 \text{ mr}, 0.2)\}$  where the first entry is the angle of the direction in the center of the pixel, and the second entry is the associated probability. The usual form of the probabilistic vector would result in two angles (e.g.,  $\theta, \emptyset$ ) being given (from the two dimensional focal plane) and would be specified in terms of a unit vector and associated probability as shown in equation 2.2. This form of expression facilitates using the concept of an elemental base pixel and rotation matrix as described in section D of chapter II.

If the probabilistic vector were to be mapped directly into the  $\theta\emptyset$  plane (or the  $\theta$  line in the one dimensional case used for this example), the probability density would be as shown in the graph to the left of the focal plane in figure 6.5. The probability density for each pixel is obtained by dividing the total probability assigned to that pixel (i.e. its normalized contrast) by its angular subtense. For the two dimensional case, this would allow the techniques developed in chapter III to be used directly. Note that no correction for the position of the pixel in the  $\theta\emptyset$  plane is necessary (as per definition 3.9) because the probability density is derived as an assumed

uniform distribution over the pixel based on a discrete measurement. Also, since any finite object subtends a constant finite solid angle regardless of the orientation of the observer, the apparent subtense of the object (in  $\theta$ ) would vary with its elevation (i.e.  $\emptyset$ ) in accordance with equation 3.8.

#### I. SPECIFIC EXAMPLE OF A TELEVISION CAMERA WITH COMPUTER INTERFACE

The preceeding sections have dealt with the generalized electro-optical sensor with a partitioned focal plane. As a result, the principles set forth above apply to many devices such as focal plane arrays (e.g., charge-coupled devices with gated sensitive elements coupled directly to the individual charge storage regions), image converter and image intensifier devices with appropriate scanning or other readout of their outputs, infrared scanners (e.g., a FLIR) and television cameras with appropriate computer interfaces. From the viewpoint of availability and representative behavior, a television camera with appropriate computer interface is the most appropriate electrooptical device to use in the experimental work reported in the next chapter. Therefore, this sensor will be examined in detail.

The television camera selected for the experimental work is a COHU model 2800, with a silicon intensified, low light level vidicon and a 50 millimeter fixed focal length lens. The output from the camera will be videotaped and fed into a Colorado Video model 274 frame store which digitizes the intensity of each pixel and passes it to a Hewlett-Packard 2114B minicomputer which expresses the direction to the viewed object as a probabilistic vector. These probabilistic vectors can then be used to compute the probabilistic

attitude matrix describing the orientation of the camera. Prior to proceeding to the experimental effort, a detailed discussion of the camera and the associated equipment is presented.

The sensitive area on the vidicon is a region approximately 1/2 inch wide by 3/8 inch high on the anode of the vidicon. The deflection circuitry in the camera scans the electron beam in the vidicon over this sensitive area in a raster pattern every 1/60 of a second (one field), and uses a 2 to 1 interlace (all odd numbered lines are scanned first, then all even numbered lines). This gives one complete frame (two fields) every 1/30 of a second. The complete frame consists of 525 horizontal lines of which 482 occur between the vertical blanking pulses thus presenting useable image information. The device which memorizes a complete frame is called a frame store. This provides useable resolution of 482 lines by 251 pixels per line.

Each pixel is represented by an 8 bit (256 level) brightness level which represents the "normalized " (i.e. multiplied by a characteristic scale factor) amount of in band energy (joules) received by the sensitive area of the vidicon covered by that pixel during one frame (i.e. 1/60 second). This is proportional to the probability that the viewed object is within the field of view of that particular pixel. The sensitive area of the vidicon is located at the focal plane of the optical system (i.e., camera lens) when the scene containing the viewed object is in focus.

To determine the field-of-view of each pixel, it is necessary to calculate the  $\Delta D$  on the focal plane for each pixel in both the

horizontal and vertical directions. Since a linear raster scan and uniform video sampling is used, all pixels on the focal plane will represent the same sized regions on the focal plane. As a first approximation the width of each pixel on the focal plane will be approximately 0.0505 mm and the height will be 0.0198 mm, resulting in a neatly partitioned focal plane of 482 rows and 251 columns (i.e., 120,982 pixels).

In assigning indices to the pixels, it is necessary to take into account the numbering scheme used in the frame store, and the conventions used in the computer interface. The frame store operates by sampling the video with a high speed analog-to-digital converter and storing the 8 bit result in a charged-coupled dynamic random access memory. Design of the memory makes it convenient to organize it in terms of 512 lines of 256 samples each. This type of memory requires a constant refresh which is accomplished by accessing each memory location in turn synchronously with the scan of the electron beam in the camera. However, the horizontal retrace of each horizontal line occurs during 5 of the 256 samples (i.e. pixels) thus leaving only the pixels in columns numbered 4 through 254 containing useable image information. A similar retrace effect occurs in the vertical which results in only lines numbered 29 through 510, which is a characteristic of the particular hardware used. Other frame stores and camera combinations on the market could provide slightly different amounts of pixel resolution depending on the number of active lines in the raster and the sampling rate used. Using the numbering scheme of the frame store and the arrangement of the pixels in the active area

of the vidicon, figure 6.6 below shows the row and column numbers assigned to valid pixels in the frame store.

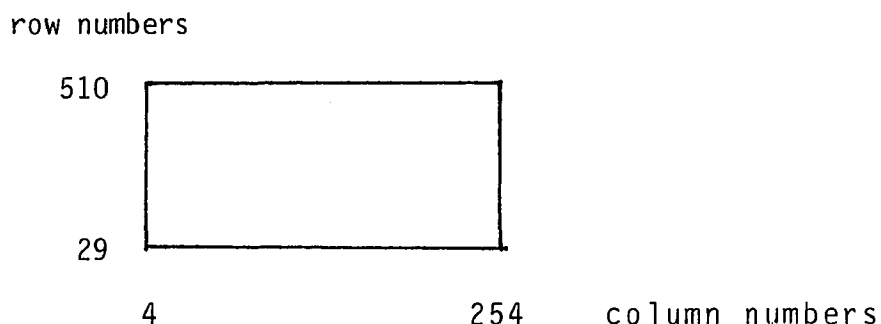


Figure 6.6 Numbering Scheme Used in Frame Store for Valid Pixels

To further complicate matters, the frame store uses a technique which offsets the sampling one half period on every other field (i.e. the odd numbered rows). This is done to improve the "apparent resolution" of the stored image when each pixel is represented as a correspondingly bright spot at the center of each pixel. The detail of this offset is shown in figure 6.7 below.

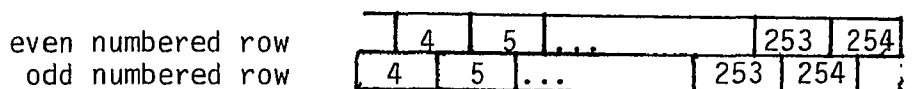


Figure 6.7 Detail of Pixel Offset for Odd and Even Numbered Rows

The net effect of this scheme is to place the geometric center of the sensitive area of the focal plane (i.e. vidicon surface) at the middle right hand edge of pixel 128,269. Using the simplified model shown in figure 6.1, the solid angle corresponding to each pixel can be easily calculated since the limits of the pixel in terms of the distance from the optical axis are now easily expressed as a function of the row and column numbers assigned to each pixel.

Unfortunately, the nominal size of the raster scan given above

is not a calibrated value for every television camera, also, various delays in the videotape equipment can result in an apparent horizontal shift of the scene when viewed on the display of the frame store. Thus, calculations based on the characteristics "specified" above may not be sufficiently accurate for some purposes. For this reason, it is necessary to perform a calibration of the composite system to determine the mapping between the pixels and their respective sets of directions.

The solid angles represented by adjacent pixels are contiguous and non-overlapping because of the 1 to 1 mapping of directions into the corresponding position on the focal plane and the non-overlapping of the partitioned regions on the focal plane. Therefore, the procedures developed in the discussion of discrete probabilistic vectors given in chapter II apply. Since the individual pixels are of differing solid angular coverage, it may be inappropriate to represent them in the form of a base pixel and matrix, unless the solid angle subtended is small enough to be considered as an elemental solid angle (in this case, the shape of the IFOV does not matter). Given the premise, that the partitions of the focal plane are sufficiently small, then except for the direction represented by the center of the IFOV of the respective pixels, the pixels can be considered as effectively indistinguishable.

In his text on Range Instrumentation, Ehling goes into a considerable amount of detail in describing the various techniques used in calibrating cameras for directional measurement. All of these methods start out by using the theory of central projection



which assumes the "equivalent geometry" shown in figure 6.1 and asserts that the image in the focal plane is the two dimensional central projection of the three dimensional image space. Thus, assuming the use of the center of the thin lens as the common origin of the image and object space coordinate systems, the relationship between the position of the point image (x,y) on the focal plane and the viewed point in object space (X,Y,Z) is given by equation 6.6.

$$\begin{bmatrix} x \\ y \\ 1 \end{bmatrix} = [ {}_iM_o ] \begin{bmatrix} X \\ Y \\ Z \end{bmatrix} \quad (\text{eq. 6.6})$$

Here  $[ {}_iM_o ]$  is the transformation matrix relating object to image space. In general, this transformation matrix is quite complicated as it contains both the orientation of the camera and the distortions introduced by the optical system (atmospheric induced distortions are usually accounted for separately). The standard approach has been to attack the orientation segment of the problem first by assuming a distortionless lens and examining a large set of point images (up to approximately 200<sup>+</sup>) in some cases, to over-determine the orientation and arrive at a statistical "best estimate" of the individual matrix coefficients. This set of coefficients was then considered to define the orientation of the camera.

Next, the orientation matrix was used to determine the "correct" coordinates  $(x_c, y_c)$  of each point (X,Y,Z). The difference vector between the correct and the actually observed points (i.e.  $(x-x_c), (y-y_c)$ ) is due to the distortions of the camera optics and is independent of the orientation of the camera. The traditional approach then forms a

least squares, best fit approximation to the magnitude of this difference vector as a function of the radial distance from the center of the focal plane to the observed image location using an iterative procedure. This is based on the assumption of a radially symmetric optical system and aperture with the condition that lenses with significant tangential distortion have been rejected by quality control procedures during manufacture of the optical system.

Assuming the orientation of the camera was unchanged (or re-measured) the observed  $(x,y)$  of a point image of a viewed object first had a calculated error vector added to it before operating by the inverse of the transformation matrix, to obtain the direction to the viewed object.

The results of the present research allow several improvements to be made to the traditional procedure. In the discussion of ReAtMent errors in chapter V, it was noted that the practice of statistically estimating the attitude matrix on a coefficient by coefficient basis can result in an invalid matrix which is neither orthogonal nor unitary. The orientation matrix can be determined by observing two known points via the Two Vector Method. By using many points pairwise, it is possible to overdetermine the orientation matrix and express it as a probabilistic matrix.

This approach has the advantage that as the number of computations increases the distortion induced variations in the PAR and AR should tend toward a gaussian distribution. By discarding those pairs of observed points, which result in values of the PAR, AR being outside a given number of standard deviations from the mean value, (assuming

that these variations are a byproduct of the distortions in the optical system), a better measurement of the actual orientation matrix can be obtained. This can be expressed in terms of a probabilistic matrix.

Given the actual orientation matrix, it is then possible to calculate the distortion, bearing in mind that the "point" on the focal plane in which a point source is imaged, is really a pixel with a finite angular subtense. What this effectively means is that the distortions of less than one pixel are essentially undetectable, and that calculated distortions of less than one pixel are questionable. To explore this, consider, for example, that the actual distortion is  $1/3$  of a pixel dimension at some particular point in the focal plane. If the calibration point used should image in the center third of that pixel, no distortion will be detected. If that point should image in the remainder of the pixel, then a difference of one pixel would be detected. Thus, it is necessary that a probabilistic approach be taken in determining the distortion. Also, as the assumption of a symmetric circular lens and aperture is not valid for all applications, it is necessary to examine this problem in detail.

In general, it is desirable to design the directional measurement system to be limited in resolution by pixel size rather than by other factors such as lens distortion, precision of the mounting assembly, mechanical attitude measurement means, etc. Thus, if the overall system is designed properly, there is at most one pixel of distortion (the case where the point should image near the edge of the pixel and falls on the adjacent pixel instead). This is covered within

the probabilistic vector theory without difficulty.

However, when it is necessary to obtain the greatest possible directional accuracy, it is often the distortions of the optical system rather than the partition size of the focal plane that becomes the limiting factor, as is the case of some of the cameras discussed by Ehling. Assuming this case, the appropriate procedure is to compute the orientation as described above and then estimate the distortion for each spot imaged. Since the distortion is a function of the camera and not of its orientation, it is possible to acquire a great deal of distortion information by using many orientations of the camera. It is not necessarily true in all optical systems that the presence of tangential distortion is such a significant defect in the optical system that it would never appear in any instrument used as a directional sensor. This is principally because the instrument may not be intended primarily as a directional sensor. In any case, the distortion should be modeled as a thick three dimensional surface. The base plane (i.e.  $x,y$ ) would be the focal plane and the height would be the magnitude of the radial distortion. Alternatively, (and much more difficult to visualize and portray) the distortion can be considered as a nonuniform vector field where each correction vector leads from the actual image point to the place where the image should be from a distortionless lens. For the case where there is only radial distortion, the representation of the distortion as a three dimensional surface is more reasonable, since the direction of the distortion is understood.

The net effect of distortion is that the position of the image

reported by the sensor must first be corrected by the inverse distortion before it can be used in the actual computations. Once this is done, the set of corrected pixels which contain the object are normalized for contrast and the set of directions representing the centroids of the respective pixels can be expressed as a probabilistic vector.

Based on this discussion and the apparatus available, the particulars of a calibration scheme for the television camera to account for distortion, and to provide a mapping of the field-of-view for the respective pixels, can be devised. Once this is done, the television camera can be used as a directional sensor which reports the direction to an object directly, in terms of a probabilistic vector.

## CHAPTER VII: EXPERIMENTS IN ReAtMent

### A. OBJECT

The purpose of including an experimental section in this otherwise theoretical study is to give the reader an appreciation for the concepts developed and how they can be demonstrated with relatively simple equipment. Thus, the main thrust of this work will be an exploration of the fundamental concepts as implemented in an electro-optical sensor, rather than the application of this original research to any specific practical problem.

The basic validity of the Two Vector Method can be illustrated using a simple surveyor's theodolite to measure the direction of three physical vectors (i.e. lines-of-sight to an identifiable object) in both a reference and current orientation of the theodolite. Two of the physical vectors would be used to compute the attitude matrix relating the current orientation to the reference orientation of the theodolite. The remaining physical vector would have its description in the reference orientation operated upon by the attitude matrix to compute its description in the current orientation. This computed description would then be compared to the actually observed physical vector in the current orientation and the accuracy of the attitude matrix established.

This experiment represents the special case of a probabilistic vector with one member (the direction defined by the crosshairs in the theodolite telescope). While interesting, this would provide little more than an exercise in arithmetic. To adequately demonstrate the probabilistic techniques developed in the research, it is necessary

to conduct the same basic experiment using a sensor which is capable of measuring the physical vectors in terms of probabilistic vectors such as the television camera described in chapter VI.

Thus, a experiment will be conducted which illustrates the following concepts: 1. The normalized contrast of an object provides a measure of the probability that the object lies within the set of directions defined by the set of pixels in which the image of the object appears., 2. The Two Vector Method is useable to measure the relative attitude matrix and is can accurately predict the current apparent direction of a previously measured physical vector., 3. The technique discussed in section I of chapter III can be used to compute the probabilistic attitude matrix., and 4. The probabilistic attitude matrix can be used to express a reorientation of a single sensor.

#### B. DESIGN OF THE EXPERIMENT

The television camera, frame store, and computer described in section I of chapter VI will be used. The purposes of the experiment detailed above allow many conditions to be optimized to reduce or eliminate many of the problems that would arise in attempting a practical implementation of the concepts developed in a ReAtMent system.

First, the background will be made as uniform and as dark as possible to permit easy, unambiguous identification of the illuminated objects to be viewed for defining the three physical vectors to be measured. This avoids the necessity for providing a mechanism for identifying and separating the objects to be viewed from a cluttered

background. Thus, any bright object detected in the scene is known to be a desired object to be used in defining a physical vector.

Second, the three objects to be viewed will be the ends of a fiber optics bundle. All three fiber optics bundles will be illuminated by a single light source, and therefore will maintain a constant relative brightness to each other. This will tend to eliminate variations in apparent size by changes in brightness levels.

Third, the ends of the fiber optics bundles will be mounted in a piece of wood to provide a fixed spatial relationship between them and help to provide a uniform background. By utilizing a non-symmetric pattern of the three ends, it is possible to immediately and uniquely identify each of the three ends. This provides a mechanism to verify that any two of the three vectors may be used to compute the probabilistic attitude matrix.

Fourth, the experiment will be conducted with the television camera mounted on a machinists table, such that the axis of rotation passes through the nodal point of the lens. The machinists table is mounted on an optical table which also supports the wooden block holding the ends of the fiber optics bundles. This insures that the relative placement of the camera and the wooden block does not inadvertently change during the course of the experiment. The disadvantage of this arrangement is the relatively short range between the viewed objects and the sensor.

Fifth, the experimental setup will be in the same room with the computer acquiring and processing the data. This removes many of the problems associated with the control over, and verification of the



experimental procedure. Thus, if inconsistencies are discovered, it is a relatively simple matter to repeat the experiment and verify the data.

Sixth, since it was shown in section G of chapter II that the Two Vector Method, originally developed for the reorientation of a single sensor, can be generalized to more than one remotely located sensor, performing the experiment with one sensor is sufficient to validate the realizability of a ReAtMent system utilizing the concepts developed under this research.

### C. DIRECTIONAL CALIBRATION OF THE TELEVISION CAMERA

This essential first step in performing the experiment necessitated an in-depth study of the various techniques available. Since these techniques apply not only to the television camera of the present experiment, but also to the directional calibration of other sensors, it is worthwhile to cover the techniques explored in some detail.

The basic problem is to express the  $\theta\phi$  of a pixel as a function of its xy indices. The implicit assumption in representing a physical vector by a discrete probabilistic vector is that the reported members of the probabilistic vector have essentially the same very small solid angle which is represented by the associated central direction. If for example, the field-of-view of the sensor was very wide, then the variation in pixel subtense (see section F of chapter VI) would have to be accounted for by partitioning the larger pixels into appropriate subpixels with proportionally smaller probabilities. This discussion rapidly leads to the question of how one defines the

width and height of a pixel. Since the concept of a pixel arises from an infinitesimally small picture element, which in reality has a finite size, it is impossible to arrive at a clean cut definition of the size of the pixel. The best that can be done is to define the leakage that can be tolerated into adjacent pixels before it is said that the viewed object subtends more than one pixel.

The major problem associated with the various attempted calibration schemes is the precision to which the "known quantities" of the geometrical figure can be measured. All calibration schemes use the front nodal point of the lens as the apex of the triangle which includes two known targets. These targets must be detectable by the sensor and should be as small as possible so as to subtend an angle smaller than one pixel. Also, since the triangle is a planar figure, the targets should have a cylindrical shape with the axis of the cylinder roughly perpendicular to the triangle. This shape and orientation allows the angular subtense of the target to be nearly independent of the aspect angle from which the target is viewed.

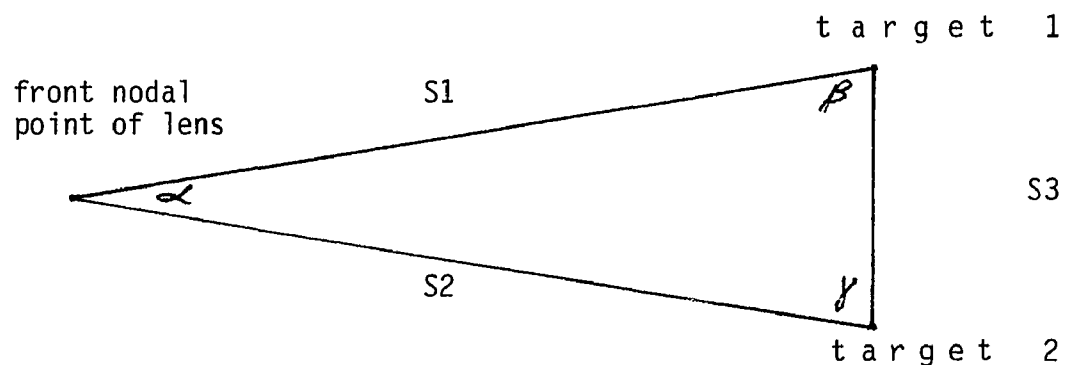


Figure 7.1 The Calibration Triangle

Thus, the target will appear as a thin line to the sensor. This line can be oriented, by rotating the sensor, to appear perpendicular to the dimension of the pixel to be measured. This calibration triangle is illustrated in figure 7.1.

Since the sensor forms an image, it is possible to move along the targets to determine the points at which the sides of the triangle,  $S_1$  and  $S_2$ , intersect the targets, and thus to measure the length of side  $S_3$ . The uncertainty associated with this measurement is on the order of the diameter of the target cylinder. Thus, for the case where the diameter of the target cylinder is negligible compared to the length of the side  $S_3$ , this error also becomes negligible.

The location of the nodal point also introduces some uncertainty into the measurement as the nodal point is located inside the lens assembly and is thus virtually impossible to locate accurately without extensive measurements. The best that can be done is to assume that the nodal point is on the optical axis and thus in the center of the lens assembly. Given detailed knowledge of the lens assembly, it may be possible to locate the front nodal point more accurately, but again, the physical inaccessability makes it very difficult to locate to within much better than a few millimeters. This introduces errors in the lengths of the sides  $S_1$  and  $S_2$ . Fortunately, since  $S_1$  and  $S_2$  are typically much longer than  $S_3$ , the effect of this error is generally quite small.

This inability to accurately locate the nodal point makes it quite difficult to set up a test jig where the axis of rotation passes

directly through the nodal point and is perpendicular to the dimension of the pixel to be measured. This dilemma is further aggravated by the fact that the optical axis does not necessarily pass through the center of the lens assembly and impact the center pixel in the active region of the sensor. Thus, it is quite difficult to accurately manufacture a suitable test jig to measure the subtense of the pixels of the sensor.

There are two possible solutions to this problem. One solution is to use a bright target point that is very far away. This makes the effect of the axis of rotation passing through other than the front nodal point of the lens effectively negligible. However, this is not appropriate for experiments in which the lens must be focused on objects a relatively short distance away, as in a lab experiment. The principal reason for this is the lens elements not being perfectly centered on the optical axis. This results in a movement of the image as the focus is changed. The other solution is to focus the lens on a variable size target which is known to be initially much smaller than a pixel and is at the same distance as the object which is to be observed. When the size of the object is changed, the leakage into adjacent pixels can be measured to determine the size of each pixel. Alternatively the endpoints of the variable size target can be measured to determine the number of pixels subtended.

This calibration procedure was first attempted with the camera held in a fixed position to view an arm holding two vertical cylinders (one at each end) which was mounted on a machinists table. The geometrical figure formed is shown in figure 7.2.

The machinists table was first aligned so that the vertical cylinders appeared as a single line to the camera. The table was then rotated by a fixed angular increment and the set of pixels were determined in which contained the image of the vertical cylinders. The angular separation of the two cylinders was determined by equations 7.1 and 7.2. Thus, a plot could be developed of angle vs pixel number and the horizontal subtense of the pixels could be calculated. The sensor was subsequently rotated 90 degrees about its optical axis to measure the vertical subtense of the pixel.

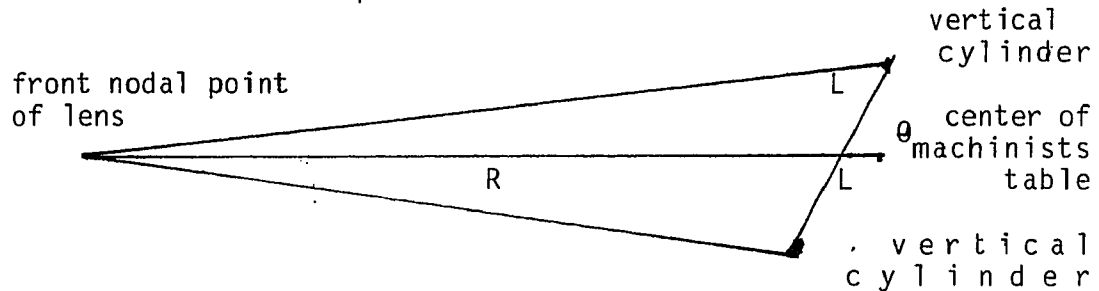


Figure 7.2 Machinists Table Calibration Figure

$$\psi_1 = \tan^{-1} \left( \frac{L \sin \theta}{R + L \cos \theta} \right) \quad (\text{eq. 7.1})$$

$$\psi_2 = \tan^{-1} \left( \frac{L \sin \theta}{R - L \cos \theta} \right) \quad (\text{eq 7.2})$$

This experiment was run and found to produce reasonable results. However, several difficulties became apparent which made this approach unsuitable for the experimental setup to be used. The major difficulty in a lab environment was the depth of focus of the lens. As the angle  $\theta$  approached zero, where the two vertical cylinders were to appear as a single line, the cylinders went out of focus, thus blurring and causing their apparent angular subtense to exceed one pixel. When this experiment was attempted with a somewhat larger apparatus at a sufficient range so that the cylinders remained in focus,

the required size of the apparatus rapidly became unwieldy, almost to the point of impracticality. Also, problems of maintaining the relative immobility of the machinists table and the sensor became very difficult. The experience gained in this effort led to the conclusion that this approach was not appropriate for the purposes of the present experiment.

The next approach attempted involved imaging a calibrated slit on a selected pixel and varying the slit width to measure the subtense of the pixel. Having measured the subtense of the various pixels, a reasonable estimate could be made of the solid angle subtended by each pixel and its central direction. Measurements were made using a calibrated slit with back illumination provided by an incandescent bulb behind a plastic diffusive cover. Given a specified amount of leakage into adjacent pixels, as the definition of the width of the pixel, experimentation revealed that by varying the intensity of the light (and/or the gain, contrast, and black level setting of the frame store), a variety of pixel widths could be obtained from the same slit size. Experimentation also revealed that while the apparent width could be increased, it could not be decreased below the actual subtense of the slit. This lends validity to the concept of leakage defining the width of the pixel, but was felt to be too subjective to be used in the present experiment.

By calculating the size of the center pixel for a 50mm lens using the "spec" values for the active area of the vidicon as 3/8 inch high by 1/2 inch wide, and the 481 lines by 250 pixels per line resolution of the frame store, the center pixel was calculated to be

0.396 milliradian high by 1.016 milliradians wide. Using equation 6.4, the end pixels were calculated to have a  $d\theta/dD$  of 0.984 and  $d\phi/dD$  of 0.9915. This means that with the 50 mm lens used, there was less than a 2 percent variation in the size of the pixels. Thus, for all practical purposes, the pixels can be considered to be effectively the same size.

It was decided to mount the camera on the machinists table (which had a 2 arc second resolution) such that the first element of the lens was directly over the axis of rotation of the machinists table. This is shown in figure 7.3. The camera viewed the calibrated slit set to its smallest calibrated width (0.02 mm). At a distance of 38 inches (0.9652 meters) the slit physically subtends much less than a pixel. The camera lens was set at minimum focus to give a precisely repeatable

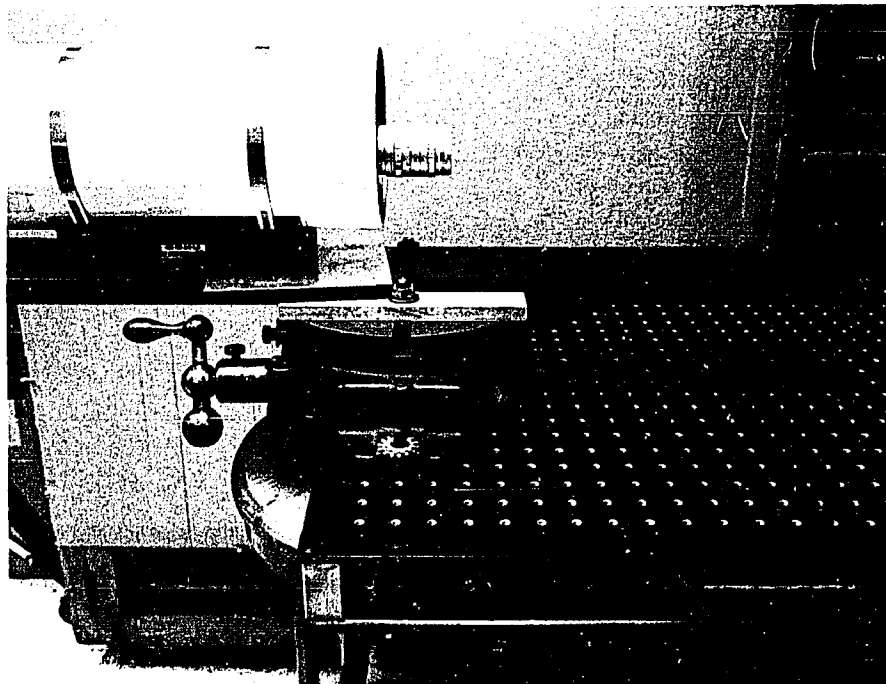


Figure 7.3 Detail of Camera Mounting on Machinists Table

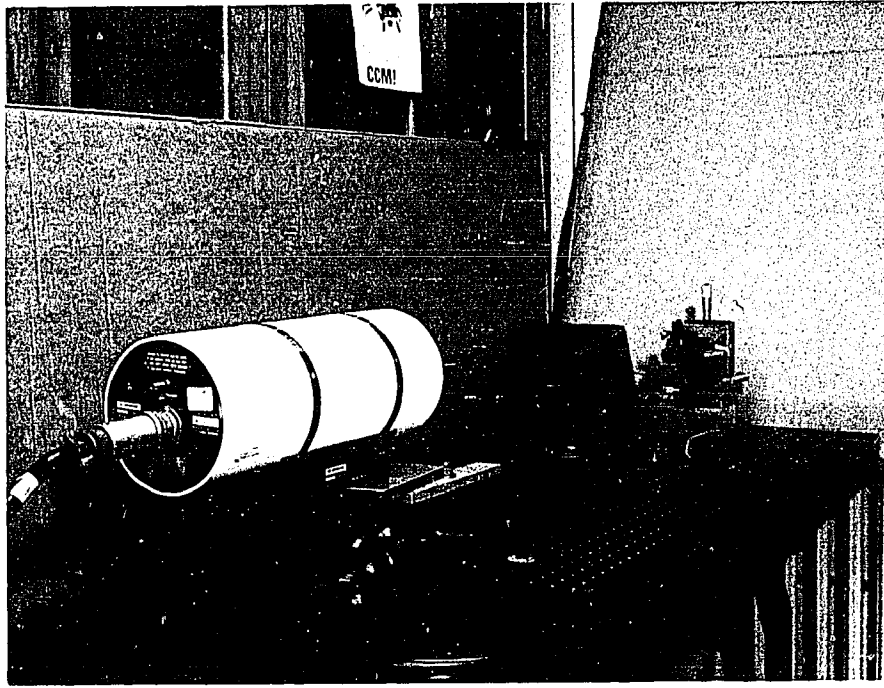


Figure 7.4 Camera Viewing Illuminated Slit During Calibration setting, and an F stop of 22 was used to minimize background features. This setup is shown in figure 7.4

A program was written in BASIC to read in two horizontal lines from the frame store. These lines pass through the image of the slit. The maximum and minimum were found for each line. The contrast of each pixel was then computed using equation 7.3.

$$C = \frac{(\text{intensity of pixel} - \text{min intensity})}{(\text{max intensity} + \text{min intensity})} \quad (\text{eq. 7.3})$$

The mean and standard deviation of the contrast in each line were then computed. A set of pixels was selected which had contrasts greater than 3 standard deviations above the mean contrast. This set of pixels is known to contain the image of the slit because the calibration setup was designed to make the slit the brightest object



in the scene. The contrast of this set of pixels was then normalized so as to sum to one and the probability that the slit was in the direction subtended by each of the respective pixels was computed. The resulting set of pixels, with their associated probabilities, and the reading from the machinists table were then stored on a disc file.

The intensity of the light illuminating the slit, room ambient lighting, video gain and zero setting of the frame store, and aperture of the camera were adjusted to give a set of no more than two pixels as the image of the slit for this program. The validity of this choice of conditions was demonstrated prior to taking data by rotating the machinists table and observing that it was possible to get the slit to image in exactly one pixel on one line, and two pixels on the adjacent line. This arises because of the approximately one-half pixel offset due to the frame store as illustrated in figure 6.7. With all reasonable precautions taken to insure the integrity of the data, a calibration was performed for the horizontal width of each pixel.

In plotting the results using a curve fitting program on a desktop calculator (HP 9830), the index of the pixel with the highest probability was used as the Y coordinate and the angle of the machinists table expressed in milliradians was used for the X coordinate. The data was shown to be effectively linear by the coefficient of the  $x^2$  term being less than 4 percent of the coefficient of the  $x^1$  term. For the even numbered lines, the zero angle crossing was found to be at 137.1677 pixels while for the odd numbered lines, the zero

crossing occurred at 136.6862 pixels. This confirms the one half pixel offset between the odd and even horizontal lines. The slope of the curve for the two horizontal lines were virtually identical (-1.1149 and -1.1147 pixels per milliradian respectively). This also lends some validity to the calibration procedure.

The cylindrical camera housing was then rotated 90 degrees about its long axis and remounted to the machinists table to place the nodal point of the lens as nearly as possible over the axis of rotation of the machinists table. This maneuver allowed the slit to remain fixed relative to the machinists table and effectively interchanged the horizontal and vertical axes of the calibration setup. To compensate for this change, the program was modified to read in one column of pixels instead of two horizontal lines, allowing the same procedure and consequent data reduction to be used. The curvefit program yielded a zero crossing of 252.498 with a slope of 2.6366 pixels per milliradian.

Consistant results were obtained. From the 3 to 4 height to width ratio of the standard television image and the use of 481 lines by 250 pixels per line, the expected ratio of pixel height to width should be about 0.389. The calibration performed resulted in a mean pixel height of 0.379 milliradians and a width of 0.897 milliradians for a ratio of 0.42. This 10 percent variation can be accounted for by the experimental errors inherent in the calibration setup and the adjustments/idiosyncrasies of the particular camera used.

The zero crossings observed during the calibration define the zero angles of the respective horizontal and vertical calibration

setups. There is no guarantee that this defines the direction of the optical axis. A much more elaborate test setup would be required to determine the direction of the optical axis in the camera coordinate system. Fortunately, for the purposes of the experimental work at hand, the choice of a zero direction is somewhat arbitrary, since a relative motion, (i.e. a rotation ) is to be measured.

#### D. MEASUREMENT OF PROBABILISTIC VECTORS

The camera was set up on the machinists table as it was for the horizontal pixel calibration described above. A wooden board was used to hold the three ends of the fiber optics bundles in a fixed orientation (two points 2 inches apart horizontally and one point 1 inch below the top right hand point). The board had a 1/16 inch hole ,tapered in the back, for each fiber allowing the fiber to be inserted firmly. The 1/16 inch front of the hole defined the illuminated aperture. The main fiber optic bundle was split into the three smaller bundles and the common end of the bundle was illuminated by a small incandescent bulb. The details of this setup are visible in the photograph shown in figure 7.5.

The camera and target board were setup as shown in figure 7.6. The black cardboard to the left of the target board was used to hide the glow from the light illuminating the fiber optic bundle and the pilot light on the power supply so that it would not appear to the camera. The target board was set up 44 inches from the axis of rotation of the machinists table. This arrangement provided a satisfactory image of the illuminated points on the target board against a very nearly uniform background.

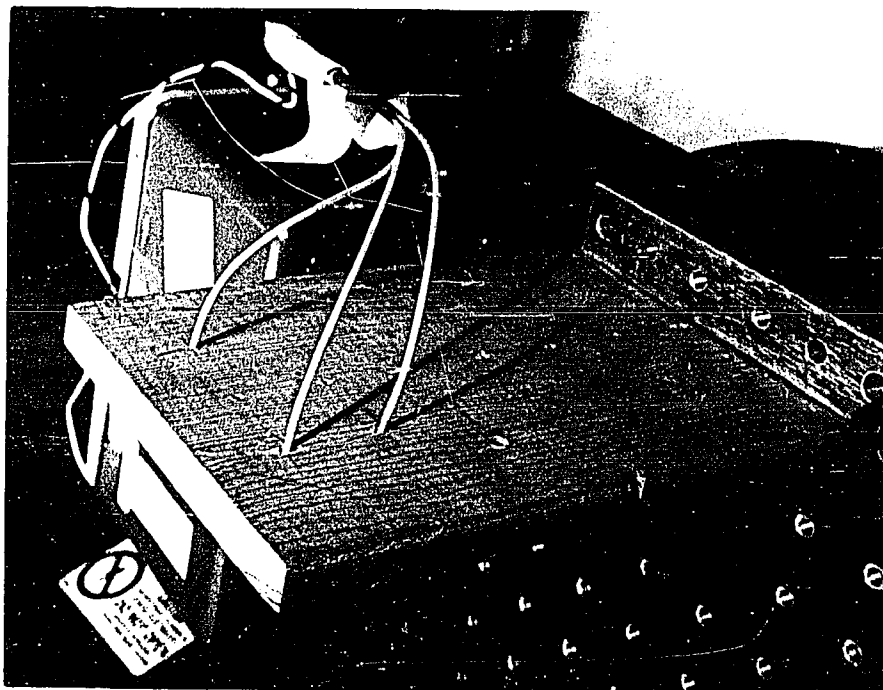


Figure 7.5 Detail of the Fiber Optic Bundles in the Target Board

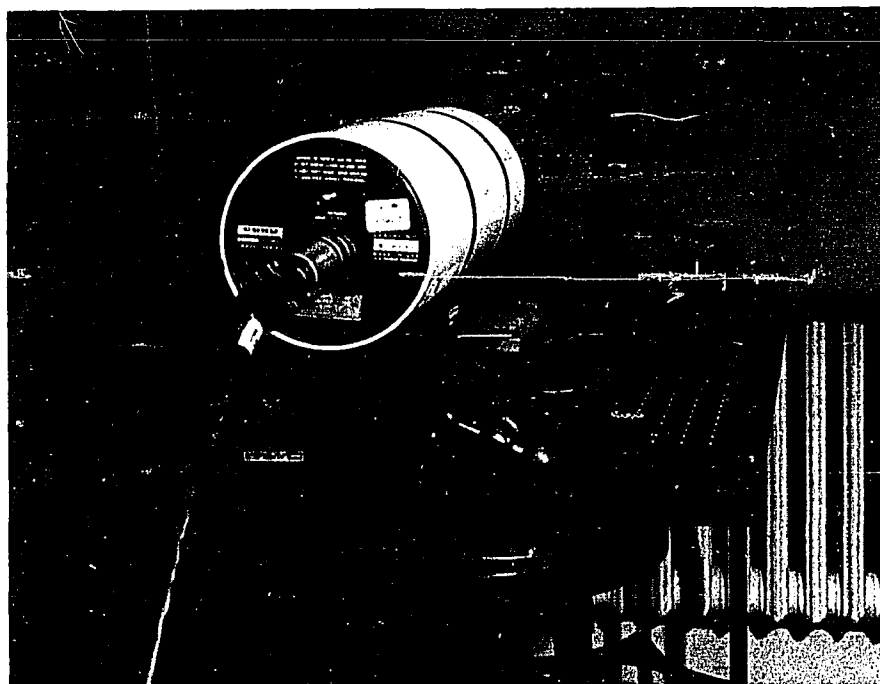


Figure 7.6 View of Setup to Measure Probabilistic Vectors

A program was written in BASIC to draw a 21 pixel wide by 31 pixel high box around the image of each illuminated spot on the frame store defining the "known background" used in computing the probabilistic vector. The program then stored the intensity of these pixels in a separate array for each physical vector. Next, the maximum and minimum intensities were found and used to convert the pixel intensities into contrast, using equation 7.3. The mean and standard deviation of the contrast was found and a set of pixels (defined as having contrasts greater than three sigma above the mean) was extracted. The contrasts of this set of pixels were then normalized to compute the probabilities of the illuminated spot lying within the directions defined by the respective pixels. The horizontal and vertical indices of each pixel in the set, with its associated probability, was then written into a disc file. Since each pixel is of essentially the same, small angular subtense (and therefore can be considered to represent a discrete direction in space) and each pixel has an associated probability, this set of pixels can then be considered to fit the definition of a probabilistic vector.

Thus, it is possible to measure the direction to each of the illuminated ends of the fiber optic bundles (i.e. a physical vector) in terms of a probabilistic vector using an electrooptical sensor.

#### E. THE EXPERIMENT

Once the preliminary work of calibration and arriving at a practical method of measuring probabilistic vectors had been accomplished, the experiment itself could be done. As described above, the camera was mounted on the machinists table so that the axis of

rotation passed through the nodal point of the lens, and the angle of rotation could be read from the machinists table, and compared with the AR of the computed attitude matrix. Three physical vectors are measured. Two are used to compute the probabilistic matrix. The third is used to compare a computed probabilistic vector (in the current orientation) with the measured probabilistic vector describing the actual observation of that physical vector in that orientation. This gives a measure of the accuracy of the probabilistic matrix.

In order to establish the validity of the data, it was decided to take four trials in each of three orientations. This use of multiple trials for the same orientation allows the repeatability of the measurement to be shown. The presence of variations in the observed probabilistic vectors could be accounted for in terms of small relative motions over the 10 to 15 minutes required for the BASIC program to acquire the data and write the results to disc. Also, apparent intensity changes can be explained by drift in the gain and zero settings of the frame store as well as the automatic gain control circuitry of the camera. In all cases, as shown by the data presented in table 7.1, the repeatability of the data was verified.

The procedure used in actually performing the experiment was to first adjust the gain and contrast settings of the frame store and the aperture of the camera (focus being held constant at minimum to preserve calibration) in order to produce probabilistic vectors with between 3 and 5 members. A typical image from the frame store is shown in figure 7.7 with a corresponding view from behind the camera

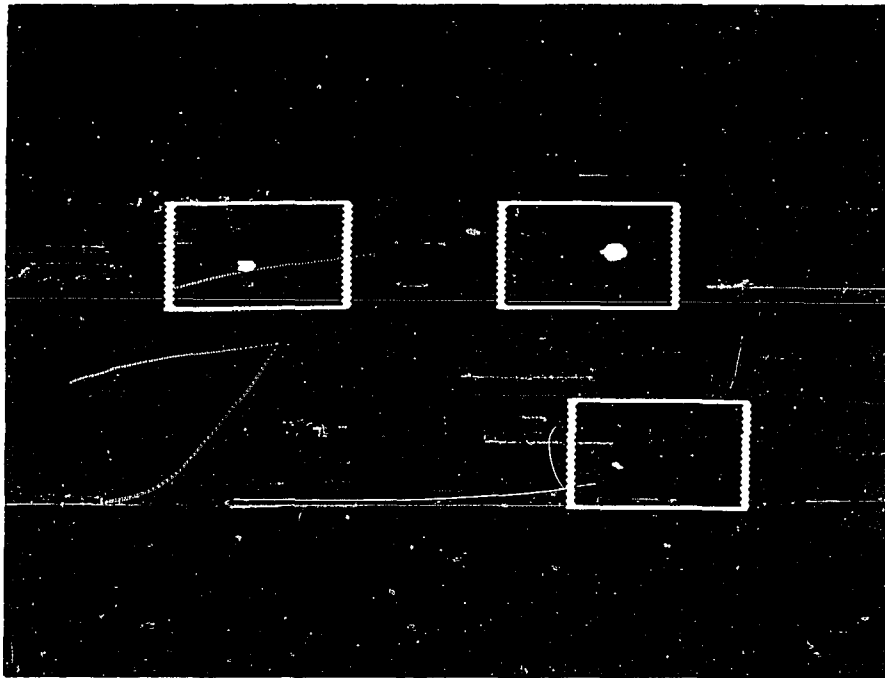


Figure 7.7 Typical Frame Store Image



Figure 7.8 View of Target Board from Behind the Camera

in figure 7.8. The box around each spot in figure 7.7 shows the size of the area "known by design" to contain exactly one viewable object whose direction defines the physical vector to be measured. If you look closely at this figure, the one-half pixel offset between the odd and the even lines of the frame store is visible in the vertical edges of the boxes. The geometrical size of the illuminated circular spot subtends 1.42 milliradians for an area of approximately  $1.58 \text{ mr}^2$ , since a pixel subtends  $0.379 \times 0.879$  or approximately  $0.34 \text{ mr}^2$ , the image could be expected to subtend roughly 5 pixels. Thus, the adjustments of the instrumentation have been set properly. The first orientation was intended to be the reference orientation with the second arising from a rotation of the machinists table by 2 degrees and the third 7 degrees from the reference. The maximum intensity and number of pixels in each probabilistic vector is shown below in table 7.1. Thus, for example, in orientation 1, physical vector 1 had 3 pixels with a maximum intensity of 19, physical vector 2 had 5 pixels

Orientation#	Vector 1		Vector 2		Vector 3	
	#pixels	max	#pixels	max	#pixels	max
1	3	19	5	52	2	44
1.1	3	21	5	54	4	39
1.2	3	23	5	54	4	38
1.3	3	16	4	67	3	46
2	4	30	6	93	6	55
2.1	5	33	5	88	5	56
2.2	6	34	6	85	4	56
2.3	5	50	6	97	4	69
3	4	147	6	190	3	42
3.1	6	171	6	214	4	42
3.2	7	185	7	237	5	65
3.3	7	187	8	250	5	68

Table 7.1 Number of Members and Maximum Value of Measured Probabilistic Vectors



with a maximum intensity of 52, and physical vector 3 had 2 pixels with a maximum intensity of 44. The minimum intensity in each case was zero.

Analysis of this data shows several interesting points. For those cases where there were less than 5 members, this could be explained by some pixels having contrasts below the 3 sigma threshold required for inclusion in the probabilistic vector. Similarly, for those cases with more, there were additional pixels with contrasts above the required level. The increased intensities of vectors 1 and 2 while that of vector 3 remained relatively constant may be explained by a slight shift in the position of the target board. This is reasonable considering that the illumination comes from the ends of a fiber optics bundle and is therefore essentially directional in nature, or just that when viewed from the aspect angle corresponding to the third orientation, the camera is more directly in the beam emitted by the end of the fiber optic bundle. (In retrospect, it may be more desirable to use a diffuser to produce an illumination pattern more nearly independent of angle). Also, when comparing the reported pixel indices for the respective probabilistic vectors, it was noticed that these indices appeared to change consistently as expected with the angle of the machinists table. This lends additional validity to the data taken and the calibration procedure used. (It should be noted that the camera was mounted on the machinists table three times, once for the horizontal calibration, once for the vertical calibration, and once again for the experiment.)

Thus, the experiment resulted in the measurement of three phys-

ical vectors reported as probabilistic vectors as seen in three different orientations of the sensor. Furthermore, the technique of measuring probabilistic vectors with an electrooptical sensor has been validated.

#### F. DATA REDUCTION

Given the data measured in the experiment, it is necessary to apply the concepts developed during this research in order to compute the probabilistic matrix representing the attitude of the sensor. The approach taken is described in section I of chapter III. A flowchart of the data reduction process is shown below in figure 7.9.

This flowchart is configured to stress the important aspects of the data reduction process without becoming lost in the fine details of the programming. A complete listing of the program is given in appendix A, with a list of variables used in appendix B. The raw data taken for orientations 1, 2, and 3 are shown in appendix C, with a sample run of the program for the first case shown in appendix D. Being thus assured that the details are adequately documented, the flowchart will be discussed in detail, step by step.

First, the measured probabilistic vectors were stored in a disc data file in the format of orientation number, # of entries, and then for each member, the x and y pixel indices with the associated probability; this occurred when the experiment was run. The present program reads this data from the disc and asks which two physical vectors are to be used for the computation of the probabilistic matrix. These are assigned to A and B for the reference orientation

and D and E for the current orientation. The remaining physical vector is assigned to C for the reference orientation and both F and R for the current orientation. A,B,C,D,E,and F are stored in unit vector, probability format while R is retained in the original pixel indices, probability format for later comparison with the computed probabilistic vector S. If desired, the data read from the disc can be printed for documentation purposes.

Now we come to the heart of the program, the calculation of the probabilistic matrix. Nested loops are used to form every combination of members from A,B,D,E. Each combination is input to the routine calculating the PAR and both possible ARs according to the Two Vector Method. At this point, the two values of the AR are compared, and if essentially the same, (i.e., within a specified tolerance), then the combination of members of the respective probabilistic vectors is considered to have produced a valid computation of the PAR, AR which can be used to generate a member of the probabilistic matrix. The probability of the joint occurrence of this set of members of the respective probabilistic vectors (i.e. the product of all 4 associated probabilities) is then assigned to this member of the probabilistic matrix, Q. The PAR is then converted into pixel indices form and compared with the previously generated (and quantized) PARs. If a match is found, then the values of the currently computed and previously found values of the AR are compared. If this is also effectively the same, then the currently computed member of the probabilistic matrix is considered to be the same as an already existing member, and the probability associated with the currently

computed member is assigned to the existing member. If no match is found, then the new member is added to the probabilistic matrix. On the other hand, if the two computed values of the AR from the Two Vector Method do not agree, then the combination of the members of the probabilistic matrix are invalid (i.e. there is no single rotation that would map both A into D and B into E) and the next combination is tried.

In this fashion, the probabilistic matrix is computed. Since the total probability associated with the members of the probabilistic matrix may no longer sum to one, the associated probabilities are normalized to assign a total probability of unity to the probabilistic matrix.

Next, the validity of this matrix is tested by using it to transform a probabilistic vector measured in the reference orientation C, into the predicted probabilistic vector that would describe it in the current orientation, S. Again, nested loops are used to compute  $S=[Q]C$  using every combination of members of Q and members of C. Similar members of S are combined (i.e. if they have the same pixel indices, the associated probabilities are added and assigned to the existing member of S). The probabilities of the members of S are then normalized to sum to unity, and S is sorted by pixel indices to allow easy comparison with the actually observed probabilistic vector representing the same physical vector, R.

By looking at the pixels comprising R and those comprising S, it is possible to get a feel for the similarity of shape and direction,

but this is hard to express numerically. Therefore, for each probabilistic vector, the spread (i.e. expected value of the angle between a member and the central direction) and the central direction are printed out. Also, the expected value of the angle between R and S is computed.

This angle between R and S represents the transformation error generated as a result of using the measured attitude matrix as opposed to the actual attitude matrix, for this particular physical vector. This angle is therefore a practical measure of the error of the probabilistic matrix. However, it should be clearly understood that this angle is not necessarily the maximum transformation error which could occur. Referring back to section D of chapter V, the error matrix was defined as the product of the measured and the inverse of the actual attitude matrices. The PAR of the error matrix is that direction for which no transformation error would occur. The AR of the error matrix represents the maximum transformation error that could occur for a physical vector perpendicular to the PAR of the error matrix. Since there is no guarantee that the physical vector used for C and F is perpendicular to the PAR of the error matrix, the maximum transformation error of the computed probabilistic matrix is at least as great as the angle between R and S.

During the experiment, the actual axis and angle of rotation in the camera coordinate system was known only approximately since a relative attitude was to be measured. The fairly extensive calibration and pre-experiment alignment, essential to accurately measure the "correct" attitude of the camera independently, are beyond the

scope of the relatively simple experimental work described in this chapter.

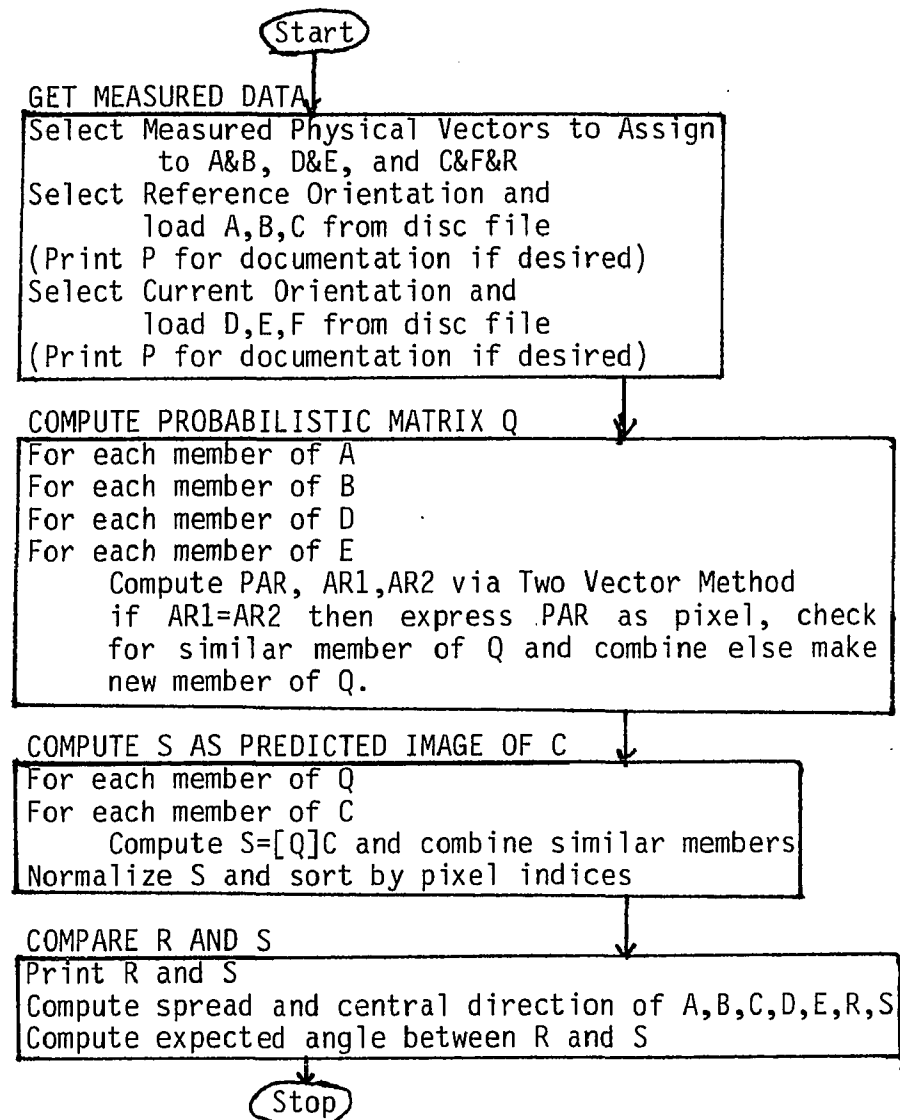


Figure 7.9 Simplified Flowchart of Data Reduction Program

## G. RESULTS

The three physical vectors were measured four times in each of three orientations. The number of pixels, distribution, and relative probabilities were essentially constant for any single

physical vector and orientation. Thus, the repeatability of the measured data allows any trial of each orientation to be used. For convenience, the primary trials were selected. The data reduction program described in the above was run for several cases with the successful results tabulated in table 7.2. Looking at the sample run of the program shown in appendix D, the probabilistic matrix members are printed out in PAR, AR form. Taking the first line as an example, the PAR was found to be  $0.002 \hat{i} + 0.036 \hat{j} + 0.999 \hat{k}$  which corresponds to the Z axis as per the design of the experiment. The AR is found as 33.6 milliradians which corresponds to approximately 1.93 degrees which correlates well with the expected 2 degree rotation designed into the experiment. Thus, the valid members of [Q] agree with the values anticipated and thus provide a validation of the Two Vector Method being able to accurately determine the rotation of the sensor from the measured physical vectors.

Orientation		#pixels/spread (mr)			<FS	#memb	Raw Prob
Reference	Current	Vector C	Vector F	Vector S	(mr)	in Q	in Q
1	2	2/0.27	6/0.45	5/0.45	2.00	3	0.155
2	1	6/0.45	2/0.27	20/0.7	1.16	3	0.399
1	3	2/0.27	3/0.35	8/0.21	4.61	4	0.049
3	1	3/0.35	2/0.27	17/1.10	3.71	9	0.188

Table 7.2 Results of Experimental Data Reduction

Thus, for the case where the reference orientation is the first orientation and the current is the second (see the first line of table 7.2): The third physical vector measured in the reference orientation, vector C, had 2 pixels with a spread of 0.27 mr. This same physical vector measured in the current orientation, vector F, had 6 members with a spread of 0.45 mr. The probabilistic vector computed from [Q]C,

vector  $S$ , has 5 pixels with a spread of 0.45 mr. The angle between the computed,  $S$ , and observed,  $F$ , descriptions of the same physical vector is shown as 2 mr, and serves as a measure of the error resulting from the use of this probabilistic attitude matrix. The computed matrix  $[Q]$  had 3 valid members whose total raw probability (i.e. before normalization) was 0.155. This arises from the sum of the joint probabilities of the combinations of members from the measured probabilistic vectors which resulted in valid members of  $[Q]$ .

The most significant correlation appearing in table 7.2 shows the angle between  $S$  and  $F$  decreasing (i.e., accuracy improves) as the raw probability (i.e. total unnormalized probability) of  $Q$  increases. This is due to valid combinations of the members of the 4 probabilistic vectors used to compute  $Q$  occurring more often. It is significant to note that the relatively small number of members in the probabilistic matrix relative to the number of combinations of pixels in the probabilistic vectors used. For example, each of the cases shown required 480 computations of the PAR, AR from which a maximum of 9 different potentially valid realizations of the attitude matrix were selected. The accuracy of those selected is illustrated by the close agreement between the computed,  $S$ , and observed,  $R$ , vectors in the current orientation of the camera.

It has been mentioned that there were some unsuccessful results. These were termed unsuccessful because none of the combinations of one pixel from each probabilistic vector resulted in sufficient agreement between the two computed values of the AR to be considered as valid. While this is distressing at first, it is possible due the quantization



effects of pixel size, and the possibility of error in measuring the subtense of the pixels. Clearly, the measured pixel size can not be too much in error as several successful runs were made, but the size of the errors indicate that this may be possible. It may be possible to partition the pixels into subpixels (with proportionally smaller probabilities) and achieve more accurate results. This arises primarily because of the quantization effects which affect the correlation between which pixels corresponding portions of the same image appear in different orientations of the sensor. However, partitioning pixels is impractical in the present experiment due to the significantly longer computation times (which increase as roughly the fourth power of the average number of members in the probabilistic vectors) and the intent of the experiment which is to illustrate the concepts and techniques involved rather than arriving at as accurate a result as possible for some practical application.

Considering that the experiment was run with probabilistic vectors having a relatively small number of pixels and that the accuracy of the results agree to within a few pixels, it can be said that the main purposes of the experiment have been fulfilled. An electrooptical sensor has been demonstrated as a physical vector measurement device. The calibrated sensor measured the same two physical vectors in different orientations and used the Two Vector Method to compute the probabilistic attitude matrix, thus validating the Two Vector Method as a ReAtMent technique. The concepts developed during the research have been validated.

## CHAPTER VIII: CONCLUSIONS AND RECOMMENDATIONS FOR FURTHER RESEARCH

### A. CONCLUSIONS

The preceeding chapters have progressed from the fundamental concepts, through mathematical analysis, and culminated in an experimental verification of the viability of the developed techniques. It is worthwhile to briefly recap the major concepts developed during the course of this dissertation.

First, the concept of a probabilistic vector representing the direction to an object in physical, as contrasted to mathematical, geometry was shown. Normalized contrast is used as a measure of the probability that a portion of an object lies within a specified solid angle, a pixel.

Second, the concept of a probabilistic matrix representing the physical attitude of a sensor was shown. This probabilistic interpretation of the unique attitude (represented by a rotation of the sensor about an axis passing through the front nodal point of the lens by a finite angle) arises from the probabilistic vectors used to measure the directions needed to compute the attitude.

Third, the Two Vector Method was validated. This method uses the mathematical relationship between the representations of two physical vectors (i.e. directions in space) as observed in the local coordinate system of the sensor in both a reference and a current orientation to compute the equivalent single axis, PAR, and angle, AR, by which the sensor could have been rotated to bring it from the reference to the current orientation in a single motion. The Two Vector Method can be extended to any number of sensors, provided they measure the

same set of two physical vectors.

Fourth, the PAR, AR computed from the Two Vector Method can be used to compute the coefficients of a valid transformation matrix. The probabilistic representation of the transformation (i.e. attitude) matrix is a more accurate way of expressing the calculated attitude rather than averaging computed matrices on a component by component basis.

Fifth, the necessary mathematics to adequately describe and compute the various functions of probabilistic vectors have been derived for both the continuous and discrete probabilistic vectors. The resulting equations and integrals for operation with probabilistic vectors are guaranteed to be computable by their physical realizability, however, the difficulties involved preclude their practical application. On the other hand, operations with discrete probabilistic vectors have been shown to be implementable with a combination of ordinary vector operations and keeping track of associated probabilities. By recognizing inconsistent (i.e. mathematically impossible) combinations and disregarding them, it is possible to improve the accuracy of discrete probabilistic computations which is impossible with continuous probabilistic computations. This is due to the lack of adequate mathematical formalism to express the IF-THEN logic required to recognize inconsistent combinations of parameters.

Sixth, the practical concepts of what constitutes a valid physical vector, what characteristics are required of a viable ReAtMent system, and what techniques are available to measure directional

information have been discussed from the viewpoint of an engineer who must make informed choices in implementing a ReAtMent system.

And, seventh, an experiment was conducted in great detail to illustrate the above concepts, insure the integrity of the data taken, and data reduction techniques used. This experiment illustrated the practical problems encountered with sensor calibration, pixel size, and data reduction/interpretation. But, more importantly, the experiment validated the concepts described above, and hopefully will provide a springboard for further research.

#### B. RECOMMENDATIONS FOR FURTHER RESEARCH

The author has enjoyed several years of investigation resulting in the present work described above, but this is only a preliminary step in the field of Remote Attitude Measurement.

The major areas which should be targeted for further research are (in no particular order): The development of a suitable mathematical formalism to describe the IF-THEN relationship and logic within an integral to allow inconsistent combinations of parameters to be excluded while maintaining the formal tractability of the integral; The refinement of calibration techniques suitable for directional measurement sensors, refinement of the normalized contrast method of assessing probabilities to account for variations in apparent angular subtense due to aspect angle (i.e. directional energy radiation characteristics) of the source; and, refinement in the computational techniques used in ReAtMent.

A logical extension of the present work would be to implement the Two Vector Method in an actual ReAtMent system, using the prob-

abilistic concepts developed. In addition to the ReAtMent system itself, techniques used to align the device whose attitude is to be measured with the component of the ReAtMent System attached to it, should be investigated from a probabilistic viewpoint. Calibration of the ReAtMent system by independent means is also an area which requires advanced study.

In summary, the author has developed several tools (the probabilistic vector, probabilistic matrix, and the Two Vector Method) which will hopefully advance the study of ReAtMent and find practical application in future ReAtMent systems.

# APPENDIX A. LISTING OF DATA REDUCTION PROGRAM

```

10 REM PROGRAM TO PROCESS PROBABILISTIC VECTORS
19 DIM G[255,4]
20 DIM P[255,4],A[10,4],B[10,4],C[10,4],R[10,3]
21 DIM D[10,4],E[10,4],F[10,4],Q[255,5],S[255,3]
22 LET Z0=4.000000E-04
23 REM Z0 IS ANGULAR ACCURACY TOLERANCE
27 PRINT "ENTER VECTOR NUMBERS FOR A,B,C (MUST BE SET OF 1,2,3)"
28 READ I1,I2,I3
29 PRINT I1,I2,I3
30 PRINT "ENTER REFERENCE ORIENTATION NUMBER"
31 CALL (28)
32 REM CALL(28) REWINDS DISK DATA FILE
35 READ N8
36 PRINT N8
37 IF N8#-999 THEN 40
38 REM CHECK FOR END OF DATA FILE
39 STOP
40 GOSUB 1000
45 IF N8#N9 THEN 40
50 GOSUB 1100
52 REM GOSUB 1500 TO PRINT PROB VECTORS IN THIS ORIENTATION
55 CALL (28)
56 REM REWIND DATA FILE
60 PRINT "ENTER CURRENT ORIENTATION NUMBER"
64 READ N8
65 PRINT N8
70 GOSUB 1000
75 IF N8#N9 THEN 70
79 CALL (28)
80 GOSUB 1200
82 REM GOSUB 1500 TO PRINT PROB VECTORS IN THIS ORIENTATION
90 LET Q9=0
95 PRINT "A9,B9,C9=";A9;B9;C9
96 PRINT "D9,E9,F9=";D9;E9;F9
100 FOR L=1 TO A9
101 REM FOR EVERY MEMBER OF A
102 LET V1=A[L,1]
104 LET V2=A[L,2]
106 LET V3=A[L,3]
108 LET V7=A[L,4]
110 FOR K=1 TO B9
111 REM FOR EVERY MEMBER OF B
112 LET W1=B[K,1]
114 LET W2=B[K,2]
116 LET W3=B[K,3]
118 LET W7=B[K,4]
120 FOR J=1 TO D9
121 REM FOR EVERY MEMBER OF D
122 LET V4=D[J,1]
124 LET V5=D[J,2]

```

```

126 LET V6=D[J,3]
128 LET V8=D[J,4]
130 FOR I=1 TO E9
131 REM FOR EVERY MEMBER OF E
132 LET W4=E[I,1]
134 LET W5=E[I,2]
136 LET W6=E[I,3]
138 LET W8=E[I,4]
139 REM COMPUTE PROB MATRIIX USING TWO VECTOR METHOD
140 GOSUB 6000
150 NEXT I
160 NEXT J
170 NEXT K
180 NEXT L
185 LET S9=0
186 LET S=0
189 REM NORMALIZE PROB OF MATRIX TO UNITY
190 FOR I=1 TO Q9
191 LET S=S+Q[I,3]
192 NEXT I
193 FOR I=1 TO Q9
194 LET Q[I,3]=Q[I,3]/S
195 NEXT I
196 PRINT "PROBABILISTIC MATRIX IN PAR,AR,PROB FORMAT"
197 REM COMPUTE S USING PROB MATRIX
200 FOR J=1 TO Q9
210 LET X=-8.97000E-04*(Q[J,1]-(Q[J,2]-2*INT(Q[J,2]/2))/2-128)
220 LET Y=3.79000E-04*(Q[J,2]-269)
230 LET P1=COS(X)*COS(Y)
232 LET P2=SIN(X)*COS(Y)
234 LET P3=SIN(Y)
236 LET P4=Q[J,4]
237 PRINT P1;P2;P3;P4;Q[J,3]
239 REM COMPUTE MATRIX COEFFICIENTS FOR THIS MEMBER
240 GOSUB 7000
260 FOR I=1 TO C9
270 LET S1=M1*C[I,1]+M2*C[I,2]+M3*C[I,3]
272 LET S2=M4*C[I,1]+M5*C[I,2]+M6*C[I,3]
274 LET S3=M7*C[I,1]+M8*C[I,2]+M9*C[I,3]
275 IF S1=0 THEN 290
276 LET X=ATN(S2/S1)
282 IF S1>0 THEN 290
290 LET Y=ATN(S3/SQR(S1^2+S2^2))
300 GOSUB 5000
301 REM CONVERT ANGLE TO PIXEL
302 REM NOW SEE IF SIMILAR MEMBER ALREADY IN S
320 LET I2=0
330 FOR I1=1 TO S9

```

```

332 IF S[I1,1]#X THEN 340
334 IF S[I1,2]#Y THEN 340
336 LET I2=1
338 LET S[I1,3]=S[I1,3]+Q[J,3]
340 NEXT I1
350 IF I2=1 THEN 360
352 LET S9=S9+1
354 LET S[S9,1]=X
356 LET S[S9,2]=Y
358 LET S[S9,3]=Q[J,3]*C[I,4]
360 NEXT I
365 NEXT J
370 PRINT "COMPUTED PROBABILISTIC VECTOR IS"
371 LET S=0
372 FOR I=1 TO S9
373 LET S=S+S[I,3]
374 NEXT I
375 FOR I=1 TO S9
376 LET S[I,3]=S[I,3]/S
377 NEXT I
378 GOSUB 1800
379 REM SORT S BEFORE PRINTING
380 PRINT "X","Y","PROB"
390 FOR I=1 TO S9
400 PRINT S[I,1],S[I,2],S[I,3]
410 NEXT I
420 PRINT "OBSERVED PROBABILISTIC VECTOR IS"
430 PRINT "X","Y","PROB"
440 FOR I=1 TO R9
450 PRINT R[I,1],R[I,2],R[I,3]
460 NEXT I
463 IF S9=0 THEN 470
464 REM COMPUTE CENTRAL DIRECTION, SPREAD & ANGLE BETWEEN R&S
465 GOSUB 4500
466 REM NOW DO NEXT CASE
470 GOTO 10
1000 REM ROUTINE TO READ PROBABILISTIC VECTORS FROM DISK
1010 CALL (19)
1011 CALL (21)
1012 REM CALL(19) ALLOWS DISK INPUT
1013 REM CALL(20) DIRECTS OUTPUT TO DISK TO SUPPRESS ?
1020 INPUT N9
1030 INPUT P0
1040 FOR I=1 TO P0
1041 CALL (21)
1050 INPUT P[I,1]
1051 INPUT P[I,2]
1052 INPUT P[I,3]

```



```

1053 INPUT P[1,4]
1058 CALL (22)
1059 REM CALL(22) RETURNS OUTPUT TO TTY
1060 NEXT I
1070 CALL (20)
1071 REM CALL(20 ) RETURNS INPUT TO KEYBOARD
1080 RETURN
1100 REM LOAD A,B,C WITH PHYSICAL VECTORS 11,12,13
1102 LET A9=B9=C9=0
1110 FOR I=1 TO P0
1112 LET X=-8.97000E-04*(P[1,2]-(P[1,3]-2*INT(P[1,3]/2))/2-128)
1114 LET Y=3.79000E-04*(P[1,3]-269)
1120 IF P[1,1]#11 THEN 1130
1121 LET A9=A9+1
1122 LET A[A9,1]=COS(X)*COS(Y)
1123 LET A[A9,2]=SIN(X)*COS(Y)
1124 LET A[A9,3]=SIN(Y)
1125 LET A[A9,4]=P[1,4]
1126 GOTO 1160
1130 IF P[1,1]#12 THEN 1140
1131 LET B9=B9+1
1132 LET B[B9,1]=COS(X)*COS(Y)
1133 LET B[B9,2]=SIN(X)*COS(Y)
1134 LET B[B9,3]=SIN(Y)
1135 LET B[B9,4]=P[1,4]
1136 GOTO 1160
1140 IF P[1,1]#13 THEN 1160
1141 LET C9=C9+1
1142 LET C[C9,1]=COS(X)*COS(Y)
1143 LET C[C9,2]=SIN(X)*COS(Y)
1144 LET C[C9,3]=SIN(Y)
1145 LET C[C9,4]=P[1,4]
1160 NEXT I
1170 RETURN
1200 REM LOAD D,E,F WITH PHYSICAL VECTORS 11,12,13
1202 LET D9=E9=F9=0
1210 FOR I=1 TO P0
1212 LET X=-8.97000E-04*(P[1,2]-(P[1,3]-2*INT(P[1,3]/2))/2-128)
1214 LET Y=3.79000E-04*(P[1,3]-269)
1220 IF P[1,1]#11 THEN 1230
1221 LET D9=D9+1
1222 LET D[D9,1]=COS(X)*COS(Y)
1223 LET D[D9,2]=SIN(X)*COS(Y)
1224 LET D[D9,3]=SIN(Y)
1225 LET D[D9,4]=P[1,4]
1226 GOTO 1260
1230 IF P[1,1]#12 THEN 1240
1231 LET E9=E9+1

```

```

1232 LET E[E9,1]=COS(X)*COS(Y)
1233 LET E[E9,2]=SIN(X)*COS(Y)
1234 LET E[E9,3]=SIN(Y)
1235 LET E[E9,4]=P[I,4]
1236 GOTO 1260
1240 IF P[I,1]#I3 THEN 1260
1241 LET F9=F9+1
1242 LET F[F9,1]=COS(X)*COS(Y)
1243 LET F[F9,2]=SIN(X)*COS(Y)
1244 LET F[F9,3]=SIN(Y)
1245 LET F[F9,4]=P[I,4]
1246 LET R[F9,1]=P[I,2]
1247 LET R[F9,2]=P[I,3]
1248 LET R[F9,3]=P[I,4]
1249 LET R9=F9
1260 NEXT I
1270 RETURN
1500 REM ROUTINE TO PRINT OUT PROBABILISTIC VECTORS READ FROM DISK
1510 PRINT "ID#      X      Y      PROB"
1520 FOR I=1 TO P0
1530 PRINT P[I,1];P[I,2];P[I,3];P[I,4]
1540 NEXT I
1550 RETURN
1800 REM SORT COMPUTED PROB VECTOR
1809 REM S IS USED HERE AS A FLAG
1810 LET S=0
1812 FOR I=1 TO S9-1
1820 IF S[I,1]>S[I+1,1] THEN 1840
1830 IF S[I,1]<S[I+1,1] THEN 1850
1835 IF S[I,2]<S[I+1,2] THEN 1850
1840 LET I1=S[I,1]
1841 LET I2=S[I,2]
1842 LET I3=S[I,3]
1843 LET S[I,1]=S[I+1,1]
1844 LET S[I,2]=S[I+1,2]
1845 LET S[I,3]=S[I+1,3]
1846 LET S[I+1,1]=I1
1847 LET S[I+1,2]=I2
1848 LET S[I+1,3]=I3
1849 LET S=1
1850 NEXT I
1860 IF S=1 THEN 1810
1865 PRINT
1866 IF S=1 THEN 1810
1870 RETURN
4000 REM ROUTINE TO COMPUTE CENTRAL DIRECTION OF PIXEL
4001 REM AND ANGULAR SPREAD
4005 LET I1=I2=I3=0

```

```

4006 REM I1,I2,I3 NOW USED AS DUMMY VARIABLES
4010 FOR I=1 TO G9
4020 LET I1=I1+G[I,1]*G[I,4]
4030 LET I2=I2+G[I,2]*G[I,4]
4040 LET I3=I3+G[I,3]*G[I,4]
4050 NEXT I
4060 LET S=SQR(I1*I2+I2*I2+I3*I2)
4070 LET I1=I1/S
4072 LET I2=I2/S
4073 LET I3=I3/S
4080 LET I4=0
4090 FOR I=1 TO G9
4100 LET I5=(G[I,2]*I3-G[I,3]*I2)*2+(G[I,3]*I1-G[I,1]*I3)*2
4102 LET I5=I5+(G[I,1]*I2-G[I,2]*I1)*2
4103 LET I5=SQR(I5)
4104 LET I5=ATN(I5/(G[I,1]*I1+G[I,2]*I2+G[I,3]*I3))
4110 LET I4=I4+G[I,4]*I5
4120 NEXT I
4130 RETURN
4500 REM ROUTINE TO COMPUTE AND PRINT CENTRAL DIRECTION
4501 REM AND SPREAD OF A,B,C,D,E,F
4510 LET G9=A9
4512 FOR I=1 TO G9
4514 LET G[I,1]=A[I,1]
4515 LET G[I,2]=A[I,2]
4516 LET G[I,3]=A[I,3]
4517 LET G[I,4]=A[I,4]
4518 NEXT I
4520 GOSUB 4000
4530 PRINT "CENTRAL DIRECTION OF A IS";I1;I2;I3;"SPREAD=";I4
4540 LET G9=B9
4550 FOR I=1 TO G9
4551 LET G[I,1]=B[I,1]
4552 LET G[I,2]=B[I,2]
4553 LET G[I,3]=B[I,3]
4554 LET G[I,4]=B[I,4]
4555 NEXT I
4556 GOSUB 4000
4560 PRINT "CENTRAL DIRECTION OF B IS";I1;I2;I3;"SPREAD=";I4
4570 LET G9=C9
4580 FOR I=1 TO G9
4581 LET G[I,1]=C[I,1]
4582 LET G[I,2]=C[I,2]
4583 LET G[I,3]=C[I,3]
4584 LET G[I,4]=C[I,4]
4585 NEXT I
4590 GOSUB 4000
4591 LET S1=I1

```

```

4592 LET S2=I2
4593 LET S3=I3
4600 PRINT "CENTRAL DIRECTION OF C IS";I1;I2;I3;"SPREAD=";I4
4610 LET G9=D9
4620 FOR I=1 TO G9
4621 LET G[I,1]=D[I,1]
4622 LET G[I,2]=D[I,2]
4623 LET G[I,3]=D[I,3]
4624 LET G[I,4]=D[I,4]
4625 NEXT I
4630 GOSUB 4000
4640 PRINT "CENTRAL DIRECTION OF D IS";I1;I2;I3;"SPREAD=";I4
4650 LET G9=E9
4660 FOR I=1 TO G9
4661 LET G[I,1]=E[I,1]
4662 LET G[I,2]=E[I,2]
4663 LET G[I,3]=E[I,3]
4664 LET G[I,4]=E[I,4]
4665 NEXT I
4666 GOSUB 4000
4670 PRINT "CENTRAL DIRECTION OF E IS ";I1;I2;I3;"SPREAD=";I4
4680 LET G9=F9
4690 FOR I=1 TO G9
4691 LET G[I,1]=F[I,1]
4692 LET G[I,2]=F[I,2]
4693 LET G[I,3]=F[I,3]
4694 LET G[I,4]=F[I,4]
4695 NEXT I
4696 GOSUB 4000
4700 PRINT "CENTRAL DIRECTION OF F IS";I1;I2;I3;"SPREAD=";I4
4710 LET G9=S9
4720 FOR I=1 TO G9
4722 LET X=-8.97000E-04*(S[I,1]-(S[I,2]-2*INT(S[I,2]/2))/2-128)
4723 LET Y=3.79000E-04*(S[I,2]-269)
4724 LET G[I,1]=COS(X)*COS(Y)
4725 LET G[I,2]=SIN(X)*COS(Y)
4726 LET G[I,3]=SIN(Y)
4727 LET G[I,4]=S[I,3]
4728 NEXT I
4730 GOSUB 4000
4740 PRINT "CENTRAL DIRECTION OF S IS";I1;I2;I3;"SPREAD=";I4
4750 REM COMPUTE ANGLE BETWEEN S AND F
4760 LET I4=0
4770 FOR I=1 TO G9
4780 FOR J=1 TO F9
4790 LET I5=(G[I,2]*F[J,3]-G[I,3]*F[J,2])^2
4791 LET I5=I5+(G[I,3]*F[J,1]-G[I,1]*F[J,3])^2
4792 LET I5=I5+(G[I,1]*F[J,2]-G[I,2]*F[J,1])^2

```

```

4793 LET I5=SQR(I5)
4794 LET I5=ATN(I5/(G[I,1]*F[J,1]+G[I,2]*F[J,2]+G[I,3]*F[J,3]))
4795 LET I4=I4+I5*G[I,4]*F[J,4]
4798 NEXT J
4799 NEXT I
4800 PRINT "ANGLE BETWEEN COMPUTED PROB VECTOR AND OBSERVED"
4801 PRINT " PHYSICAL VECTOR IS ";I4
4895 RETURN
5000 REM ROUTINE TO CONVERT ANGLE TO PIXEL
5005 LET Y=INT(.5+(Y+269*3.79000E-04)/3.79000E-04)
5010 IF Y=2*INT(Y/2) THEN 5040
5020 LET X=INT((-X/8.97000E-04)+128.5)
5030 GOTO 5050
5040 LET X=INT((-X/8.97000E-04)+128)
5050 RETURN
6000 REM TWO VECTOR METHOD
6005 REM COMPUTE DIFFERENCE VECTORS
6010 LET D1=V1-V4
6011 LET D2=V2-V5
6012 LET D3=V3-V6
6020 LET D4=W1-W4
6021 LET D5=W2-W5
6022 LET D6=W3-W6
6030 LET S=SQR(D12+D22+D32)
6031 LET D1=D1/S
6032 LET D2=D2/S
6033 LET D3=D3/S
6040 LET S=SQR(D42+D52+D62)
6041 LET D4=D4/S
6042 LET D5=D5/S
6043 LET D6=D6/S
6044 REM CHECK FOR PARALLEL DIFFERENCE VECTORS
6045 LET S=D1*D4+D2*D5+D3*D6
6046 IF 1-S2<Z02 THEN 6300
6048 REM COMPUTE PAR
6050 LET P1=D2*D6-D3*D5
6051 LET P2=D3*D4-D1*D6
6052 LET P3=D1*D5-D2*D4
6060 LET S=SQR(P12+P22+P32)
6061 LET P1=P1/S
6062 LET P2=P2/S
6063 LET P3=P3/S
6065 REM COMPUTE FIRST AR, CALL IT A1
6070 LET S=V1*P1+V2*P2+V3*P3
6071 LET D1=V1-S*P1
6072 LET D2=V2-S*P2
6073 LET D3=V3-S*P3
6074 LET D4=V4-S*P1

```

```

6075 LET D5=V5-S*P2
6076 LET D6=V6-S*P3
6077 LET S=SQR(D12+D22+D32)
6078 LET D1=D1/S
6079 LET D2=D2/S
6080 LET D3=D3/S
6081 LET S=SQR(D42+D52+D62)
6082 LET D4=D4/S
6083 LET D5=D5/S
6084 LET D6=D6/S
6085 LET S1=(D2*D6+D3*D5)*P1+(D3*D4-D1*D6)*P2+(D1*D5-D2*D4)*P3
6086 LET A1=D1*D4+D2*D5+D3*D6
6088 REM COMPUTE SECOND AR, CALL IT A2
6090 LET S=W1*P1+W2*P2+W3*P3
6091 LET D1=W1-S*P1
6092 LET D2=W2-S*P2
6093 LET D3=W3-S*P3
6094 LET D4=W4-S*P1
6095 LET D5=W5-S*P2
6096 LET D6=W6-S*P3
6097 LET S=SQR(D12+D22+D32)
6098 LET D1=D1/S
6099 LET D2=D2/S
6100 LET D3=D3/S
6101 LET S=SQR(D42+D52+D62)
6102 LET D4=D4/S
6103 LET D5=D5/S
6104 LET D6=D6/S
6105 LET S2=(D2*D6+D3*D5)*P1+(D3*D4-D1*D6)*P2+(D1*D5-D2*D4)*P3
6106 LET A2=D1*D4+D2*D5+D3*D6
6107 IF A1>0 THEN 6110
6108 LET A1=ATN(S1/A1)+3.14159
6109 GOTO 6111
6110 LET A1=ATN(S1/A1)
6111 IF S2>0 THEN 6114
6112 LET A2=ATN(S2/A2)+3.14159
6113 GOTO 6116
6114 LET A2=ATN(S2/A2)
6115 REM SEE IF VALID COMPUTATION WITH A1 NEARLY EQUAL TO A2
6116 IF ABS(A1-A2)>1.000000E-07 THEN 6220
6117 IF P1=0 THEN 6125
6120 LET X=ATN(P2/P1)
6122 IF P1>0 THEN 6130
6124 LET X=X+3.14159
6125 IF P12+P22≠0 THEN 6130
6126 LET X=0
6127 LET Y=SGN(P3)*1.57078
6128 GOTO 6140

```

```

6130 LET Y=ATN(P3/SQR(P1^2+P2^2))
6140 GOSUB 5000
6141 REM TO CONVERT ANGLES TO PIXELS
6150 REM SEE IF SIMILAR MEMBER ALREADY IN Q
6160 LET I2=0
6161 FOR I1=1 TO Q9
6170 IF Q[I1,1]#X THEN 6180
6172 IF Q[I1,2]#Y THEN 6180
6173 IF ABS(Q[I1,4]-A1)>Z0 THEN 6180
6174 LET I2=1
6176 LET Q[I1,3]=Q[I1,3]*Q[I1,5]+V7*V8*W7*W8
6177 LET Q[I1,5]=Q[I1,5]+1
6178 LET Q[I1,3]=Q[I1,3]/Q[I1,5]
6179 GOTO 6220
6180 NEXT I1
6190 IF I2=1 THEN 6220
6195 REM N0, MUST MAKE NEW MEMBER OF Q
6200 LET Q9=Q9+1
6210 LET Q[Q9,1]=X
6212 LET Q[Q9,2]=Y
6214 LET Q[Q9,3]=V7*V8*W7*W8
6216 LET Q[Q9,4]=(A1+A2)/2
6217 LET Q[Q9,5]=1
6220 RETURN
6300 REM ALTERNATE COMPUTATION OF PAR
6310 LET D1=V2*W3-V3*W2
6312 LET D2=V3*W1-V1*W3
6314 LET D3=V1*W2-V2*W1
6316 LET D4=V5*W6-V6*W5
6318 LET D5=V6*W4-V4*W6
6320 LET D6=V4*W5-V5*W4
6330 GOTO 6050
7000 REM COMPUTE MATRIX COEFFICIENTS
7010 LET P5=P4/2
7021 LET M1=COS(P5)^2-(1-2*P1^2)*SIN(P5)^2
7022 LET M2=-P3*SIN(P4)+2*P1*P2*SIN(P5)^2
7023 LET M3=P2*SIN(P4)+2*P1*P3*SIN(P5)^2
7024 LET M4=P3*SIN(P4)+2*P2*P1*SIN(P5)^2
7025 LET M5=COS(P5)^2-(1-2*P2^2)*SIN(P5)^2
7026 LET M6=-P1*SIN(P4)+2*P2*P3*SIN(P5)^2
7027 LET M7=-P2*SIN(P4)+2*P3*P1*SIN(P5)^2
7028 LET M8=P1*SIN(P4)+2*P3*P2*SIN(P5)^2
7029 LET M9=COS(P5)^2-(1-2*P3^2)*SIN(P5)^2
7030 RETURN
8000 REM DATA FOR PRODUCTION RUN OF PROGRAM
8001 REM I1,I2,I3,ORIENTATION #,ORIENTATION #
8010 DATA 1,2,3,1,2
8015 DATA 1,2,3,2,1

```

```
8040 DATA 1,2,3,1,3
8045 DATA 1,2,3,3,1
8070 DATA -999
9999 END
```



## APPENDIX B VARIABLE LIST FOR DATA REDUCTION PROGRAM

$P[-,-]$  Array of measured probabilistic vectors for an orientation  
 $P[-,1]$  Corresponding physical vector number  
 $P[-,2]$  X index of pixel  
 $P[-,3]$  Y index of pixel  
 $P[-,4]$  Probability associated with pixel  
  
 $A[-,-]$  First probabilistic vector in reference orientation  
 $B[-,-]$  Second probabilistic vector in reference orientation  
 $C[-,-]$  Third probabilistic vector in reference orientation  
 $D[-,-]$  First probabilistic vector in current orientation  
 $E[-,-]$  Second probabilistic vector in current orientation  
 $F[-,-]$  Third probabilistic vector in current orientation  
 $A,B,C,D,E,F[-,1]$  i component of unit vector  
 $[-,2]$  j component of unit vector  
 $[-,3]$  k component of unit vector  
 $[-,4]$  probability associated with this member  
  
 $R[-,-]$  is the actually observed third probabilistic vector  
 $S[-,-]$  is the computed third probabilistic vector  
 $R[-,-]$  and  $S[-,-]$  are defined in the same format as  $P[-,-]$   
  
 $Q[-,-]$  PAR,AR,probability form of probabilistic attitude matrix  
 $Q[-,1]$  X index of pixel containing PAR  
 $Q[-,2]$  Y index of pixel containing PAR  
 $Q[-,3]$  Probability associated with this member  
 $Q[-,4]$  AR  
 $Q[-,5]$  # of similar members compressed into this member  
  
Z0 Angular accuracy quantization tolerance  
N9 Orientation number of data in file  
P9,A9,B9,C9,D9,E9,F9,Q9,S9,R9 # of entries in respective matrix  
P1,P2,P3 i,j,k components of PAR in Two Vector Method(TVM)  
A1,A2 value of AR computed from V and W respectively  
P4 value of AR used to compute matrix  
P5 AR/2  
M1,M2,M3,M4,M5,M6,M7,M8,M9 components of the attitude matrix  
V1,V2,V3,V7 i,j,k component and probability of V1 in TVM  
V4,V5,V6,V8 i,j,k component and probability of V2 in TVM  
W1,W2,W3,W7 i,j,k component and probability of W1 in TVM  
W4,W5,W6,W8 i,j,k component and probability of W2 in TVM  
S1,S2,S3 i,j,k components of R  
  
D1,D2,D3,D4,D5,D6,S,N8,I1,I2,I3,I4,I5,X,Y, are dummy variables

# APPENDIX C. MEASURED PROBABILISTIC VECTORS

ORIENTATION NUMBER 1			
ID#	X	Y	PROB
1	217	96	.410256
1	218	94	.179487
1	218	95	.410256
2	217	158	.177419
2	217	159	.360215
2	217	160	.27957
2	217	161	.182796
3	164	153	.128205
3	164	154	.589744
3	165	153	.282051
ORIENTATION NUMBER 2			
ID#	X	Y	PROB
1	179	90	.261905
1	179	92	.357143
1	180	89	8.33333E-02
1	180	91	.297619
2	178	154	6.81818E-02
2	178	156	.13961
2	179	154	.136364
2	179	155	.301948
2	179	156	.185065
2	179	157	.168831
3	127	149	6.21469E-02
3	127	150	.310734
3	127	151	6.21469E-02
3	128	149	.231638
3	128	150	.180791
3	128	151	.152542
ORIENTATION NUMBER 3			
ID#	X	Y	PROB
1	179	90	.252336
1	179	91	9.34579E-02
1	179	92	.308411
1	180	89	.102804
1	180	91	.242991
2	178	156	.125899
2	179	154	.158273
2	179	155	.316547
2	179	156	.23741
2	179	157	.16187
3	127	149	.116162
3	127	150	.282828
3	128	149	.217172
3	128	150	.19697
3	128	151	.186869

ENTER VECTOR NUMBERS FOR A,B,C  
 (MUST BE SET OF 1,2,3)  
     1                    2                    3  
 ENTER REFERENCE ORIENTATION NUMBER  
     1  
 ENTER CURRENT ORIENTATION NUMBER  
     2  
 A9,B9,C9= 4          5          2  
 D9,E9,F9= 4          6          6  
 PROBABILISTIC MATRIX IN PAR,AR,PROB FORMAT  
 2.23812E-03  3.57687E-02  .999358  3.36565E-02  .209367  
 1.15031E-03  1.79952E-02  .999837  3.40941E-02  .395895  
 2.39181E-03  3.68971E-02  .999316  3.41185E-02  .394738  
 COMPUTED PROBABILISTIC VECTOR IS  
     X                    Y                    PROB  
     125                  152                  .515644  
     125                  153                  .117815  
     126                  151                  .198795  
     126                  152                  .06231  
     127                  151                  .10544  
 OBSERVED PROBABILISTIC VECTOR IS  
     X                    Y                    PROB  
     127                  149                  .062147  
     127                  150                  .310734  
     127                  151                  .062147  
     128                  149                  .231638  
     128                  150                  .180791  
     128                  151                  .152542  
 CENTRAL DIRECTION OF A IS .994677 -7.93886E-02 -6.56940E-02  
 SPREAD= 4.09404E-04  
 CENTRAL DIRECTION OF B IS .995995 -7.92473E-02 -4.13975E-02  
 SPREAD= 4.30172E-04  
 CENTRAL DIRECTION OF C IS .998541 -3.20896E-02 -4.34306E-02  
 SPREAD= 2.74032E-04  
 CENTRAL DIRECTION OF D IS .996672 -4.57972E-02 -6.74379E-02  
 SPREAD= 4.07678E-04  
 CENTRAL DIRECTION OF E IS .998047 -4.52920E-02 -4.30192E-02  
 SPREAD= 4.55297E-04  
 CENTRAL DIRECTION OF F IS .998982 6.17642E-04 -4.51157E-02  
 SPREAD= 4.58144E-04  
 CENTRAL DIRECTION OF S IS .999011 2.45450E-03 -4.43991E-02  
 SPREAD= 4.59837E-04  
 ANGLE BETWEEN COMPUTED PROB VECTOR AND OBSERVED  
 PHYSICAL VECTOR IS 2.00270E-03

## SELECTED BIBLIOGRAPHY

- Almar, I., "The Accuracy of Synchronous Visual Observations under the INTEROBS Program in 1962", Smithsonian Astrophysical Observatory Observations of Artificial Earth Sattelites, No.2,1963 p. 87-93
- Bar-Itzhak, "Optimum Normalization of a Computed Quaternion of Rotation", IEEE Transactions on Aerospace and Electronic Systems, Vol. AES-7, p. 401,402, March 1971
- Barnard, T.W. et al., "Remote Attitude Sensing with Polarization Modulated Light", IEEE Transactions on Aerospace and Electronic Systems, Vol. AES-8 No. 2, Mar. 1972
- Boulay, J. L., et al., "Attitude Control of a Pilotless Aircraft by Radioactive Probes", (NATO, AGARD: Reunion Sur L'Instrumentation et le Guidage des Avions sans Pilote, Florence, Italy, Oct. 4-8, 1976), ONERA, TP No. 1976-122, 1976 11 pgs (original in French)
- Bork, A. M., "Vectors Versus Quaternions", American Journal of Physics, Vol. 34, No. 3 . 202-211, March 1966
- Brewer, M. J., "Evaluation of the EROS IV Sattelite Horizon Crossing Indicator Performance", Journal of Spacecraft and Rockets, Vol. 12, No. 4, p. 235-241, April 1975
- Bright, H. R., "A Methodology for Determining the Flight Path of a Six Degree of Freedom Aircraft and its Orientation with Respect to a Ground Site", AD-A015011, July 1975
- Cauffman, D. P., "Matrix Transformations for Spacecraft Attitude Determination", Planet and Space Science, Vol. 20, p. 1607-1611, 1972
- Cantrell, B. H., "Application of Speed Improvement Technique in Coordinate Transformations for Multiple Platform Sensor Integration Problem, NRL Memorandum Report 3520, May 1977
- Collyer, P. W., "Flexure Monitor System for Spacecraft", American Institute of Aeronautics and Astronautics Guidance and Control Conference, Stanford, California, Aug. 14-16, 1972, AIAA paper, 72-855, Vol. II
- Conrad, R. G., et al., "Techniques for Remote Sensing of Missile Position and Attitude", AD-A021974, technical report RD-76-11, 1 Oct. 1975
- Desvignes, F., "Optical Attitude Sensors- A Review for Spacecraft Control", Symposium on Automatic Control in Space, 7th,

- Rottach-Egern, West Germany, May 17-21, 1976, Preprints Vol. 1 (A77-2477 10-12) Duesseldorf, VDI/VDE-Gesellschaft Mess-und-Regelungstechnik, 1976, p. 183-204
- Elmer, F. J., "Method of Determining Relative Orientation of Physical Systems", US Patent #4,134,681, 16 Jan 1979
- Ehling, E. H., Range Instrumentation, Prentice Hall, Englewood Cliffs, N.J. 1967
- Falconi, O., "Maximum Sensitivities of Optical Direction and Twist Measuring Instruments", Journal of the Optical Society of America, Vol. 54, No. 11, Nov. 1964
- Fang, A. C., "An approach to Attitude Determination for a Spin Stabilized Spacecraft (IMP 1)", NASA-TN-D-6925 G1059 , Aug. 1972
- Frew, A. M. et al., "An Integrated System for Precision Attitude Determination and Control", AIAA paper 71-692, August 1971, American Institute of Aeronautics and Astronautics; Guidance Control and Flight Mechanics Conference, Hofstra University, Hempstead, N.Y. Aug 16-18, 1971
- Flom, T. et al., "Multiple Target Tracking and Target Attitude Determination", p. 9-19 (after 1974, no other publication data available) reference to ITT final report "Development of Generation #3 Scanning Laser Radar", Contract NAS 8-20833, Phase III, Jan., 1974
- Gardina, C. R., comments on Bar-Itzhack op. cit., IEEE Transactions on Aerospace and Electronic Systems, p. 392-393, May 1974
- Garner, D., "The Electrofluidic Autopilot", Sport Aviation, August, 1980, Vol.29, No. 8, p. 16-24
- Glazer, J. et al., "The Effects of Tracking Station Coordinate Uncertainties on GEOS-2 Orbital Accuracy", NASA TM-X-65998
- Golub, G. H. et al., "Singular Value Decomposition and Least Squares Solutions", Numer. Math. 14 , p. 403-420, 1979
- Greaves, J. R. , "Manual Photogrammetric Attitude Determination" NASA CR-139117
- Grubin, C., "Derivation of the Quaternion Scheme via the Euler Axis and Angle", Journal of Spacecraft and Rockets, Vol. 7. no. 10, p. 1261-1263, 1970
- Grubin, C., "Vector Representation of Rigid Body Rotation", American Journal of Physics, Vol. 30, no. 6, p. 416,417, June 1962

- Hatcher, N. M., "Attitude Sensor for Space Vehicles", US. Patent #3,381,569 7 May 1968
- Hext, G. R., "The Estimation of Second Order Tensors, with Related Tests and Designs", Biometrika 50 p. 353-373, 1963
- Hill, M. L. et al., "Investigations Related to the Use of Atmospheric Electric Fields for Aircraft and RPV Stabilization", AD A022-051, John Hopkins University, Laurel Md., Applied Physics Lab, June 1975
- Hutchison, T. C. et al., "A Precise Optical Instrumentation Radar", IEEE Transactions on Aerospace and Electronic Systems, Vol. AES-2 No. 2, March 1966, p. 158-168
- Kronsbein, J., "Kinematics, Quaternions, Spinors, and Pauli's Spin Matrices", American Journal of Physics, Vol. 35, No. 4, April 1967, p. 335-342
- Kurjan, D., "Aircraft Altitude Determination in an Angle Measuring Navigation Satellite System", NASA-CR-124625
- Kruse, P. W. et al., Elements of Infrared Technology, New York, John Wiley & Sons Inc. 1962
- Lee, H. B., "Accuracy Limitations of Range-Range (Spherical) Multi-Lateration Systems", MIT Lincoln Labs, PB-228135/0, TN-1973-43
- Newcombe, A. L. Jr., "Attitude Sensor", US Patent #3,780,966, 25 Dec. 1973
- Mardia, K. V., Statistics of Directional Data, New York, Academic Press, 1972
- Mikelson, D., "Design and Laboratory Testing of a Self Contained High Altitude Navigation System, Phase 1, Final Report", "July 1977, Space and Missile Systems Organization/YAD-SAMSO TR-77123
- O'Connor, B. J. et al., "Attitude Determination for a Strapdown IMU", Symposium on Automatic Control in Space, 7th, Rottach-Egern, West Germany, May 17-21, 1976, Preprints, Vol. 2 (A77-24777 10-12), Duesseldorf, VDI/VDE-Gesellschaft Mess-und-Regelungstechnik, 1976, p. 397-411
- Papoulis, A., Probability, Random Variables and Stochastic Processes McGraw Hill, New York, 1965
- Poole, H. H., Fundamentals of Display Systems, Spartan Books, Washington, 1966

- Perrotta, G., "System Consideration on the use of Radiofrequency Sensors as Attitude Detectors for the Fine Pointing of Antennas on board Communications Satellites", International Scientific-Technical Conference on Space, 16th, Rome, Italy, March 18-20, 1976 (Proceedings, A76-4595 23-12) Rome, Rassenga Internazionale Elettronica Nucleare Aerospaziale, 1976 pg. 341-330
- Pietila, R. et al., "A Vector Autopilot System", IEEE AES Vol. 12, No. 3, May 1976, p. 341,347
- Polhemus, W.L., "Miss Distance Position and Attitude Measurement System for Missile Tracking during Target Approach", NAECON 75, Proceedings of the National Aerospace and Electronics Conference, Dayton, Ohio, June 10-12, 1975, (A75-37623,18-01), New York, IEEE, 1975, p. 563-568
- Rogers, C. J. et al., "High Altitude Attitude Determination System Star Sensor Study (HAADS)", AD-B017-336L, March 1977
- Simcox, D.G. et al., "An Attitude Determination Experiment for Evaluation of In Flight Performance of Two New Spacecraft Attitude Sensors", American Institute of Aeronautics and Astronautics, Mechanics, and Control of Flight Conference, Anaheim, Ca. Aug. 5-9, 1974, AIAA paper 74-892
- Singer, S. F., "Torques and Attitude Sensing in Earth Satellites", Academic Press.
- Spinney, V. W., "Application of the Global Positioning System as an Attitude Reference for Near Earth Users", New Frontiers in Aerospace Navigation: Proceedings of the Bicentennial National Aerospace Symposium, Warminster, Pa. April 27,28, 1976 (A77-20655 07-C4) Washington, DC, Institute of Navigation 1976, p. 132-136
- Stephens, M. A., "Vector Correlations", Biometrika 66, 1979, p.41-48
- Stephenson, R. J., "Development of Vector Analysis from Quaternions", American Journal of Physics, Vol. 34, No.3, March 1966 p. 194-201
- Sukhanov, K. G., "Determination of the Coordinates and Attitude of a Spacecraft on a Planetary Surface", (original in Russian), Kosmicheski Issledovania, Vol 13, Sept.-Oct. 1975, p. 658-688 Translation #76 A 32456 also in Cosmic Research, Vol 13, No. 5, March 1976, pg. 591-600
- Todman, D. et al., "Study of Strapdown Inertial Optical Attitude Measurement Systems", Jan. 77 NTIS-HCA17/MFA01, Vol. 1,2,3, ESS/SS-738
- Williams, C. E., "Attitude Determination of TRIAD and TIP XII and XIII Gravity Gradient Stabilized Satellites", AD-031650 APL/JHC TG-1313, DEc. 1977

Wilcox, J. C., "A New Algorithm for Strapped Down Inertial Navigation",  
IEEE Transactions on Aerospace and Electronic Systems, Vol.  
AES-3, No. 5, Sept. 1967

Wolf, W. L.(Ed), Handbook of Military Infrared Technology, University  
of Michigan, 1965

Wolf, W. L. (Ed), The Infrared Handbook, Infrared Information and  
Analysis (IRIA) Center, Environmental Research Institute of  
Michigan, 1978



## INDEX

Alternate computation of vector components perpendicular to PAR 36  
Angle Between Two Pixels 33  
Angle of Rotation (AR) 13,16,39,40  
Aperture Stop 87  
Apparent size and shape 80  
Assembly Language 68  
Atmospheric Scattering and Adsorbtion 80  
Attitude Matrix Coefficients 16,17  
Averaging Coefficients 73  
  
Base Pixel and Matrix 10,22  
BASIC Language 69  
  
Calibration triangle 118  
Camera Calibration 108,117  
Central Direction 136  
Change of pixel width with position in focal plane 85  
Choice of programming language 68  
Circled Variables 22  
Closure of physical geometric figure 60  
Coefficient Estimation 109  
Communication means 71  
Computability of Integrals 29  
Computational Means 65  
Computations required for Two Vector Method 65,106  
Computerized analysis 30  
Continuous Probabilistic Vector 8  
Contrast 5,124  
Crossproduct Between Two Pixels 32  
  
Data reduction 133  
Data repeatability 130  
Density of a pixel 22  
Design of experiment 115  
Depth of focus 121  
Detectable energy difference 80  
Detectable volume element 3  
Device to be pointed 61  
Difference between two pixels 30  
Direction of optical axis in TV camera 126  
Direction to an object 3,81  
Directional properties of EO systems 85  
Discrete probabilistic vector 9,37  
Discrete sampling of vidicon 100  
Distortion 89,90,109  
Dummy variable 22  
  
Error budget 74  
Error matrix 77

- Electromagnetic attitude measurement 53
- Electrooptical attitude measurement 54
- Euler angles 45
  
- Fiber optics 127,141
- Field of View (FOV) 4
- Field stop 87
- Firmware 68
- FLIR 89
- Fluidic rate sensor 48
- Flowchart 134,138
- Focal plane partitioning 94
  - Continuous 97
  - Discrete 96
- Frame store 105
- Front nodal point 102
- Fundamental assumption 2
  
- Geometric ray trace 83
- General ReAtMent problem 12
- Generalization of Two Vector Method for separated observers 17,18
- Generalized ReAtMent system 59,60
- Gravitimetric Attitude Measurement 49
- Gyroscope 47
  
- IF-THEN logic 143,144
- Inertial Attitude Measurement 46
- Instantaneous Field of View (IFOV) 4
- Invalid matrix 73
  
- Jacobian 23,24
  
- Laser gyroscope 47
- Leakage 91
  
- Magnetic attitude measurement 51
- Mapping Probability into the  $\theta, \emptyset$  plane 8,9,20,26,103
- Mathematical geometry 2
- Measuring probabilistic vectors with E0 sensors 79
- Mechanical attitude measurement 43
- Minimum range for an object to define a physical vector 82
- Modulation Transfer Function (MTF) 5
- Most Likely Pixel (MLP) 82
- Mutually Orthogonal 8
  
- Negative of a pixel 31
- Nodal points 83,85,86
- Normalized contrast 7
- Normalized probability 41
  
- Object Direction and Range Measurement Means 70
- Optical Directional Measurement Model 83

- Parametric study 64,77
- Partial attitude measurement 50
- Partitioning of objects 2,62
- Partitioned focal plane 83,85
- Partitioning pixels into subpixels 139
- Photogrammetric attitude measurement 52
- Photoconductive 93
- Photoemissive 97
- Photovoltaic 97
- Physical geometry 2,19,76
- Physical vector 17,49,50,51
  - Measurement means 63
- Pixel 4
- Pixel subtense 24
- Pointwise orthogonal 8
- Polarization 55
- Position measurement means 61
- Principal Axis of Rotation (PAR) 13
- Principal point 87
- Probabilistic analysis of a ReAtMent system 19
- Probabilistic matrix 39,134,135
- Probabilistic vector 7.8
  - Normalization 41
  - Spread of 136
  - Use of 41
- Pyroelectric 93
  
- Quantization Error in Angular Measurement 81
  
- Ray trace 86
- ReAtMent 1,52,53,54
  - Application considerations 57
  - Error budget 74
  - Summary of considerations 78
- Recommendations for further research 142
- Results 137,138
  
- Scanning optical system 89
- Sensitive area of vidicon 105
- Simple general ReAtMent system 72
- Sonar attitude measurement 54
- Spirit level 50
- State of the Art in ReAtMent 43
  - Accuracy and limiting factors 57
  - Summary 55
- Stationarity 19
- Statistical analysis theorems used 20,21
- Successive rotations 43,44
- Successive transformations 44
- Sum of two pixels 26

Television camera and frame store 104  
Theodolite 56  
Transformation error 74,136  
Two Vector Method 13  
    Computation 65  
  
Uniform Vector Field 17